EUROPEAN ORGANIZATION FOR PARTICLE PHYSICS

CERN-PPE/97-154
2 December 1997

A Combination of Preliminary Electroweak Measurements and Constraints on the Standard Model

The LEP Collaborations* ALEPH, DELPHI, L3, OPAL, the LEP Electroweak Working Group† and the SLD Heavy Flavour Group‡

Prepared from Contributions of the LEP and SLD experiments to the 1997 summer conferences.

Abstract

This note presents a combination of published and preliminary electroweak results from the four LEP collaborations and the SLD collaboration which were prepared for the 1997 summer conferences. Averages are derived for hadronic and leptonic cross-sections, the leptonic forward-backward asymmetries, the τ polarisation asymmetries, the $\mathrm{b\overline{b}}$ and $\mathrm{c\overline{c}}$ partial widths and forward-backward asymmetries and the $\mathrm{q\overline{q}}$ charge asymmetry. The major changes with respect to results presented last year are updated results of A_{LR} from SLD, and the inclusion of the first direct measurements of the W mass and triple-gauge-boson couplings performed at LEP. The results are compared with precise electroweak measurements from other experiments. The parameters of the Standard Model are evaluated, first using the combined LEP electroweak measurements, and then using the full set of electroweak results.

---

*The LEP Collaborations each take responsibility for the preliminary data of their own experiment.

†D. Abbaneo, J. Alcaraz, P. Antilogus, T. Behnke, B. Bertucci, A. Blondel, C. Burgard, R. Clare, P.E.L. Clarke, S. Dutta, M. Elsing, R. Faccini, D. Fassouliotis, M.W. Grünewald, A. Gurtu, K. Hamacher, J.B. Hansen, R.W.L. Jones, P. de Jong, T. Kawamoto, M. Kobel, E. Lançon, W. Lohmann, C. Mariotti, M. Martinez, C. Matteuzzi, M.N. Minard, K. Mönig, P. Molnar, A. Nippe, S. Olshevski, Ch. Paus, M. Pepe-Altarelli, S. Petzold, B. Pietrzyk, G. Quast, D. Reid, P. Renton, J.M. Roney, R. Sekulin, R. Tenchini, F. Teubert, M.A. Thomson, J. Timmermans, M.F. Turner-Watson, H. Wahlen, C.P. Ward, D.R. Ward, N.K. Watson, A. Weber.

‡N. de Groot, E. Etzion, B. Schumm, D. Su.

1 Introduction

The four LEP experiments have previously presented [1] parameters derived from the Z resonance using published and preliminary results based on data recorded until the end of 1995. Since then additional results have become available. To allow a quick assessment, a box highlighting the updates is given at the beginning of each section. During 1996 LEP ran at energies of 161 and 172 GeV, allowing the production of W boson pairs for the first time in high energy e^+e^- collisions. Using these data several properties of the W boson have been measured and are included in this note. Published and preliminary fermion pair production cross-section and asymmetry results from data taken in 1995 and 1996 at energies well above the Z resonance are also included which are particularly sensitive to the γZ interference. These results are denoted as LEP-II results.

The LEP-I data (1990-1995) consist of the hadronic and leptonic cross-sections, the leptonic forward-backward asymmetries, the τ polarisation asymmetries, the $b\overline{b}$ and $c\overline{c}$ partial widths and forward-backward asymmetries and the $q\overline{q}$ charge asymmetry. The measurements of the $b\overline{b}$ and $c\overline{c}$ partial widths and left-right-forward-backward asymmetries for b and c quarks from SLD are treated consistently with the LEP data. Many technical aspects of their combination have already been described in References 2, 3 and references therein. It should be noted that several measurements included in this combination are still preliminary.

This note is organised as follows:

Section 2 Z line shape and leptonic forward-backward asymmetries;

Section 3 τ polarisation;

Section 4 Heavy flavour analyses;

Section 5 Inclusive hadronic charge asymmetry;

Section 6 W-boson properties, including m_W, branching ratios, production cross-sections and anomalous triple-gauge-boson couplings;

Section 7 Interpretation of the results, including the combination of results from LEP, SLD, neutrino interaction experiments and from CDF and DØ;

Section 8 Prospects for the future.

2 Z Lineshape and Lepton Forward-Backward Asymmetries

Updates with respect to last year:
ALEPH has reanalysed the full data set, resulting primarily in changes in the τ asymmetry. The results from DELPHI have been updated to include the analysis of the μ and τ pair data recorded in 1995 and improvements to the analysis of the 1994 τ pair data. The L3 results are unchanged. The results from OPAL have been updated to include the hadronic cross-sections measured during the 1995 energy scan and the experimental systematic uncertainties have also been reduced. In addition, ALEPH and DELPHI have used the most recent determination of the LEP energy and errors; L3 and OPAL have evaluated the effect of the energies on their results.
New fermion pair production cross-section measurements from the LEP running periods well above the Z resonance since October 1995 are included for all experiments. The results are interpreted within the framework of the S-Matrix ansatz.

2.1 Results from the Z Peak Data

The 1995 energy scan resulted in each experiment collecting approximately 40 pb^{-1} of data, of which 18 pb^{-1} was recorded at two off-peak points with centre-of-mass energies, $\sqrt{s}$, 1.8 GeV above and below the Z peak. This almost doubled the data available for measurements of m_Z and Γ_Z.

The results presented here are based on these data combined with those recorded in previous years. This includes the data taken during the energy scans in 1990 and 1991 in the range[1] $|\sqrt{s} - m_Z| < 3$ GeV, the data collected at the Z peak in 1992 and preliminary analyses of the energy scan in 1993 ($|\sqrt{s} - m_Z| < 1.8$ GeV) and the peak running in 1994. The total statistics and the systematic errors on the individual analyses of the four LEP collaborations are given in Tables 1 and 2. Details of the individual analyses can be found in References 4–7.

		ALEPH	DELPHI	L3	OPAL	LEP
$q\overline{q}$	'90-'91	451	357	416	454	1678
	'92	680	697	678	733	2788
	'93 prel.	640	677	646	646	2609
	'94 prel.	1654	1241	1307	1524	5726
	'95 prel.	739	584	311	344	1978
	total	4164	3556	3358	3701	14779
$\ell^+\ell^-$	'90-'91	55	36	40	58	189
	'92	82	70	58	88	298
	'93 prel.	78	74	64	82	298
	'94 prel.	190	135	127	184	636
	'95 prel.	80	67	28	42	217
	total	485	382	317	454	1638

Table 1: LEP statistics in units of 10^3 events used for the analysis of the Z line shape and lepton forward-backward asymmetries. Not all experiments have used the full 1995 data set for the present results, in particular this applies to the data recorded before the start of the high precision energy scan.

	ALEPH			DELPHI			L3			OPAL		
	'93 prel.	'94 prel.	'95 prel.	'93 prel.	'94 prel.	'95 prel.	'93 prel.	'94 prel.	'95 prel.	'93 prel.	'94 prel.	'95 prel.
$\mathcal{L}^{\mathrm{exp.}\,(b)}$	0.067%	0.073%	0.080%	0.24%	0.09%	0.09%	0.10%	0.078%	0.128%	0.046%	0.046%	0.046%
σ_{had}	0.068%	0.072%	0.073%	0.10%	0.10%	0.10%	0.052%	0.051%	0.10%	0.084%	0.084%	0.094%
σ_{e}	0.30%	0.30%	0.31%	0.59%	0.54%	0.75%	0.30%	0.23%	1.0%	0.23%	0.24%	$^{(a)}$
σ_{μ}	0.12%	0.12%	0.12%	0.28%	0.30%	0.40%	0.31%	0.31%	1.0%	0.16%	0.15%	$^{(a)}$
σ_{τ}	0.20%	0.20%	0.20%	0.60%	0.60%	0.60%	0.67%	0.65%	0.60%	0.43%	0.46%	$^{(a)}$
$A_{\mathrm{FB}}^{\mathrm{e}}$	0.0018	0.0019	0.0020	0.0025	0.0022	0.0021	0.003	0.003	0.01	0.0016	0.0016	0.002
A_{FB}^{μ}	0.0005	0.0005	0.0005	0.0010	0.0015	0.0015	0.0008	0.0008	0.005	0.001	0.001	0.001
A_{FB}^{τ}	0.0009	0.0007	0.0009	0.0020	0.0020	0.0020	0.003	0.003	0.003	0.002	0.002	0.002

Table 2: Experimental systematic errors for the analysis of the Z line shape and lepton forward-backward asymmetries at the Z peak. The errors quoted do not include the common uncertainty due to the LEP energy calibration. The treatment of correlations between the errors for different years is described in References 4–7.
$^{(a)}$No preliminary result quoted yet.
$^{(b)}$In addition, there is a theoretical error for the calculation of the small angle Bhabha cross-section of 0.11% [8], which has been treated as common to all experiments. For the present, the previous error of 0.16% [9] is used by DELPHI for 1993.

[1] In this note $\hbar = c = 1$.

For the averaging of results the LEP experiments provide a standard set of 9 parameters describing the information contained in hadronic and leptonic cross sections and leptonic forward-backward asymmetries [2, 10]. These parameters are convenient for fitting and averaging since they have small correlations. They are:

- The mass and total width of the Z boson, where the definition is based on the Breit-Wigner denominator $(s - m_{\mathrm{Z}}^2 + is\Gamma_{\mathrm{Z}}/m_{\mathrm{Z}})$ (s-dependent width) [11].
- The hadronic pole cross-section of Z exchange:

$$\sigma_{\mathrm{h}}^0 \equiv \frac{12\pi}{m_{\mathrm{Z}}^2} \frac{\Gamma_{\mathrm{ee}}\Gamma_{\mathrm{had}}}{\Gamma_{\mathrm{Z}}^2} \,. \qquad (1)$$

  Here Γ_{ee} and Γ_{had} are the partial widths of the Z for decays into electrons and hadrons.

- The ratios:

$$R_{\mathrm{e}} \equiv \Gamma_{\mathrm{had}}/\Gamma_{\mathrm{ee}}, \quad R_\mu \equiv \Gamma_{\mathrm{had}}/\Gamma_{\mu\mu} \text{ and } R_\tau \equiv \Gamma_{\mathrm{had}}/\Gamma_{\tau\tau}. \qquad (2)$$

  Here $\Gamma_{\mu\mu}$ and $\Gamma_{\tau\tau}$ are the partial widths of the Z for the decays $\mathrm{Z} \to \mu^+\mu^-$ and $\mathrm{Z} \to \tau^+\tau^-$. Due to the large mass of the τ lepton, a small difference of 0.2% is expected between the values for R_{e} and R_μ, and the value for R_τ, even under the assumption of lepton universality [12].

- The pole asymmetries, $A_{\mathrm{FB}}^{0,\mathrm{e}}$, $A_{\mathrm{FB}}^{0,\mu}$ and $A_{\mathrm{FB}}^{0,\tau}$, for the processes $\mathrm{e^+e^-} \to \mathrm{e^+e^-}$, $\mathrm{e^+e^-} \to \mu^+\mu^-$ and $\mathrm{e^+e^-} \to \tau^+\tau^-$. In terms of the real parts of the effective vector and axial-vector neutral current couplings of fermions, $g_{V\mathrm{f}}$ and $g_{A\mathrm{f}}$, the pole asymmetries are expressed as:

$$A_{\mathrm{FB}}^{0,\mathrm{f}} \equiv \frac{3}{4}\mathcal{A}_{\mathrm{e}}\mathcal{A}_{\mathrm{f}} \qquad (3)$$

  with:

$$\mathcal{A}_{\mathrm{f}} \equiv \frac{2g_{V\mathrm{f}}g_{A\mathrm{f}}}{g_{V\mathrm{f}}^2 + g_{A\mathrm{f}}^2} \,. \qquad (4)$$

The imaginary parts of the vector and axial-vector coupling constants as well as real and imaginary parts of the photon vacuum polarisation are accounted for explicitly in the fitting formulae and are fixed to their Standard Model values.

The fitting procedure takes effects of initial-state radiation [11] as well as t-channel and s/t-interference contributions in the case of $\mathrm{e^+e^-}$ final states into account. The set of 9 parameters does not describe hadron and lepton-pair production completely, because it does not include the interference of the s-channel Z exchange with the s-channel γ exchange. For the results presented in this section and used in the rest of the note, the γ-exchange contributions and the hadronic γZ interference terms are fixed to their Standard Model values. The leptonic γZ interference terms are expressed in terms of the effective couplings. An alternative analysis, where all γZ interference terms are independently determined from the LEP data, is presented in Section 2.2.

The four sets of 9 parameters provided by the LEP experiments are presented in Table 3. The covariance matrix of these parameters is constructed as described in Reference 10. It is constructed from the covariance matrices of the individual LEP experiments and common systematic errors. These common errors arise from the theoretical uncertainty in the luminosity normalisation affecting the hadronic pole cross-section, $\Delta\sigma_{\mathrm{h}}^0/\sigma_{\mathrm{h}}^0 = 0.11\%$, from the uncertainty of the LEP centre-of-mass energy spread of about 1 MeV [13], resulting in $\Delta\Gamma_{\mathrm{Z}} \approx 0.2$ MeV, and from the uncertainty in the LEP energy calibration. The combined parameter set and its correlation matrix are given in Tables 4 and 5.

	ALEPH	DELPHI	L3[a]	OPAL[b]
m_Z(GeV)	91.1883±0.0031	91.1866±0.0029	91.1883±0.0029	91.1838±0.0029
Γ_Z(GeV)	2.4951±0.0043	2.4893±0.0040	2.4996±0.0043	2.4958±0.0043
σ_h^0(nb)	41.520±0.068	41.566±0.079	41.411±0.074	41.46±0.07
R_e	20.66±0.09	20.89±0.13	20.78±0.11	20.83±0.14
R_μ	20.82±0.06	20.69±0.08	20.84±0.10	20.79±0.07
R_τ	20.77±0.07	20.88±0.13	20.75±0.14	20.98±0.11
$A_{FB}^{0,e}$	0.0176±0.0037	0.0189±0.0050	0.0148±0.0063	0.0107±0.0054
$A_{FB}^{0,\mu}$	0.0170±0.0025	0.0154±0.0027	0.0176±0.0035	0.0156±0.0026
$A_{FB}^{0,\tau}$	0.0167±0.0028	0.0222±0.0039	0.0233±0.0049	0.0189±0.0034
χ^2/d.o.f.	178/177	183/162	142/159	96/144[c]

Table 3: Line shape and asymmetry parameters from 9-parameter fits to the data of the four LEP experiments.

[a] These results use the energies as given in Ref. [14]. L3 has estimated that using the new energies the mass would shift by +0.3 MeV and the width by +0.3 MeV, and these values have been used in subsequent fits.

[b] These results use the energies as given in Ref. [14]. OPAL has estimated that using the new energies the mass would shift by +0.5 MeV and the width by 0.0 MeV, and these values have been used in subsequent fits.

[c] This parameter set has been obtained from a parameter transformation applied to the 15 parameters of the OPAL fit [7], which treats the γZ interference terms for leptons as additional free parameters while fixing the hadronic γ/Z interference term to the Standard Model. The parameters for the leptonic γZ interference terms have been constrained by the leptonic couplings in the transformation. The χ^2/d.o.f. for the transformation from the 15 to the standard 9 parameters is 11/6.

Parameter	Average Value
m_Z(GeV)	91.1867±0.0020
Γ_Z(GeV)	2.4948±0.0025
σ_h^0(nb)	41.486±0.053
R_e	20.757±0.056
R_μ	20.783±0.037
R_τ	20.823±0.050
$A_{FB}^{0,e}$	0.0160±0.0024
$A_{FB}^{0,\mu}$	0.0163±0.0014
$A_{FB}^{0,\tau}$	0.0192±0.0018

Table 4: Average line shape and asymmetry parameters from the data of the four LEP experiments given in Table 3, without the assumption of lepton universality. The χ^2/d.o.f. of the average is 21/27.

	m_Z	Γ_Z	σ_h^0	R_e	R_μ	R_τ	$A_{FB}^{0,e}$	$A_{FB}^{0,\mu}$	$A_{FB}^{0,\tau}$
m_Z	1.00	0.05	−0.01	0.00	−0.03	−0.02	0.02	0.05	0.04
Γ_Z	0.05	1.00	−0.16	0.00	−0.01	0.00	0.00	0.00	0.00
σ_h^0	−0.01	−0.16	1.00	0.06	0.11	0.08	0.00	0.00	0.00
R_e	0.00	0.00	0.06	1.00	0.05	0.04	−0.02	0.01	0.00
R_μ	−0.03	−0.01	0.11	0.05	1.00	0.06	0.00	0.01	0.00
R_τ	−0.02	0.00	0.08	0.04	0.06	1.00	0.00	0.00	0.01
$A_{FB}^{0,e}$	0.02	0.00	0.00	−0.02	0.00	0.00	1.00	0.01	0.01
$A_{FB}^{0,\mu}$	0.05	0.00	0.00	0.01	0.01	0.00	0.01	1.00	0.02
$A_{FB}^{0,\tau}$	0.04	0.00	0.00	0.00	0.00	0.01	0.01	0.02	1.00

Table 5: The correlation matrix for the set of parameters given in Table 4.

The measurement of the LEP beam energies, and the associated uncertainties, are important in the determination of the mass and width of the Z. In the previous note [1], the treatment of the LEP energies was based on Reference 14. Since then, the studies of the sources of uncertainty in the energy measurements have been almost finalized [15]. The ALEPH and DELPHI collaborations have reanalysed their data using these new determinations of energies and errors. L3 and OPAL have not yet updated their analyses, but have estimated the impact on m_Z and Γ_Z from changes in the overall energy scale; however, improvements due to reduced LEP energy errors have not been included in their results. The uncertainty causes errors of $\Delta m_Z \approx 1.5$ MeV and $\Delta\Gamma_Z \approx 1.5$ MeV [15].

The estimation of the common errors which arise from the LEP energy calibration is more complicated than in previous years due to the correlations in the LEP energy error matrix between the 1993 and 1995 scans. The procedure adopted is the same approximate method as has been used for the previous note [1]. Two fits are performed to a data set from a single experiment. The first fit takes into account all errors as evaluated, whereas in the second fit all errors except those due to the LEP energy uncertainty are halved. The procedure results in two covariance matrices, $V_1 = V_E + V_O$ and $V_2 = V_E + V_O/4$, where V_E contains the components due to energy, and V_O contains all other components. V_E is obtained algebraically from V_1 and V_2, and is then used as a correlated part of the full covariance matrix when combining the data from experiments. The result[2] is insensitive to which of the experiments is used to provide the data.

If lepton universality is assumed, the set of 9 parameters given above is reduced to a set of 5 parameters. R_ℓ is defined as $R_\ell \equiv \Gamma_{\mathrm{had}}/\Gamma_{\ell\ell}$, where $\Gamma_{\ell\ell}$ refers to the partial Z width for the decay into a pair of massless charged leptons. The data of each of the four LEP experiments are consistent with lepton universality (the difference in χ^2 over the difference in d.o.f. with and without the assumption of lepton universality is 4/4, 4/4, 2/4 and 3/4 for ALEPH, DELPHI, L3 and OPAL, respectively). Table 6 gives the five parameters m_Z, Γ_Z, σ_h^0, R_ℓ and $A_{\mathrm{FB}}^{0,\ell}$ for the individual LEP experiments, assuming lepton universality. Tables 7 and 8 give the combined result and the corresponding correlation matrix. Figure 1 shows, for each lepton species and for the combination assuming lepton universality, the resulting 68% probability contours in the R_ℓ-$A_{\mathrm{FB}}^{0,\ell}$ plane. For completeness the partial decay widths of the Z boson are listed in Table 9.

[2]This procedure was previously checked [1] by performing a global fit to the hadronic cross-section data for all experiments for the years 1993, 1994 and 1995. This procedure included all common errors without any approximations being necessary, and was therefore exact apart from the fact the data from earlier years and the leptonic channels were not used. The results agreed with those of the method described in the text.

	ALEPH	DELPHI	L3[(a)]	OPAL[(b)]
m_Z(GeV)	91.1883±0.0031	91.1866±0.0029	91.1883±0.0029	91.1836±0.0029
Γ_Z(GeV)	2.4951±0.0043	2.4893±0.0040	2.4996±0.0043	2.4958±0.0043
σ_h^0(nb)	41.520±0.068	41.557±0.079	41.411±0.074	41.456±0.071
R_ℓ	20.754±0.043	20.759±0.062	20.788±0.066	20.834±0.056
$A_{FB}^{0,\ell}$	0.0170±0.0017	0.0178±0.0021	0.0187±0.0026	0.0160±0.0019
χ^2/d.o.f.	182/181	187/166	144/163	96/144[(c)]

Table 6: Line shape and asymmetry parameters from 5-parameter fits to the data of the four LEP experiments, assuming lepton universality. R_ℓ is defined as $R_\ell \equiv \Gamma_{had}/\Gamma_{\ell\ell}$, where $\Gamma_{\ell\ell}$ refers to the partial Z width for the decay into a pair of massless charged leptons.
[(a)] These results use the energies as given in Ref. [14]. L3 has estimated that using the new energies the mass would shift by +0.3 MeV and the width by +0.3 MeV, and these values have been used in subsequent fits.
[(b)] These results use the energies as given in Ref. [14]. OPAL has estimated that using the new energies the mass would shift by +0.5 MeV and the width by 0.0 MeV, and these values have been used in subsequent fits.
[(c)] This parameter set has been obtained by a parameter transformation applied to the 15 parameters of the OPAL fit. The χ^2/d.o.f. for the transformation from the 15 to the standard 5 parameters is 14/10.

Parameter	Average Value
m_Z(GeV)	91.1867±0.0020
Γ_Z(GeV)	2.4948±0.0025
σ_h^0(nb)	41.486±0.053
R_ℓ	20.775±0.027
$A_{FB}^{0,\ell}$	0.0171±0.0010

Table 7: Average line shape and asymmetry parameters from the results of the four LEP experiments given in Table 6, assuming lepton universality. R_ℓ is defined as $R_\ell \equiv \Gamma_{had}/\Gamma_{\ell\ell}$, where $\Gamma_{\ell\ell}$ refers to the partial Z width for the decay into a pair of massless charged leptons. The χ^2/d.o.f. of the average is 23/31.

	m_Z	Γ_Z	σ_h^0	R_ℓ	$A_{FB}^{0,\ell}$
m_Z	1.00	0.05	−0.01	−0.02	0.06
Γ_Z	0.05	1.00	−0.16	0.00	0.00
σ_h^0	−0.01	−0.16	1.00	0.14	0.00
R_ℓ	−0.02	0.00	0.14	1.00	0.01
$A_{FB}^{0,\ell}$	0.06	0.00	0.00	0.01	1.00

Table 8: The correlation matrix for the set of parameters given in Table 7.

Without Lepton Universality		
Γ_{ee}	(MeV)	83.94±0.14
$\Gamma_{\mu\mu}$	(MeV)	83.84±0.20
$\Gamma_{\tau\tau}$	(MeV)	83.68±0.24
With Lepton Universality		
$\Gamma_{\ell\ell}$	(MeV)	83.91±0.10
Γ_{had}	(MeV)	1743.2±2.3
Γ_{inv}	(MeV)	500.1±1.8

Table 9: Partial decay widths of the Z boson, derived from the results of the 9-parameter (Tables 4 and 5) and the 5-parameter fit (Tables 7 and 8). In the case of lepton universality, $\Gamma_{\ell\ell}$ refers to the partial Z width for the decay into a pair of massless charged leptons.

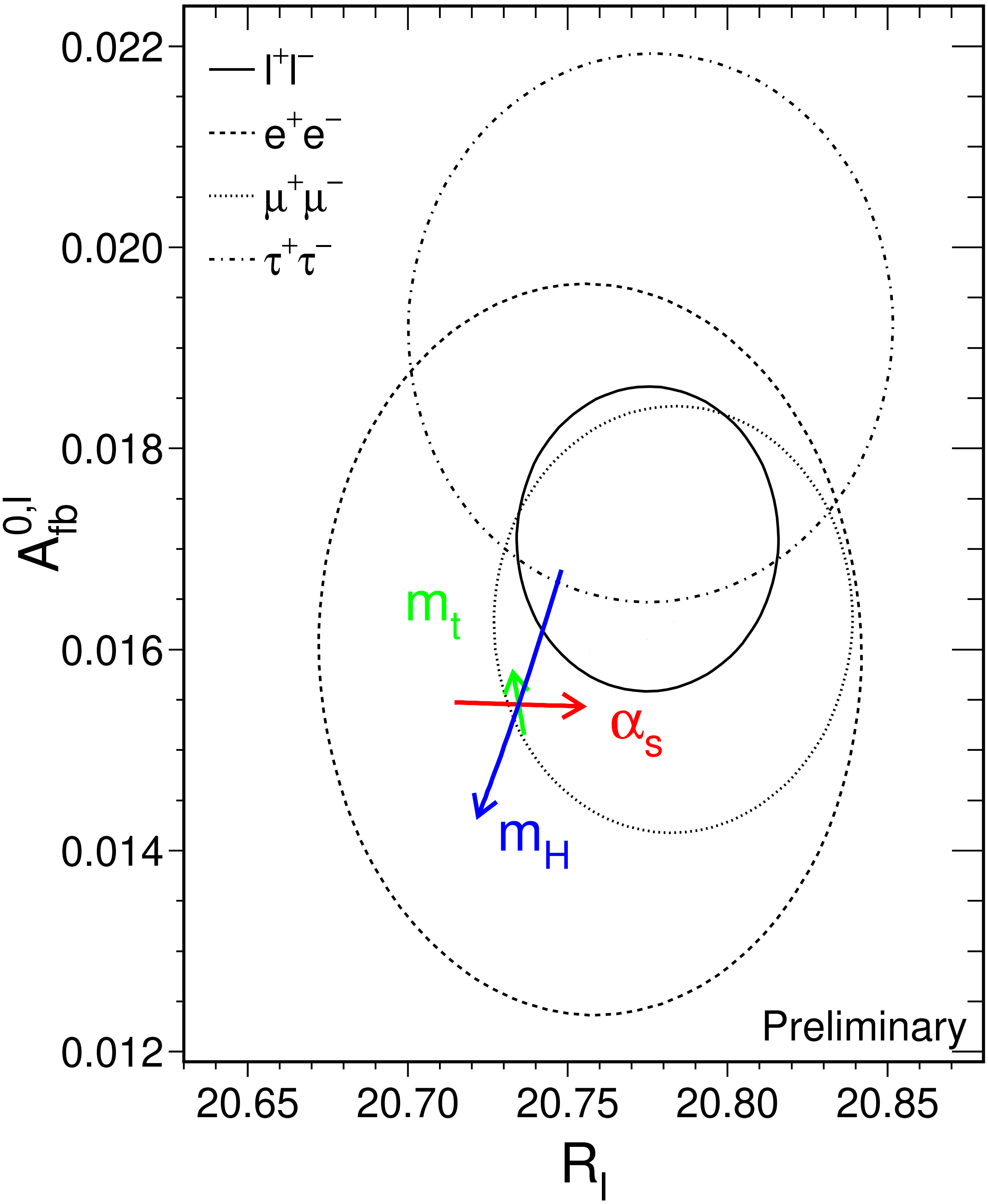

Figure 1: Contours of 68% probability in the R_ℓ-$A_{\rm FB}^{0,\ell}$ plane. For better comparison the results for the τ lepton are corrected to correspond to the massless case. The Standard Model prediction for $m_{\rm Z} = 91.1867$ GeV, $m_{\rm t} = 175.6$ GeV, $m_{\rm H} = 300$ GeV, and $\alpha_s(m_{\rm Z}^2) = 0.118$ is also shown. The lines with arrows correspond to the variation of the Standard Model prediction when $m_{\rm t}$, $m_{\rm H}$ or $\alpha_s(m_{\rm Z}^2)$ are varied in the intervals $m_{\rm t} = 175.6 \pm 5.5$ GeV, $m_{\rm H} = 300^{+700}_{-240}$ GeV, and $\alpha_s(m_{\rm Z}^2) = 0.118 \pm 0.003$, respectively. The arrows point in the direction of increasing values of $m_{\rm t}$, $m_{\rm H}$ and α_s.

2.2 Measurement of γZ Interference including LEP-II Data

In Section 2.1 a model dependence is introduced into the parametrisation of the lineshape and asymmetries by the treatment of the γZ interference contribution to the hadronic cross-section, because quark couplings to the Z are not individually measured for each flavour. This term is therefore taken from the Standard Model. A more general approach is to parametrise the γZ interference term independently of the Z exchange amplitude. Several model independent formalisms exist [16, 17]. For the analysis performed here the framework described in Reference 17 based on the S-Matrix ansatz is used.

In addition to the measurements of cross-section and forward-backward asymmetry in the vicinity of the Z resonance (LEP-I) the results from the 1995 and 1996 LEP runs at centre-of-mass energies from 130 GeV to 172 GeV (LEP-II) are included [18–21]. For a large fraction of these high-energy events, initial-state radiation photons lower the effective centre-of-mass energy, $\sqrt{s'}$, of the annihilation process to values close to the Z mass, m_{Z} (radiative return to the Z). These radiative events dilute the sensitivity of the cross-section and forward-backward asymmetry measurements to the γZ interference parameters. By applying a cut $\sqrt{s'} \gg m_{\mathrm{Z}}$, the high-energy events are isolated and used to constrain these parameters. The total statistics of these high-energy measurements of the four LEP collaborations are given in Table 10. These data are particularly important for the S-Matrix analysis, and significantly improve the precision of the results.

		ALEPH	DELPHI	L3	OPAL	LEP
hadrons	total	4439	4397	4305	4355	17486
	s' cut	1096	1224	1179	1049	4548
$\mu^+\mu^-$ & $\tau^+\tau^-$	total	519	412	379	450	1760
	s' cut	254	190	181	225	850

Table 10: Number of hadronic and $\mu^+\mu^-$ plus $\tau^+\tau^-$ events collected by the LEP experiments at centre-of-mass energies between 130 and 172 GeV. The s' cuts to separate events at high effective s' of the experiments vary between $0.8 < \sqrt{s'/s} < 0.9$. For the selection of the total data sample the experiments also apply loose s' cuts.

In the S-Matrix ansatz the lowest-order total cross-section, σ^0_{tot}, and forward-backward asymmetry, A^0_{fb}, for $\mathrm{e^+e^-}$ annihilation into a fermion-antifermion pair are given by [17]:

$$\sigma^0_a(s) = \frac{4}{3}\pi\alpha^2\left[\frac{g^a_{\mathrm{f}}}{s} + \frac{j^a_{\mathrm{f}}(s-\overline{m}^2_{\mathrm{Z}}) + r^a_{\mathrm{f}}\, s}{(s-\overline{m}^2_{\mathrm{Z}})^2 + \overline{m}^2_{\mathrm{Z}}\overline{\Gamma}^2_{\mathrm{Z}}}\right] \qquad \text{for } a = \mathrm{tot}, \mathrm{fb} \tag{5}$$

$$A^0_{\mathrm{fb}}(s) = \frac{3}{4}\frac{\sigma^0_{\mathrm{fb}}(s)}{\sigma^0_{\mathrm{tot}}(s)}\,. \tag{6}$$

The S-Matrix parameters r_{f}, j_{f} and g_{f} are real numbers which express the size of the Z exchange, γZ interference and photon exchange contributions. In the approach presented here, r_{f} and j_{f} are treated as free parameters while the photon exchange contribution, g_{f}, is fixed to its QED prediction. Each final state is thus described by four free parameters: two for cross-sections, $r^{\mathrm{tot}}_{\mathrm{f}}$ and $j^{\mathrm{tot}}_{\mathrm{f}}$, and two for forward-backward asymmetries, $r^{\mathrm{fb}}_{\mathrm{f}}$ and $j^{\mathrm{fb}}_{\mathrm{f}}$. In models with only vector and axial-vector couplings of the Z boson, *e.g.* the Standard Model, these four S-Matrix parameters are not independent of each other and are approximatively [17]:

$$r^{\mathrm{tot}}_{\mathrm{f}} \propto \left[g^2_{\mathrm{Ae}} + g^2_{\mathrm{Ve}}\right]\cdot\left[g^2_{\mathrm{Af}} + g^2_{\mathrm{Vf}}\right] \tag{7}$$

$$j^{\mathrm{tot}}_{\mathrm{f}} \propto g_{\mathrm{Ve}}g_{\mathrm{Vf}} \tag{8}$$

$$
\begin{aligned}
r_{\rm f}^{\rm fb} &\propto g_{A\rm e} g_{V\rm e} \cdot g_{A\rm f} g_{V\rm f} &(9)\\
j_{\rm f}^{\rm fb} &\propto g_{A\rm e} g_{A\rm f} \,. &(10)
\end{aligned}
$$

The S-Matrix ansatz is defined using a Breit-Wigner denominator with s-independent width for the Z resonance, $s - \overline{m}_{\rm Z}^2 + i\overline{m}_{\rm Z}\overline{\Gamma}_{\rm Z}$. The results described in Section 2.1 used an s-dependent width. Because of this, there is a shift in the Z mass and width between the two parameterisations. These shifts are given by

$$
\begin{aligned}
m_{\rm Z} &\equiv \overline{m}_{\rm Z}\sqrt{1+\overline{\Gamma}_{\rm Z}^2/\overline{m}_{\rm Z}^2} \approx \overline{m}_{\rm Z} + 34.1 \text{ MeV and}\\
\Gamma_{\rm Z} &\equiv \overline{\Gamma}_{\rm Z}\sqrt{1+\overline{\Gamma}_{\rm Z}^2/\overline{m}_{\rm Z}^2} \approx \overline{\Gamma}_{\rm Z} + \ 0.9 \text{ MeV},
\end{aligned}
\qquad (11)
$$

such that $\Gamma_{\rm Z}/m_{\rm Z} = \overline{\Gamma}_{\rm Z}/\overline{m}_{\rm Z}$. These transformations have been applied to the results shown in this section, so that results are comparable to those in the rest of this note. QED radiative corrections are included by convoluting with a radiator function [11].

The experiments fit their data with a set of 16 parameters: one set of the above 4 parameters for each lepton species, $r_{\rm had}^{\rm tot}$ and $j_{\rm had}^{\rm tot}$ for the hadronic final states (asymmetries are not used), and $m_{\rm Z}$ and $\Gamma_{\rm Z}$. These results are presented in Table 31 in Appendix A. For the averaging the procedure defined in the previous section is used. The correlated luminosity error is 0.25% at the LEP-II energies and is still negligible compared with the statistical errors. A correlated error of 0.11% relevant for the Z peak data is taken into account. The common errors originating from the LEP centre-of-mass energy calibration are determined following the procedure described in the previous section.

The data of each of the four LEP experiments are consistent with lepton universality (see the tables in Appendix A). If lepton universality is assumed, the set of 16 S-Matrix parameters is reduced to a set of 8 parameters. In Table 11 the 8 parameters of the individual LEP experiments are shown. In Tables 12 and 13 the LEP averages and their correlation matrix are provided. The Standard Model predictions agree well with the LEP averages of the S-Matrix parameters.

Large correlations appear between the S-Matrix parameters. The correlations between $\Gamma_{\rm Z}$ and the $r_{\rm f}$ parameters are a consequence of the parameter definition and were not visible in the previous section because there the parameters were chosen to be as uncorrelated as possible. A large correlation (-75%) arises between the Z-boson mass, $m_{\rm Z}$, and the hadronic γZ interference term, $j_{\rm had}^{\rm tot}$. The latter is fixed to its Standard Model value in the analysis presented in Section 2.1. This now observable correlation leads to a sizeable increase in the error on the Z-boson mass in fits where $j_{\rm had}^{\rm tot}$ is left free. In Figure 2 the 68% probability contour in the $m_{\rm Z}$-$j_{\rm had}^{\rm tot}$ plane is depicted for the complete data set and for the LEP-I data only as shown at the EPS conference in Brussels 1995 [22]. The error on the hadronic γZ interference term, and consequently the error on $m_{\rm Z}$, are reduced by using total cross-section measurements at centre-of-mass energies far away from the Z pole [17,23]. By now the LEP-II data constrain $j_{\rm had}^{\rm tot}$ well enough so that the inclusion of data taken far below the Z peak improves the errors only slightly. The TOPAZ collaboration at TRISTAN (KEK) has performed a measurement of the total hadronic cross section at $\sqrt{s} = 57.77$ GeV, $\sigma_{\rm tot}^0 = 143.6 \pm 1.5(stat.) \pm 4.5(syst.)$ pb [24]. Combining this measurement with the LEP results yields:

$$
\begin{aligned}
m_{\rm Z} &= 91.1882 \pm 0.0029 \text{ GeV} &(12)\\
j_{\rm had}^{\rm tot} &= 0.14 \pm 0.12\,, &(13)
\end{aligned}
$$

and the correlation between $m_{\rm Z}$ and $j_{\rm had}^{\rm tot}$ is reduced to -71%.

The results presented here are consistent with the results obtained in Section 2.1 where the leptonic γZ interference terms are constrained by the effective couplings and the hadronic γZ interference term is fixed to its Standard Model value.

S-Matrix fit				
	ALEPH	DELPHI	L3[a]	OPAL[a]
m_Z [GeV]	91.1951±0.0056	91.1837±0.0056	91.1854±0.0056	91.1861±0.0054
Γ_Z [GeV]	2.4939±0.0044	2.4896±0.0041	2.4999±0.0043	2.4945±0.0044
$r_{\mathrm{had}}^{\mathrm{tot}}$	2.966±0.010	2.956±0.010	2.971±0.010	2.962±0.010
r_ℓ^{tot}	0.14293±0.00055	0.14211±0.00061	0.14264±0.00066	0.14188±0.00060
$j_{\mathrm{had}}^{\mathrm{tot}}$	-0.18±0.27	0.38±0.28	0.34±0.28	0.08±0.27
j_ℓ^{tot}	-0.012±0.022	0.024±0.023	0.031±0.025	-0.013±0.027
r_ℓ^{fb}	0.00292±0.00033	0.00306±0.00040	0.00327±0.00050	0.00264±0.00037
j_ℓ^{fb}	0.840±0.025	0.761±0.026	0.788±0.033	0.733±0.025
χ^2/d.o.f.	183/197	241/203	164/191	116/163

Table 11: S-Matrix parameters from 8-parameter fits to the data of the four LEP experiments, assuming lepton universality.
[a]For the averaging procedure the L3 values of m_Z and Γ_Z are shifted by +0.3 MeV and the OPAL value of m_Z by +0.5 MeV to account for the new energy calibration.

S-Matrix fit		
Parameter	Average Value	SM Prediction
m_Z [GeV]	91.1882±0.0031	—
Γ_Z [GeV]	2.4945±0.0024	2.4932
$r_{\mathrm{had}}^{\mathrm{tot}}$	2.9637±0.0062	2.9603
r_ℓ^{tot}	0.14245±0.00032	0.14253
$j_{\mathrm{had}}^{\mathrm{tot}}$	0.14±0.14	0.22
j_ℓ^{tot}	0.004±0.012	0.004
r_ℓ^{fb}	0.00292±0.00019	0.00266
j_ℓ^{fb}	0.780±0.013	0.799

Table 12: Average S-Matrix parameters from the data of the four LEP experiments given in Table 31, assuming lepton universality. The χ^2/d.o.f. of the average is 59/56. The Standard-Model predictions are listed for $m_Z = 91.1882$ GeV, $m_t = 175.6$ GeV, $m_H = 300$ GeV, $\alpha_s(m_Z^2) = 0.118$, and $1/\alpha(m_Z^2) = 128.896$.

S-Matrix fit								
	m_Z	Γ_Z	$r_{\mathrm{had}}^{\mathrm{tot}}$	r_ℓ^{tot}	$j_{\mathrm{had}}^{\mathrm{tot}}$	j_ℓ^{tot}	r_ℓ^{fb}	j_ℓ^{fb}
m_Z	1.00	-0.13	-0.09	-0.08	-0.75	-0.43	0.14	-0.02
Γ_Z	-0.13	1.00	0.80	0.61	0.16	0.09	0.00	0.07
$r_{\mathrm{had}}^{\mathrm{tot}}$	-0.09	0.80	1.00	0.77	0.13	0.06	0.02	0.09
r_ℓ^{tot}	-0.08	0.61	0.77	1.00	0.12	0.12	0.03	0.12
$j_{\mathrm{had}}^{\mathrm{tot}}$	-0.75	0.16	0.13	0.12	1.00	0.47	-0.14	0.03
j_ℓ^{tot}	-0.43	0.09	0.06	0.12	0.47	1.00	-0.05	0.02
r_ℓ^{fb}	0.14	0.00	0.02	0.03	-0.14	-0.05	1.00	0.15
j_ℓ^{fb}	-0.02	0.07	0.09	0.12	0.03	0.02	0.15	1.00

Table 13: The correlation matrix for the set of parameters given in Table 12.

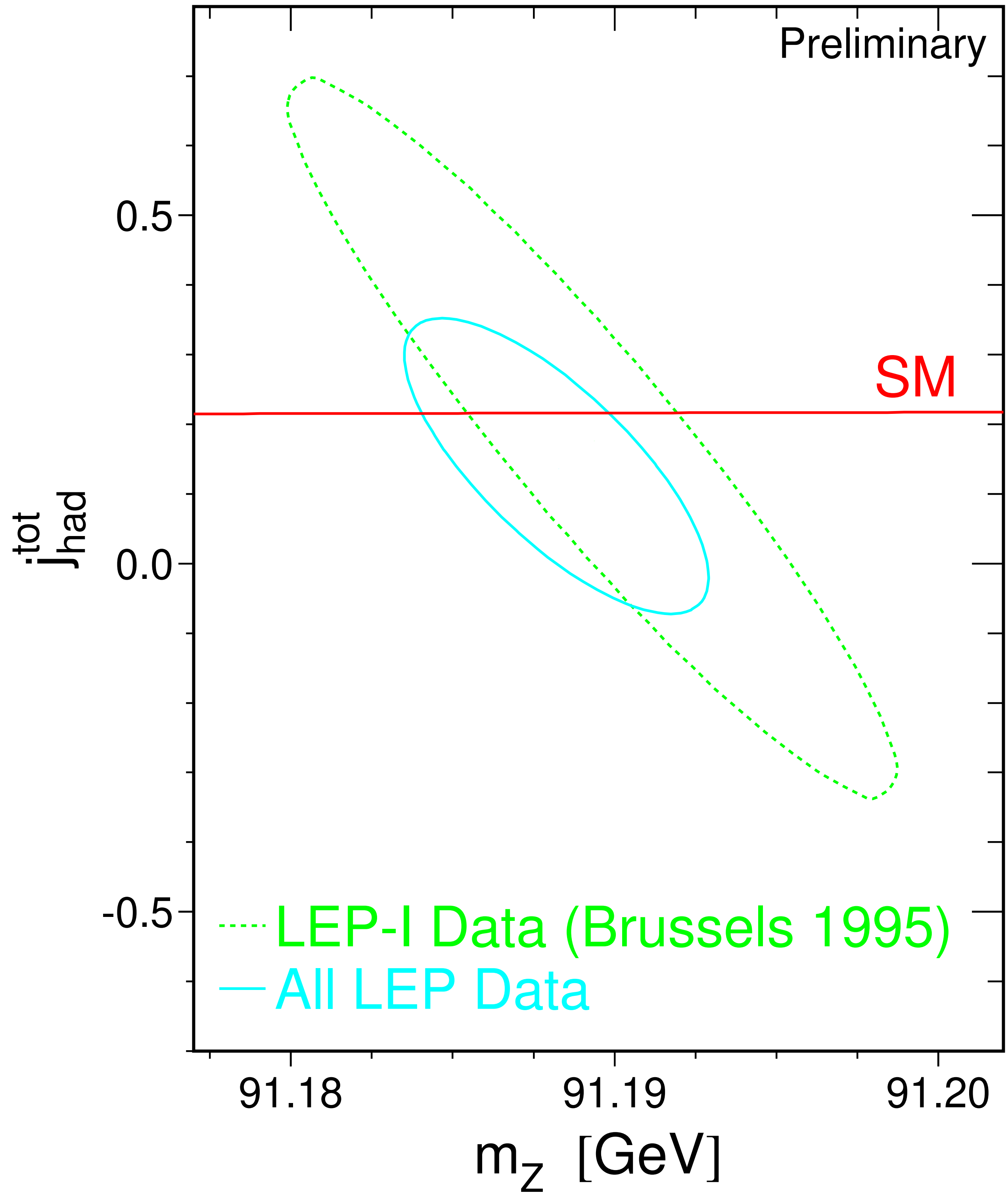

Figure 2: Contours of 68% confidence level between the mass of the Z boson, m_Z, and the hadronic γZ interference term for total cross sections, $j_{\rm had}^{\rm tot}$. Lepton universality is assumed. The solid contour corresponds to all LEP data while the dashed contour is obtained using only LEP-I results as presented at the EPS in Brussels 1995 [22]. The Standard-Model prediction for $j_{\rm had}^{\rm tot}$ is shown as the solid line.

3 The τ Polarisation

Updates with respect to last year:
L3 has reanalysed their 1994 data and has included the 1995 data.

The τ polarisation, $\mathcal{P}_\tau$, is determined by a measurement of the longitudinal polarisation of τ pairs produced in Z decays. It is defined as:

$$\mathcal{P}_\tau \equiv \frac{\sigma_R - \sigma_L}{\sigma_R + \sigma_L}, \tag{14}$$

where σ_R and σ_L are the τ-pair cross-sections for the production of a right-handed and left-handed τ^-, respectively. The distribution of $\mathcal{P}_\tau$ as a function of the polar scattering angle θ between the e^- and the τ^-, at $\sqrt{s} = m_Z$, is given by:

$$\mathcal{P}_\tau(\cos\theta) = -\frac{\mathcal{A}_\tau(1+\cos^2\theta) + 2\mathcal{A}_e\cos\theta}{1+\cos^2\theta + 2\mathcal{A}_\tau\mathcal{A}_e\cos\theta}, \tag{15}$$

with $\mathcal{A}_e$ and $\mathcal{A}_\tau$ as defined in Equation (4). Equation (15) neglects corrections for the effects of γ exchange, γZ interference and electromagnetic radiative corrections for initial- and final-state radiation. These effects are taken into account in the experimental analyses. In particular, these corrections account for the $\sqrt{s}$ dependence of the τ polarisation, $\mathcal{P}_\tau(\cos\theta)$, which is important since the off-peak data are included in the event samples for all experiments. When averaged over all production angles $\mathcal{P}_\tau$ is a measurement of $\mathcal{A}_\tau$. As a function of $\cos\theta$, $\mathcal{P}_\tau(\cos\theta)$ provides nearly independent determinations of both $\mathcal{A}_\tau$ and $\mathcal{A}_e$, thus allowing a test of the universality of the couplings of the Z to e and τ.

Each experiment makes separate $\mathcal{P}_\tau$ measurements using the five τ decay modes $e\nu\overline{\nu}$, $\mu\nu\overline{\nu}$, $\pi\nu$, $\rho\nu$ and $a_1\nu$ [25–28]. The $\rho\nu$ and $\pi\nu$ are the most sensitive channels, contributing weights of about 40% each in the average. DELPHI has also used an inclusive hadronic analysis. The combination is made using the results from each experiment already averaged over the τ decay modes.

3.1 Results

Tables 14 and 15 show the most recent results for $\mathcal{A}_\tau$ and $\mathcal{A}_e$ obtained by the four LEP collaborations [25–28] and their combination. A study of the possible common systematic errors has shown these to be small [2] and thus no such errors have been included in the combination. The statistical correlation between the extracted values of $\mathcal{A}_\tau$ and $\mathcal{A}_e$ is small ($\leq 5\%$), and is neglected.

The average values for $\mathcal{A}_\tau$ and $\mathcal{A}_e$:

$$\mathcal{A}_\tau = 0.1411 \pm 0.0064 \tag{16}$$
$$\mathcal{A}_e = 0.1399 \pm 0.0073, \tag{17}$$

are compatible, in agreement with lepton universality. Assuming $e-\tau$ universality, the values for $\mathcal{A}_\tau$ and $\mathcal{A}_e$ can be combined. This combination is performed neglecting any possible common systematic error between $\mathcal{A}_\tau$ and $\mathcal{A}_e$ within a given experiment, as these errors are also estimated to be small. The combined result of $\mathcal{A}_\tau$ and $\mathcal{A}_e$ is:

$$\mathcal{A}_\ell = 0.1406 \pm 0.0048. \tag{18}$$

Experiment		$\mathcal{A}_\tau$
ALEPH	(90 - 92), final	$0.136 \pm 0.012 \pm 0.009$
DELPHI	(90 - 94), prel.	$0.138 \pm 0.009 \pm 0.008$
L3	(90 - 95), prel.	$0.152 \pm 0.010 \pm 0.006$
OPAL	(90 - 94), final	$0.134 \pm 0.009 \pm 0.010$
LEP Average		0.1411 ± 0.0064

Table 14: LEP results for $\mathcal{A}_\tau$. The χ^2/d.o.f. for the average is 1.4/3. The first error is statistical and the second systematic. In the LEP average, statistical and systematic errors are combined in quadrature. The systematic component of the error, obtained by combining the individual systematic errors (weighted by the total errors), is ± 0.0040.

Experiment		$\mathcal{A}_\mathrm{e}$
ALEPH	(90 - 92), final	$0.129 \pm 0.016 \pm 0.005$
DELPHI	(90 - 94), prel.	$0.140 \pm 0.013 \pm 0.003$
L3	(90 - 95), prel.	$0.158 \pm 0.014 \pm 0.004$
OPAL	(90 - 94), final	$0.129 \pm 0.014 \pm 0.005$
LEP Average		0.1399 ± 0.0073

Table 15: LEP results for $\mathcal{A}_\mathrm{e}$. The χ^2/d.o.f. for the average is 2.4/3. The first error is statistical and the second systematic. In the LEP average, statistical and systematic errors are combined in quadrature. The systematic component of the error, obtained by combining the individual systematic errors (weighted by the total errors), is ± 0.0020.

4 Results from b and c Quarks

Updates with respect to last year:
Several new results on R_b are available. The $\mathcal{A}_\mathrm{c}$ measurement of SLD has improved significantly and several other measurements have been updated.

The relevant quantities in the heavy quark sector at LEP which are currently determined by the combination procedure are:

- The ratios[3] of the b and c quark partial widths of the Z to its total hadronic partial width: $R^0_\mathrm{b} \equiv \Gamma_{\mathrm{b\bar{b}}}/\Gamma_\mathrm{had}$ and $R^0_\mathrm{c} \equiv \Gamma_{\mathrm{c\bar{c}}}/\Gamma_\mathrm{had}$.
- The forward-backward asymmetries, $A^{\mathrm{b\bar{b}}}_\mathrm{FB}$ and $A^{\mathrm{c\bar{c}}}_\mathrm{FB}$.
- The semileptonic branching ratios, $\mathrm{BR}(\mathrm{b} \to \ell)$ and $\mathrm{BR}(\mathrm{b} \to \mathrm{c} \to \bar{\ell})$, and the average $\mathrm{B^0\overline{B^0}}$ mixing parameter, $\overline{\chi}$. These are often determined at the same time as the widths or asymmetries in multi-parameter fits to lepton tag samples. They are included in the combination procedure to take into account their correlations with the other parameters measured in the same fit.
- The probability that a c-quark produces a D^+, $\mathrm{D_s}$, D^{*+} meson[4] or a charmed baryon. The probability that a c-quark fragments into a D^0 is calculated from the constraint that the probabilities for the weakly decaying charmed hadrons add up to one. These quantities are determined now with good accuracy by the LEP experiments. The interpretation of the D^* rate in terms of R_c and the determination of the charm background in the lifetime tag R_b measurements can now be made without assumptions on the energy dependence of the D-meson production rates.

There are several motivations for the averaging procedure [3] presented here. Several analyses measure more than one parameter simultaneously, for example the lepton fits. Some of the measurements of electroweak parameters depend explicitly on the values of other parameters, for example R_b depends on R_c. The common tagging and analysis techniques lead to common sources of systematic uncertainty, in particular for the double-tag measurements of R_b. The starting point for the combination is to ensure that all the analyses use a common set of assumptions for input parameters which give rise to systematic uncertainties. A full description of the averaging procedure has been published in Reference 3. The input parameters have been updated and extended recently [29] to accommodate new analyses and more recent measurements. The correlations and interdependences of the input measurements are then taken into account in a χ^2 minimisation which results in the combined electroweak parameters and their correlation matrix.

In a first fit the asymmetry measurements on peak, above peak and below peak were combined at each centre-of-mass energy. The results of this fit, including the SLD results, are given in Appendix B. The dependence of the average asymmetries on centre-of-mass energy agrees with the prediction of the Standard Model. To derive the pole asymmetries, $A^{0,\mathrm{q}}_\mathrm{FB}$, from the measured quark asymmetries, all the off-peak asymmetry measurements were corrected to the peak energy before combining. Only results from this second fit are quoted here. There are therefore 11 parameters in total to be determined: the two partial widths, two asymmetries, two semileptonic branching ratios, the average mixing parameter and the probabilities for c quark to fragment into a D^+, a $\mathrm{D_s}$, a D^{*+}, or a charmed baryon.

[3] The symbols R^0_b, R^0_c denote the ratio of partial widths whereas R_b, R_c denote the experimentally measured ratios of cross-sections ($R^0_\mathrm{b} = R_\mathrm{b} + 0.0003$, $R^0_\mathrm{c} = R_\mathrm{c} - 0.0003$).

[4] Actually the product $\mathrm{P}(\mathrm{c} \to \mathrm{D}^{*+}) \times \mathrm{BR}(\mathrm{D}^{*+} \to \pi^+\mathrm{D}^0)$ is fitted since this quantity is needed and measured by the LEP experiments.

In addition the SLD collaboration has presented precise measurements of R_{b} [30], R_{c} [31] and of the left-right forward-backward asymmetry for b and c quarks [32]. Since the precision and the dominant sources of systematic uncertainty are similar at LEP and SLD it is useful to produce combined LEP+SLD averages. The left-right forward-backward asymmetries are, in contrast to the unpolarised forward-backward asymmetries, only sensitive to the final state couplings ($\mathcal{A}_{\mathrm{b}}$ and $\mathcal{A}_{\mathrm{c}}$). They are treated in the averaging procedure as physically independent quantities. However the methods used to measure the polarised and unpolarised asymmetries are very similar, so $\mathcal{A}_{\mathrm{b}}$ and $\mathcal{A}_{\mathrm{c}}$ are included in the averaging procedure in order to estimate the correlation between the SLD and the LEP asymmetries, resulting in a 13-parameter fit.

4.1 Summary of Measurements and Averaging Procedure

The measurements of R_{b} and R_{c} fall into two categories. In the first, called a single-tag measurement, a method to select b or c events is devised, and the number of tagged events is counted. This number must then be corrected for backgrounds from other flavours and for the tagging efficiency to calculate the true fraction of hadronic Z decays of that flavour. The dominant systematic errors come from understanding the branching ratios and detection efficiencies which give the overall tagging efficiency. For the second technique, called a double-tag measurement, the event is divided into two hemispheres. With N_t being the number of tagged hemispheres, N_{tt} the number of events with both hemispheres tagged and N_{had} the total number of hadronic Z decays one has:

$$\frac{N_t}{2N_{\mathrm{had}}} = \varepsilon_{\mathrm{b}} R_{\mathrm{b}} + \varepsilon_{\mathrm{c}} R_{\mathrm{c}} + \varepsilon_{\mathrm{uds}}(1 - R_{\mathrm{b}} - R_{\mathrm{c}}), \tag{19}$$

$$\frac{N_{tt}}{N_{\mathrm{had}}} = \mathcal{C}_{\mathrm{b}}\varepsilon_{\mathrm{b}}^2 R_{\mathrm{b}} + \mathcal{C}_{\mathrm{c}}\varepsilon_{\mathrm{c}}^2 R_{\mathrm{c}} + \mathcal{C}_{\mathrm{uds}}\varepsilon_{\mathrm{uds}}^2(1 - R_{\mathrm{b}} - R_{\mathrm{c}}), \tag{20}$$

where ε_{b}, ε_{c} and $\varepsilon_{\mathrm{uds}}$ are the tagging efficiencies per hemisphere for b, c and light-quark events, and $\mathcal{C}_{\mathrm{q}} \neq 1$ accounts for the fact that the tagging efficiencies between the hemispheres may be correlated. In the case of R_{b} one has $\varepsilon_{\mathrm{b}} \gg \varepsilon_{\mathrm{c}} \gg \varepsilon_{\mathrm{uds}}$, $\mathcal{C}_{\mathrm{b}} \approx 1$. The correlations for the other flavours can be neglected. These equations can be solved to give R_{b} and ε_{b}. Neglecting the c and uds backgrounds and the correlations they are approximately given by:

$$\varepsilon_{\mathrm{b}} \approx 2N_{tt}/N_t, \tag{21}$$

$$R_{\mathrm{b}} \approx N_t^2/(4N_{tt}N_{\mathrm{had}}). \tag{22}$$

The double-tagging method has the advantage that the b tagging efficiency is derived directly from the data, reducing the systematic error. The residual background of other flavours in the sample, and the evaluation of the correlation between the tagging efficiencies in the two hemispheres of the event are the main sources of systematic uncertainty in such an analysis.

The measurements included are:

- Lepton tag analyses from ALEPH [33,34], DELPHI [35,36], L3 [37] and OPAL [38]. These analyses use hadronic events with one or more leptons in the final state. Each analysis fits for several parameters chosen from R_{b}, R_{c}, $A_{\mathrm{FB}}^{\mathrm{b\bar{b}}}$, $A_{\mathrm{FB}}^{\mathrm{c\bar{c}}}$, $\mathrm{BR}(\mathrm{b} \to \ell)$ and $\mathrm{BR}(\mathrm{b} \to \mathrm{c} \to \bar{\ell})$, and $\overline{\chi}$. Correlations exist between the different measured quantities, especially between R_{b} and $\mathrm{BR}(\mathrm{b} \to \ell)$. R_{b} and the semileptonic branching ratios are measured by a double-tagging technique where for the branching ratios the lepton identification efficiency needs to be known. The dominant sources of systematic error for the lepton fits arise from the lepton identification, from other semileptonic branching ratios and from the modelling of the semileptonic decay. In addition to the single/double lepton fits ALEPH and DELPHI have measured $\mathrm{BR(b \to \ell)}$ and $\mathrm{BR(b \to c \to \bar{\ell})}$ in a lifetime tagged sample and ALEPH has measured R_c from low energy electrons assuming a value of $\mathrm{BR(c \to \ell)}$ [33, 39].

- Event-shape tag for R_b from L3 (single tag) [40].

- Lifetime (and lepton) double tag measurements for R_b from ALEPH [41], DELPHI [42], L3 [43], OPAL [44] and SLD [30]. These are the most precise determinations of R_b, and dominate the combined result. The basic features of the double-tag technique were discussed above. In the ALEPH, DELPHI and SLD measurements the charm rejection has been enhanced by using the invariant mass information where DELPHI adds also information from the energy of all particles at the secondary vertex and their rapidity. The ALEPH and DELPHI measurements make use of several different tags; this improves the statistical accuracy and reduces the systematic errors due to hemisphere correlations and charm contamination, compared with the simple single/double tag.

- Measurements of $A_\mathrm{FB}^\mathrm{b\bar{b}}$ based on lifetime tagged events with a hemisphere charge measurement from DELPHI [36], L3 [45] and OPAL [46]. These measurements contribute roughly the same weight to the combined result as the lepton fits. The preliminary ALEPH measurement prepared for the Warsaw conference has been withdrawn.

- Analyses with $\mathrm{D/D^{*\pm}}$ mesons to measure R_c from ALEPH [34], DELPHI [47] and OPAL [48]. All measurements are constructed in a way that no assumptions on the energy dependence of charm fragmentation are necessary. The available measurements can be divided into four groups:
  - inclusive/exclusive double tag (ALEPH, DELPHI, OPAL): In a first step $\mathrm{D^{*\pm}}$ mesons are reconstructed in several decay channels and their production rate is measured, which depends on the product $R_\mathrm{c} \times \mathrm{P(c \to D^{*+})} \times \mathrm{BR(D^{*+} \to \pi^+ D^0)}$. This sample of $\mathrm{c\bar{c}}$ (and $\mathrm{b\bar{b}}$) events is then used to measure $\mathrm{P(c \to D^{*+})} \times \mathrm{BR(D^{*+} \to \pi^+ D^0)}$ using a slow pion tag in the opposite hemisphere. In the ALEPH measurement R_c is unfolded internally in the analysis so that no explicit $\mathrm{P(c \to D^{*+})} \times \mathrm{BR(D^{*+} \to \pi^+ D^0)}$ is available.
  - inclusive single/double tag (DELPHI): This measurement measures the single and double tag rate using a slow pion tag. It takes advantage of the higher efficiency of the inclusive slow pion tag compared with the exclusive reconstruction. The high background, however, limits the precision of this measurement.
  - exclusive double tag (ALEPH): This analysis uses exclusively reconstructed $\mathrm{D^{*+}}$, $\mathrm{D^0}$ and $\mathrm{D^+}$ mesons in different decay channels. It has lower statistics but better purity than the inclusive analyses.
  - Reconstruction of all weakly decaying D states (ALEPH, DELPHI, OPAL): These analyses make the assumption that the production rates of $\mathrm{D^0}$, $\mathrm{D^+}$, $\mathrm{D_s}$ and Λ_c saturate the fragmentation of $\mathrm{c\bar{c}}$ with small corrections applied for the unobserved baryonic states. This is a single tag measurement, relying only on knowing the decay branching ratios of the charm hadrons. The DELPHI and OPAL analyses are also used to measure the c-hadron production ratios which are needed for the R_b analyses. This information is currently not used from the ALEPH analysis, however it clearly should be possible to use in future.

- A lifetime plus mass double tag from SLD to measure R_c [31]. This analysis uses the same tagging algorithm as the SLD R_b analysis, but requiring that the mass of the secondary vertex is smaller than the D-meson mass. Although the charm tag has a purity of about 67%, most of the background is from b which can be measured from the b/c mixed tag rate.

- Analyses with D mesons to measure $A_\mathrm{FB}^\mathrm{c\bar{c}}$ from ALEPH [49] or $A_\mathrm{FB}^\mathrm{c\bar{c}}$ and $A_\mathrm{FB}^\mathrm{b\bar{b}}$ from DELPHI [36] and OPAL [50].

- Measurements of $\mathcal{A}_{\mathrm{b}}$ and $\mathcal{A}_{\mathrm{c}}$ from SLD [32]. These results include measurements using lepton, D meson and vertex mass plus hemisphere charge tags, which have similar sources of systematic errors as the LEP asymmetry measurements. SLD also uses vertex mass for b or charm tags in conjunction with a kaon tag for $\mathcal{A}_{\mathrm{b}}$ and $\mathcal{A}_{\mathrm{c}}$ measurements, or with a vertex charge tag for $\mathcal{A}_{\mathrm{c}}$ measurement.

These measurements are presented by the LEP and SLD collaborations in a consistent manner for the purpose of combination [3]. The tables prepared by the experiments include a detailed breakdown of the systematic error of each measurement and its dependence on other electroweak parameters. Where necessary, the experiments apply small corrections to their results in order to use agreed values and ranges for the input parameters to calculate systematic errors. The measurements, corrected where necessary, are summarised in Appendix B in Tables 35-48, where the statistical and systematic errors are quoted separately. The correlated systematic entries are from sources shared with one or more other results in the table and are derived from the full breakdown of common systematic uncertainties. The uncorrelated systematic entries come from the remaining sources.

A χ^2 minimisation procedure is used to derive the values of the heavy-flavour electroweak parameters as published in Reference 3. The full statistical and systematic covariance matrix for all measurements is calculated. This correlation matrix takes correlations between different measurements of one experiment and between different experiments into account. The explicit dependencies of each measurement on the other parameters are also accounted for. The most important example is the dependence of the value of R_{b} on the assumed value of R_{c}.

Since c-quark events form the main background in the R_{b} analyses, the value of R_{b} depends on the value of R_{c}. If R_{b} and R_{c} are measured in the same analysis, this is reflected in the correlation matrix for the results. However most analyses do not determine R_{b} and R_{c} simultaneously but instead measure R_{b} for an assumed value of R_{c}. In this case the dependence is parametrised as:

$$R_{\mathrm{b}} = R_{\mathrm{b}}^{\mathrm{meas}} + a(R_{\mathrm{c}})\frac{(R_{\mathrm{c}} - R_{\mathrm{c}}^{\mathrm{used}})}{R_{\mathrm{c}}}. \tag{23}$$

In this expression, $R_{\mathrm{b}}^{\mathrm{meas}}$ is the result of the analysis assuming a value of $R_{\mathrm{c}} = R_{\mathrm{c}}^{\mathrm{used}}$. The values of $R_{\mathrm{c}}^{\mathrm{used}}$ and the coefficients $a(R_{\mathrm{c}})$ are given in Table 35 where appropriate. The dependences of all other measurements on other electroweak parameters are treated in the same way, with coefficients $a(x)$ describing the dependence on parameter x.

4.2 Treatment of the LEP Heavy Flavour Asymmetry Measurements

For the 11- and 13-parameter fits described above, the peak and off-peak asymmetries are corrected to $\sqrt{s} = 91.26$ GeV using the predicted dependence from ZFITTER [51]. The slope of the asymmetry around m_{Z} depends only on the axial coupling and the charge of the initial and final state fermions and is thus independent of the value of the asymmetry itself.

The QCD corrections to the forward-backward asymmetries depend strongly on the experimental analyses. For this reason the numbers given by the collaborations are already corrected for QCD effects. A detailed description of the procedure can be found in Reference52.

After calculating the overall averages, the quark pole asymmetries, $A_{\mathrm{FB}}^{0,\mathrm{q}}$, are derived by applying the corrections described below. The measured asymmetries are corrected to full acceptance. To relate the pole asymmetries to these numbers a few corrections that are summarised in Table 16 have to be applied. These corrections are the effects of the energy shift from 91.26 GeV to m_Z, initial state radiation, γ exchange and γZ interference. A very small correction due to the finite value of the b-quark mass is included in the correction called γZ interference. All corrections are calculated using ZFITTER.

Source	$\delta A_{\mathrm{FB}}^{\mathrm{b}}$	$\delta A_{\mathrm{FB}}^{\mathrm{c}}$
$\sqrt{s} = m_{\mathrm{Z}}$	-0.0013	-0.0034
QED corrections	$+0.0041$	$+0.0104$
γ, γZ	-0.0003	-0.0008
Total	$+0.0025$	$+0.0062$

Table 16: Corrections to be applied to the quark asymmetries. The corrections are to be understood as $A_{\mathrm{FB}}^0 = A_{\mathrm{FB}}^{meas} + \sum_i (\delta A_{\mathrm{FB}})_i$.

4.3 Results

4.3.1 Results of the 11-Parameter Fit to LEP Data

Using the full averaging procedure gives the following combined results for the electroweak parameters:

$$\begin{aligned} R_{\mathrm{b}}^0 &= 0.2174 \pm 0.0009 \\ R_{\mathrm{c}}^0 &= 0.1727 \pm 0.0050 \\ A_{\mathrm{FB}}^{0,\,\mathrm{b}} &= 0.0983 \pm 0.0024 \\ A_{\mathrm{FB}}^{0,\,\mathrm{c}} &= 0.0739 \pm 0.0048\,, \end{aligned} \tag{24}$$

where all corrections to the asymmetries and partial widths have been applied. The χ^2/d.o.f. is $51/(86-11)$. The corresponding correlation matrix is given in Table 17.

	R_{b}^0	R_{c}^0	$A_{\mathrm{FB}}^{0,\,\mathrm{b}}$	$A_{\mathrm{FB}}^{0,\,\mathrm{c}}$
R_{b}^0	1.00	-0.22	-0.03	0.02
R_{c}^0	-0.22	1.00	0.03	-0.08
$A_{\mathrm{FB}}^{0,\,\mathrm{b}}$	-0.03	0.03	1.00	0.13
$A_{\mathrm{FB}}^{0,\,\mathrm{c}}$	0.02	-0.08	0.13	1.00

Table 17: The correlation matrix for the four electroweak parameters from the 11-parameter fit.

4.3.2 Results of the 13-Parameter Fit to LEP and SLD Data

Including the SLD results on R_{b}, $\mathcal{A}_{\mathrm{b}}$ and $\mathcal{A}_{\mathrm{c}}$ into the fit the following results are obtained:

$$\begin{aligned} R_{\mathrm{b}}^0 &= 0.2170 \pm 0.0009 \\ R_{\mathrm{c}}^0 &= 0.1734 \pm 0.0048 \\ A_{\mathrm{FB}}^{0,\,\mathrm{b}} &= 0.0984 \pm 0.0024 \\ A_{\mathrm{FB}}^{0,\,\mathrm{c}} &= 0.0741 \pm 0.0048 \\ \mathcal{A}_{\mathrm{b}} &= 0.900 \pm 0.050 \\ \mathcal{A}_{\mathrm{c}} &= 0.650 \pm 0.058\,, \end{aligned} \tag{25}$$

with a χ^2/d.o.f. of 53/(94−13). The corresponding correlation matrix is given in Table 18. In deriving these results the parameters $\mathcal{A}_{\mathrm{b}}$ and $\mathcal{A}_{\mathrm{c}}$ have been treated as independent of the forward-backward asymmetries $A_{\mathrm{FB}}^{\mathrm{b\bar{b}}}(\mathrm{pk})$ and $A_{\mathrm{FB}}^{\mathrm{c\bar{c}}}(\mathrm{pk})$. In Figure 3 the results on R_{b}^0 and R_{c}^0 are shown compared with the Standard Model expectation.

	R_{b}^0	R_{c}^0	$A_{\mathrm{FB}}^{0,\mathrm{b}}$	$A_{\mathrm{FB}}^{0,\mathrm{c}}$	$\mathcal{A}_{\mathrm{b}}$	$\mathcal{A}_{\mathrm{c}}$
R_{b}^0	1.00	−0.20	−0.03	0.01	−0.03	0.02
R_{c}^0	−0.20	1.00	0.03	−0.07	0.04	−0.04
$A_{\mathrm{FB}}^{0,\mathrm{b}}$	−0.03	0.03	1.00	0.13	0.03	0.02
$A_{\mathrm{FB}}^{0,\mathrm{c}}$	0.01	−0.07	0.13	1.00	0.00	0.07
$\mathcal{A}_{\mathrm{b}}$	−0.03	0.04	0.03	0.00	1.00	0.08
$\mathcal{A}_{\mathrm{c}}$	0.02	−0.04	0.02	0.07	0.08	1.00

Table 18: The correlation matrix for the six electroweak parameters from the 13-parameter fit.

The result of the full fit to the LEP+SLC results including the off-peak asymmetries and the b semileptonic branching ratio can be found in Appendix B. It should be noted that the result on BR(b $\to \ell$) and the other non-electroweak parameters is independent of the treatment of the off-peak asymmetries and the SLD data.

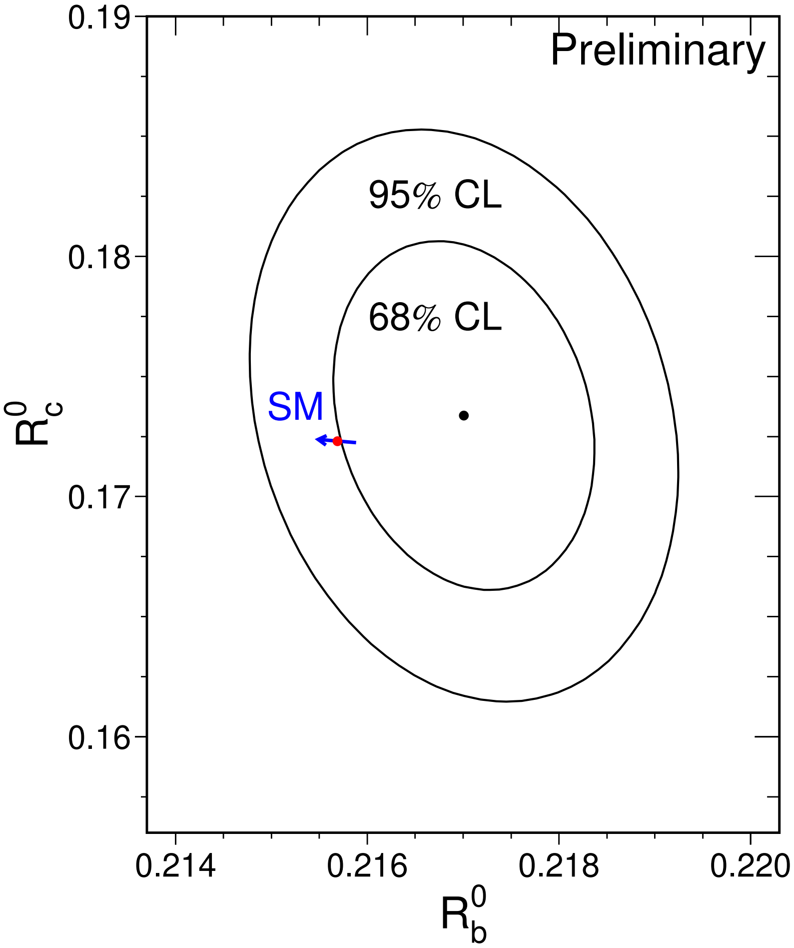

Figure 3: Contours in the R_{b}^0-R_{c}^0 plane derived from the LEP+SLD data, corresponding to 68% and 95% confidence levels assuming Gaussian systematic errors. The Standard Model prediction for $m_{\mathrm{t}} = 175.6 \pm 5.5$ GeV is also shown. The arrow points in the direction of increasing values of m_{t}.

5 The Hadronic Charge Asymmetry $\langle Q_{\mathrm{FB}} \rangle$

Updates with respect to last year:
L3 has a new preliminary result based on 1991-1994 data.

The LEP experiments ALEPH [53–55], DELPHI [56, 57], L3 [58] and OPAL [59, 60] have provided measurements of the hadronic charge asymmetry based on the mean difference in jet charges measured in the forward and backward event hemispheres, $\langle Q_{\mathrm{FB}} \rangle$. DELPHI has also provided a related measurement of the total charge asymmetry by making a charge assignment on an event-by-event basis and performing a likelihood fit [56]. The experimental values quoted for the average forward-backward charge difference, $\langle Q_{\mathrm{FB}} \rangle$, cannot be directly compared as some of them include detector dependent effects such as acceptances and efficiencies. Therefore the effective electroweak mixing angle, $\sin^2\theta_{\mathrm{eff}}^{\mathrm{lept}}$, as defined in Section 7.3, is used as a means of combining the experimental results summarised in Table 19.

Experiment		$\sin^2\theta_{\mathrm{eff}}^{\mathrm{lept}}$
ALEPH	(90-94), final	$0.2322 \pm 0.0008 \pm 0.0011$
DELPHI	(91-94), prel.	$0.2311 \pm 0.0010 \pm 0.0014$
L3	(91-94), prel.	$0.2336 \pm 0.0013 \pm 0.0014$
OPAL	(91-94), prel.	$0.2326 \pm 0.0012 \pm 0.0013$
LEP Average		0.2322 ± 0.0010

Table 19: Summary of the determination of $\sin^2\theta_{\mathrm{eff}}^{\mathrm{lept}}$ from inclusive hadronic charge asymmetries at LEP. For each experiment, the first error is statistical and the second systematic. The latter is dominated by fragmentation and decay modelling uncertainties.

The dominant source of systematic error arises from the modelling of the charge flow in the fragmentation process for each flavour. All experiments measure the required charge properties for $\mathrm{Z} \to \mathrm{b\overline{b}}$ events from the data. ALEPH also determines the charm charge properties from the data. The fragmentation model implemented in the JETSET Monte-Carlo program [61] is used by all experiments as reference; the one of the HERWIG Monte-Carlo program [62] is used for comparison. The JETSET fragmentation parameters are varied to estimate the systematic errors. The central values chosen by the experiments for these parameters are, however, not the same. The degree of correlation between the fragmentation uncertainties for the different experiments requires further investigation. The smaller of the two fragmentation errors in any pair of results is treated as common to both. The present average of $\sin^2\theta_{\mathrm{eff}}^{\mathrm{lept}}$ from $\langle Q_{\mathrm{FB}} \rangle$ and its associated error are not very sensitive to the treatment of common uncertainties. The ambiguities due to QCD corrections may cause changes in the derived value of $\sin^2\theta_{\mathrm{eff}}^{\mathrm{lept}}$. These are, however, well below the fragmentation uncertainties and experimental errors. The effect of fully correlating the estimated systematic uncertainties from this source between the experiments has a negligible effect upon the average and its error.

There is also some correlation between these results and those for $A_{\mathrm{FB}}^{\mathrm{b\bar{b}}}$ using jet charges. The dominant source of correlation is again through uncertainties in the fragmentation and decay models used. The typical correlation between the derived values of $\sin^2\theta_{\mathrm{eff}}^{\mathrm{lept}}$ between the $\langle Q_{\mathrm{FB}} \rangle$ and the $A_{\mathrm{FB}}^{\mathrm{b\bar{b}}}$ jet charge measurement has been estimated to be between 20% and 25%. This leads to only a small change in the relative weights for the $A_{\mathrm{FB}}^{\mathrm{b\bar{b}}}$ and $\langle Q_{\mathrm{FB}} \rangle$ results when averaging their $\sin^2\theta_{\mathrm{eff}}^{\mathrm{lept}}$ values (Section 7.3). Furthermore, the jet charge method contributes at most half of the weight of the $A_{\mathrm{FB}}^{\mathrm{b\bar{b}}}$ measurement. Thus, the correlation between $\langle Q_{\mathrm{FB}} \rangle$ and $A_{\mathrm{FB}}^{\mathrm{b\bar{b}}}$ from jet charge will have little impact on the overall Standard Model fit, and is neglected at present.

6 Measurement of W-Boson Properties at LEP-II

Updates with respect to last year:
This is a new section.

In 1996 the energy of LEP was increased in two steps to 161 GeV and 172 GeV, allowing the production of pairs of W bosons at LEP. The data recorded at 161 GeV, which is just above the pair production threshold, can be used to determine the W mass by comparing the measured cross-section with the predicted cross-section behaviour. At higher energies, the mass can be determined by directly reconstructing the decay products of the W boson. Thus, in 1996 the LEP collaborations were able to determine the W mass using two independent methods.

In the first run, at 161 GeV, each experiment accumulated a total luminosity of approximately 10 pb^{-1}. The final W pair cross-sections determined by the four LEP experiments [63–66] are shown in Table 20.

Experiment	$\sigma_{\mathrm{W^+W^-}}$ [pb]	Symmetrized stat. error
ALEPH	$4.23 \pm 0.73 \pm 0.19$	0.71
DELPHI	$3.67^{+0.97}_{-0.85} \pm 0.19$	0.91
L3	$2.89^{+0.81}_{-0.70} \pm 0.14$	0.92
OPAL	$3.62^{+0.93}_{-0.82} \pm 0.16$	0.88
LEP Average	3.69 ± 0.45	

Table 20: The $\mathrm{W^+W^-}$ cross-sections measured at 161 GeV. These results are all final.

These measurements have been corrected by the experiments to correspond to the set of three double-resonant Feynman diagrams (CC03 [67]). Because of the low statistics (each experiment recorded only about 30 W pair events), the errors have been determined using Poisson statistics. To ease the determination of the average W-pair cross-section, the experiments have also provided a symmetrized statistical error based on the number of expected events, given the world average W mass of 80.36 GeV [68]. This error is also shown in the table. The LEP average W-pair cross-section is

$$\sigma_{\mathrm{W^+W^-}} = 3.69 \pm 0.45 \text{ pb}, \tag{26}$$

where the smallest quoted systematic error (0.14 pb) has been taken as 100% correlated between experiments. The χ^2 per degree of freedom is 1.3/3. The LEP centre-of-mass energy averaged over the 4 experiments is determined to be 161.33 ± 0.05 [69]. Using the GENTLE [70] program and assuming the Standard Model couplings of the W boson, the predicted cross-section as a function of the W mass is calculated and is shown in Figure 4. The W mass is determined to be:

$$m_{\mathrm{W}} = 80.40^{+0.22}_{-0.21} \pm 0.03 \text{ GeV}, \tag{27}$$

where the first error is experimental, and the second error is due to the LEP energy calibration. Approximately 70 MeV of the experimental error is due to common systematics.

Each experiment also accumulated 10 pb^{-1} at the higher energy of 172 GeV. The cross-section at 172 GeV is more than a factor 3 larger than at 161 GeV, so that each experiment recorded approximately 100 W pair events at this energy. To determine the W mass, the experiments fit the reconstructed invariant mass distributions [71–74]. The results are shown in Table 21.

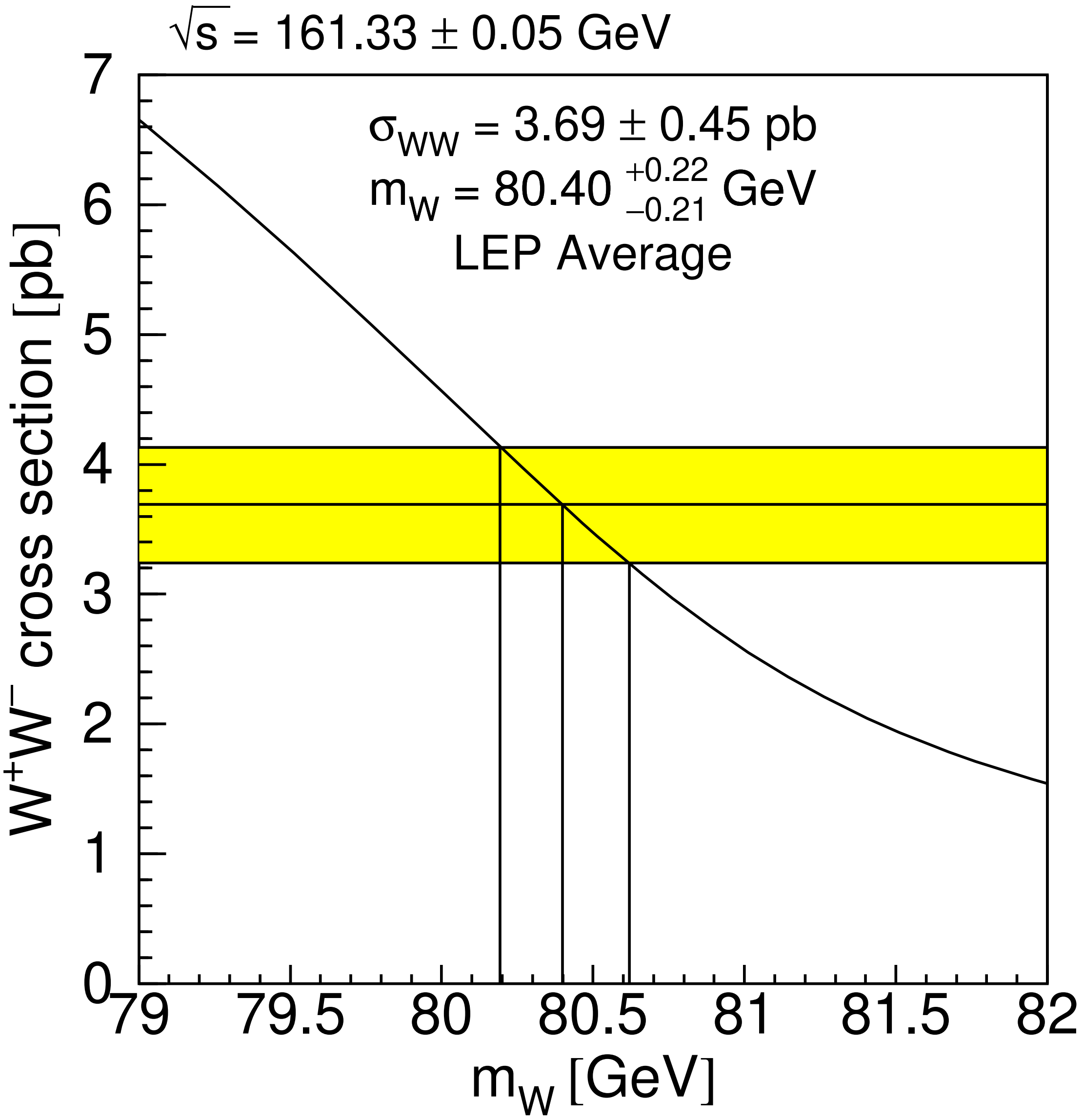

Figure 4: The cross-section of the process $e^+e^- \to W^+W^-$ as a function of the W mass. The horizontal band shows the cross-section measurement with its error. The curve shows the Standard Model prediction.

Experiment	m_W (GeV)	
	$q\bar{q}\ell\nu$	$q\bar{q}q\bar{q}$
ALEPH (prel.)	$80.38 \pm 0.43 \pm 0.12$	$81.30 \pm 0.47 \pm 0.10$
DELPHI (prel.)	$80.51 \pm 0.57 \pm 0.06$	$79.90 \pm 0.59 \pm 0.12$
L3 (final)	$80.42 \pm 0.54 \pm 0.08$	$80.91 \pm 0.42 \pm 0.13$
OPAL (prel.)	$80.53 \pm 0.41 \pm 0.10$	$80.08 \pm 0.44 \pm 0.15$
LEP Average	80.46 ± 0.24	80.62 ± 0.26

Table 21: The measurements of m_W at 172 GeV in the $q\bar{q}\ell\nu$ and $q\bar{q}q\bar{q}$ channels. The χ^2/d.o.f. for the two combinations is 0.1/3 and 5.4/3.

The systematic errors quoted include experimental sources, the LEP energy uncertainty of 30 MeV, and in the case of the $q\bar{q}q\bar{q}$ channel the potential effects of reinteraction of the hadronic decay products of the W's ("colour reconnection" and "Bose-Einstein correlations"). This last effect has been estimated by ALEPH to be 60 MeV. DELPHI, L3, and OPAL use 100 MeV as quoted in Reference 75. In the combination, the last two effects have been treated as 100% correlated between the experiments. At the current level of statistics, the mass determined from semi-leptonic decays and that from hadronic decays are consistent, and are combined to obtain:

$$m_{\mathrm{W}} = 80.53 \pm 0.17 \pm 0.05 \text{ GeV}. \tag{28}$$

Combining this last result with that of the 161 GeV data yields

$$m_{\mathrm{W}} = 80.48 \pm 0.13 \pm 0.04 \text{ GeV} \tag{29}$$

as the current LEP-II average W mass.

In addition, the LEP experiments have determined the W pair cross-section at 172 GeV, and have used the data at 161 and 172 GeV to determine the W decay branching ratios [71–74]. These results are summarised in Tables 22 and 23 and and in Figure 5.

Experiment	$\sigma_{\mathrm{W^+W^-}}$ (pb)
ALEPH (final)	$11.7 \pm 1.2 \pm 0.3$
DELPHI (prel.)	$11.58^{+1.44}_{-1.35} \pm 0.32$
L3 (final)	$12.27^{+1.41}_{-1.32} \pm 0.23$
OPAL (final)	$12.3 \pm 1.3 \pm 0.3$
LEP Average	12.0 ± 0.7

Table 22: The measurements of the W pair cross-sections at 172 GeV.

Experiment	Br(W→eν)	Br(W→ $\mu\nu$)	Br(W→ $\tau\nu$)	Br(W→hadrons)
ALEPH (final)	9.7 ± 2.2	11.2 ± 2.2	11.3 ± 2.9	67.7 ± 3.2
DELPHI (prel.)	10.2 ± 3.8	10.7 ± 3.2	13.4 ± 5.0	66.0 ± 3.7
L3 (final)	16.5 ± 3.7	8.4 ± 2.8	10.9 ± 4.2	64.2 ± 3.7
OPAL (final)	9.8 ± 2.1	7.3 ± 1.8	14.0 ± 2.9	69.8 ± 3.2
LEP Average	10.8 ± 1.3	9.2 ± 1.1	12.7 ± 1.7	67.2 ± 1.7

Table 23: The measurements of the W decay branching ratios in percent. The hadronic branching ratio is determined assuming lepton universality. There are large correlations between the individual leptonic branching ratios, which have been taken into account in determining the hadronic branching ratio.

The $\mathrm{W^+W^-}$ production process also involves the triple-gauge-boson vertices between the $\mathrm{W^+W^-}$ and the Z or photon. The measurement of these triple gauge boson couplings (TGC's) and the search for possible anomalous values is an additional physics goal at LEP-II.

The LEP experiments have presented measurements of anomalous coupling parameters [76–79] using the 1996 data set. Other experiments also measure TGC's and at present the most precise results come from the Tevatron experiments CDF [80] and DØ [81] based upon an analysis of nearly 100 pb^{-1} per experiment.

The parameterisation of anomalous TGC's is described in References 82–87. The most general Lorentz invariant Lagrangian which describes the triple gauge boson interaction has fourteen independent terms, seven describing the WWγ vertex and seven describing the WWZ vertex. Assuming

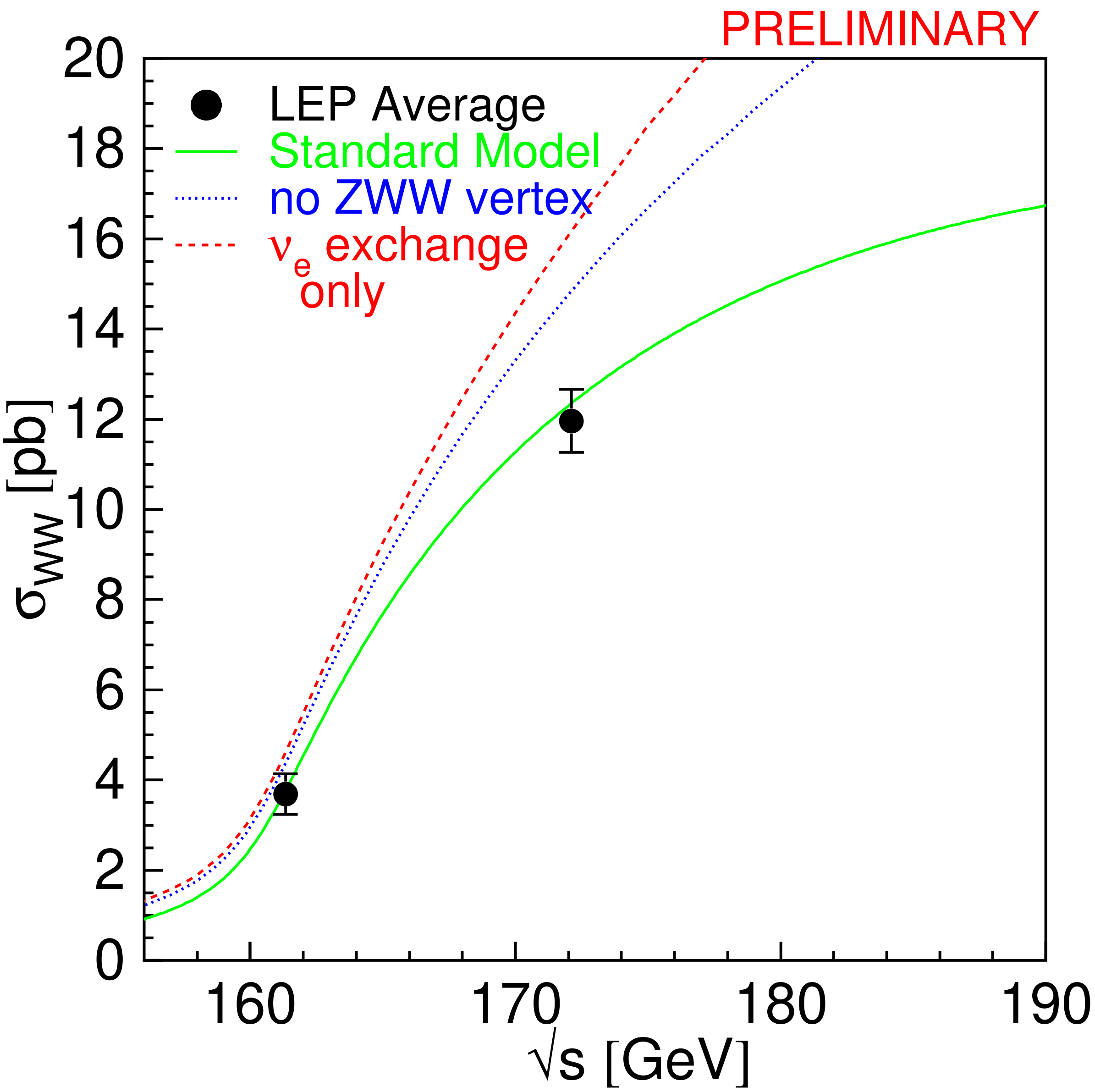

Figure 5: The W-pair cross-section as a function of the centre of mass energy. The data points are the LEP averages. Also shown is the Standard Model prediction (solid line), and for comparison the cross-section if the ZWW coupling did not exist (dotted line), or if only the t-channel ν_{e} exchange diagram existed (dashed line).

electromagnetic gauge invariance and C and P conservation the number of parameters reduces to five. One common set is $\{g_1^{\mathrm{z}}, \kappa_{\mathrm{z}}, \kappa_\gamma, \lambda_{\mathrm{z}}, \lambda_\gamma\}$ [83] where $g_1^{\mathrm{z}} = \kappa_{\mathrm{z}} = \kappa_\gamma = 1$ and $\lambda_{\mathrm{z}} = \lambda_\gamma = 0$ in the Standard Model.

Different sets of parameters have also been proposed which are motivated by SU(2)×U(1) gauge invariance and constraints arising from precise measurements at LEP-I. One such set [87] is:

$$\alpha_{W\phi} \equiv \Delta g_1^{\mathrm{z}} \cos^2\theta_{\mathrm{W}} \tag{30}$$

$$\alpha_W \equiv \lambda_\gamma \tag{31}$$

$$\alpha_{B\phi} \equiv \Delta\kappa_\gamma - \Delta g_1^{\mathrm{z}} \cos^2\theta_{\mathrm{W}} \tag{32}$$

with the constraints that $\Delta\kappa_z = -\Delta\kappa_\gamma \tan^2\theta_w + \Delta g_1^z$ and $\lambda_z = \lambda_\gamma$. The Δ indicates the deviation of the respective quantity from its Standard Model value and θ_w is the weak mixing angle. The α parameters are zero in the Standard Model.

Each of the experiments has measured several of the many possible TGC parameters and References 76–79 should be consulted for the complete set of measurements in each case. All experiments have measured at least $\alpha_{W\phi}$, α_W and $\alpha_{B\phi}$ in single-parameter fits. Here combined results for these three parameters are presented.

Anomalous TGC's can affect both the total production cross-section and the shape of the differential cross-section as a function of the W^- production angle. The relative contributions of each helicity state of the W bosons are also changed, which in turn affects the distributions of their decay products. The analyses presented by each experiment make use of different combinations of each of these quantities, and of different decay modes of the WW system. The reader should consult the References 76–79 for details. In general, however, all analyses use at least the expected variations of the total production cross-section and the W^- production angle.

The results of fits to $\alpha_{W\phi}$, α_W and $\alpha_{B\phi}$, assuming in each case that the other two anomalous couplings are zero, are shown in Table 24 for each experiment and for the LEP combined results. The combination has been performed by adding the log-likelihood curves supplied by each experiment. For this combination, the correlated systematic errors have been estimated to be small, and have been neglected. The results are consistent with the Standard Model expectations.

Experiment	$\alpha_{W\phi}$	α_W	$\alpha_{B\phi}$
ALEPH [76]	$-0.14^{+0.29}_{-0.28}$	$0.06^{+0.59}_{-0.55}$	$1.01^{+0.91}_{-2.17}$
DELPHI [77]	$0.24^{+0.26}_{-0.27}$	$0.14^{+0.46}_{-0.47}$	$0.40^{+0.71}_{-0.92}$
L3 [78]	$0.04^{+0.43}_{-0.35}$	$0.22^{+0.59}_{-0.61}$	$0.07^{+1.77}_{-1.16}$
OPAL [79]	$-0.08^{+0.30}_{-0.27}$	$0.18^{+0.54}_{-0.52}$	$0.35^{+1.34}_{-1.14}$
LEP 1-sigma	$0.02^{+0.16}_{-0.15}$	$0.15^{+0.27}_{-0.27}$	$0.45^{+0.56}_{-0.67}$
LEP 95% CL	$[-0.28,\ \ 0.33]$	$[-0.37,\ \ 0.68]$	$[-0.81,\ \ 1.50]$

Table 24: The measured values and one standard deviation errors obtained by the four LEP experiments for the anomalous TGC parameters. Both statistical and systematic errors are included. For the combined LEP results, both the central value with the one standard deviation error as well as the 95% confidence level interval are shown. For the fits to each coupling, the values of the other two are set to zero.

7 Interpretation of Results

Updates with respect to last year:
The results of the Standard Model fit with the Higgs mass as a free parameter are presented. A new fit is performed, where all data except the direct measurements of m_{W} and m_{t} are included.

7.1 The Coupling Parameters $\mathcal{A}_{\mathrm{f}}$

The coupling parameters $\mathcal{A}_{\mathrm{f}}$ are defined in terms of the effective vector and axial-vector neutral current couplings of fermions (Equation (4)). The LEP measurements of the forward-backward asymmetries of charged leptons (Section 2) and b and c quarks (Section 4) determine the products $A_{\mathrm{FB}}^{0,\mathrm{f}} = \frac{3}{4}\mathcal{A}_{\mathrm{e}}\mathcal{A}_{\mathrm{f}}$ (Equation (3)). The LEP measurements of the τ polarisation (Section 3), $\mathcal{P}_\tau(\cos\theta)$, determine $\mathcal{A}_\tau$ and $\mathcal{A}_{\mathrm{e}}$ separately (Equation (15)). The SLD collaboration measures the left-right asymmetry, A_{LR} [88], which determines the same quantity, $\mathcal{A}_{\mathrm{e}}$, as the τ polarisation. Both measurements have small systematic errors. The A_{LR} measurement benefits from a simple event production cross section counting with all $\mathrm{Z} \to$ hadrons events to achieve high statistical precision. Since there is no need for any event final state analysis beyond the event selection, the small total systematic error of 0.75%, one third of the statistical error, is basically the uncertainty in electron beam polarisation measurement only. Table 25 shows the results for the leptonic coupling parameter $\mathcal{A}_\ell$ and their combination assuming lepton universality.

Using the measurements of $\mathcal{A}_\ell$ one can extract $\mathcal{A}_{\mathrm{b}}$ and $\mathcal{A}_{\mathrm{c}}$ from the LEP measurements of the b and c quark asymmetries. The SLD measurements of the left-right forward-backward asymmetries for b and c quarks [88] are direct determinations of $\mathcal{A}_{\mathrm{b}}$ and $\mathcal{A}_{\mathrm{c}}$. Table 26 shows the results on the quark coupling parameters $\mathcal{A}_{\mathrm{b}}$ and $\mathcal{A}_{\mathrm{c}}$ derived from LEP or SLD measurements separately (Equations 24 and 25) and from the combination of LEP+SLD measurements (Equation 25). The LEP extracted values of $\mathcal{A}_{\mathrm{b}}$ and $\mathcal{A}_{\mathrm{c}}$ are in excellent agreement with the SLD measurements, and in reasonable

	$\mathcal{A}_\ell$	Cumulative Average	χ^2/d.o.f.
$A_{\mathrm{FB}}^{0,\ell}$	0.1510 ± 0.0044		
$\mathcal{P}_\tau(\cos\theta)$	0.1406 ± 0.0048	0.1461 ± 0.0033	2.5/1
A_{LR} (SLD)	0.1547 ± 0.0032	0.1505 ± 0.0023	6.0/2

Table 25: Determinations of the leptonic coupling parameter $\mathcal{A}_\ell$ assuming lepton universality. The second column lists the $\mathcal{A}_\ell$ values derived from the quantities listed in the first column. The third column contains the cumulative averages of these $\mathcal{A}_\ell$ results. The averages are derived assuming no correlations between the measurements. The χ^2 per degree of freedom for the cumulative averages is given in the last column.

	LEP ($\mathcal{A}_\ell = 0.1461 \pm 0.0033$)	SLD	LEP+SLD ($\mathcal{A}_\ell = 0.1505 \pm 0.0023$)
$\mathcal{A}_{\mathrm{b}}$	0.897 ± 0.030	0.900 ± 0.050	0.877 ± 0.023
$\mathcal{A}_{\mathrm{c}}$	0.674 ± 0.046	0.650 ± 0.058	0.653 ± 0.037

Table 26: Determinations of the quark coupling parameters $\mathcal{A}_{\mathrm{b}}$ and $\mathcal{A}_{\mathrm{c}}$ from LEP data alone (using the LEP average for $\mathcal{A}_\ell$), from SLD data alone, and from LEP+SLD data (using the LEP+SLD average for $\mathcal{A}_\ell$) assuming lepton universality.

agreement with the Standard Model predictions (0.935 and 0.668, respectively, see Table 29). However, the combination of LEP+SLD of $\mathcal{A}_{\mathrm{b}}$ is about 2.5 sigma below the Standard Model. This is due to three independent measurements: the LEP measurement of $A_{\mathrm{FB}}^{0,\mathrm{b}}$ is low compared with the Standard Model, the SLD measurement of $\mathcal{A}_{\mathrm{b}}$ is also slightly lower, and the SLD measurement of A_{LR} is high compared with the Standard Model.

7.2 The Effective Vector and Axial-Vector Coupling Constants

The partial widths of the Z into leptons and the lepton forward-backward asymmetries (Section 2), the τ polarisation and the τ polarisation asymmetry (Section 3) can be combined to determine the effective vector and axial-vector couplings for e, μ and τ. The asymmetries (Equations (3) and (15)) determine the ratio $g_{V\ell}/g_{A\ell}$ (Equation (4)), while the leptonic partial widths determine the sum of the squares of the couplings:

$$\Gamma_{\ell\ell} = \frac{G_{\mathrm{F}} m_{\mathrm{Z}}^3}{6\pi\sqrt{2}}(g_{V\ell}^2 + g_{A\ell}^2)(1+\delta_\ell^{QED}), \tag{33}$$

where $\delta_\ell^{QED} = 3q_\ell^2\alpha(m_{\mathrm{Z}}^2)/(4\pi)$ accounts for final state photonic corrections. Corrections due to lepton masses, neglected in Equation 33, are taken into account for the results presented below.

The averaged results for the effective lepton couplings are given in Table 27. Figure 6 shows the 68% probability contours in the $g_{A\ell}$-$g_{V\ell}$ plane. The signs of $g_{A\ell}$ and $g_{V\ell}$ are based on the convention $g_{A\mathrm{e}} < 0$. With this convention the signs of the couplings of all charged leptons follow from LEP data alone. For comparison, the $g_{V\ell}$-$g_{A\ell}$ relation following from the measurement of A_{LR} from SLD [88] is indicated as a band in the $g_{A\ell}$-$g_{V\ell}$-plane of Figure 6. It is consistent with the LEP data. The information on the leptonic couplings from LEP can therefore be combined with the A_{LR} measurement of SLD. The results for this combination are given in the right column of Table 27. The measured ratios of the e, μ and τ couplings provide a test of lepton universality and are also given in Table 27.

The neutrino couplings to the Z can be derived from the measured value of the invisible width of the Z, Γ_{inv} (see Table 9), attributing it exclusively to the decay into three identical neutrino generations ($\Gamma_{\mathrm{inv}} = 3\Gamma_{\nu\nu}$) and assuming $g_{A\nu} \equiv g_{V\nu} \equiv g_\nu$. The relative sign of g_ν is chosen to be in agreement with neutrino scattering data [89], resulting in $g_\nu = +0.50125 \pm 0.00092$.

7.3 The Effective Electroweak Mixing Angle $\sin^2\theta_{\mathrm{eff}}^{\mathrm{lept}}$

The asymmetry measurements from LEP can be combined into a single observable, the effective electroweak mixing angle, $\sin^2\theta_{\mathrm{eff}}^{\mathrm{lept}}$, defined as:

$$\sin^2\theta_{\mathrm{eff}}^{\mathrm{lept}} \equiv \frac{1}{4}\left(1 - \frac{g_{V\ell}}{g_{A\ell}}\right), \tag{34}$$

without making any strong model-specific assumptions.

For a combined average of $\sin^2\theta_{\mathrm{eff}}^{\mathrm{lept}}$ from $A_{\mathrm{FB}}^{0,\ell}$, $\mathcal{A}_\tau$ and $\mathcal{A}_{\mathrm{e}}$ only the assumption of lepton universality, already inherent in the definition of $\sin^2\theta_{\mathrm{eff}}^{\mathrm{lept}}$, is needed. We can also include the hadronic forward-backward asymmetries if we assume the hadronic couplings to be given by the Standard Model. This is justified within the Standard Model as the hadronic asymmetries $A_{\mathrm{FB}}^{0,\mathrm{b}}$ and $A_{\mathrm{FB}}^{0,\mathrm{c}}$ have a reduced sensitivity to weak corrections and to those corrections particular to the hadronic vertex. The results

	Without Lepton Universality: LEP	LEP+SLD
$g_{V\mathrm{e}}$	-0.0367 ± 0.0015	-0.03844 ± 0.00071
$g_{V\mu}$	-0.0374 ± 0.0036	-0.0358 ± 0.0032
$g_{V\tau}$	-0.0367 ± 0.0015	-0.0365 ± 0.0015
$g_{A\mathrm{e}}$	-0.50123 ± 0.00044	-0.50111 ± 0.00043
$g_{A\mu}$	-0.50087 ± 0.00066	-0.50098 ± 0.00065
$g_{A\tau}$	-0.50102 ± 0.00074	-0.50103 ± 0.00074
	Ratios of couplings: LEP	LEP+SLD
$g_{V\mu}/g_{V\mathrm{e}}$	1.02 ± 0.12	0.932 ± 0.087
$g_{V\tau}/g_{V\mathrm{e}}$	0.998 ± 0.060	0.949 ± 0.044
$g_{A\mu}/g_{A\mathrm{e}}$	0.9993 ± 0.0017	0.9997 ± 0.0016
$g_{A\tau}/g_{A\mathrm{e}}$	0.9996 ± 0.0018	0.9998 ± 0.0018
	With Lepton Universality: LEP	LEP+SLD
$g_{V\ell}$	-0.03681 ± 0.00085	-0.03793 ± 0.00058
$g_{A\ell}$	-0.50112 ± 0.00032	-0.50103 ± 0.00031
g_{ν}	$+0.50125 \pm 0.00092$	$+0.50125 \pm 0.00092$

Table 27: Results for the effective vector and axial-vector couplings derived from the combined LEP data without and with the assumption of lepton universality. For the right column the SLD measurement of A_{LR} is also included.

of these determinations of $\sin^2\theta_{\mathrm{eff}}^{\mathrm{lept}}$ and their combination are shown in Table 28 and in Figure 7. Also the measurement of the left-right asymmetry, A_{LR}, from SLD [88] is given. Compared with the results presented in our previous note [1], the χ^2 of the average of all determinations has decreased by 0.3.

	$\sin^2\theta_{\mathrm{eff}}^{\mathrm{lept}}$	Average by Group of Observations	Cumulative Average	χ^2/d.o.f.
$A_{\mathrm{FB}}^{0,\ell}$	0.23102 ± 0.00056			
$\mathcal{A}_{\tau}$	0.23228 ± 0.00081			
$\mathcal{A}_{\mathrm{e}}$	0.23243 ± 0.00093	0.23162 ± 0.00041	0.23162 ± 0.00041	2.6/2
$A_{\mathrm{FB}}^{0,\mathrm{b}}$	0.23236 ± 0.00043			
$A_{\mathrm{FB}}^{0,\mathrm{c}}$	0.2314 ± 0.0011	0.23223 ± 0.00040	0.23194 ± 0.00029	4.3/4
$\langle Q_{\mathrm{FB}} \rangle$	0.2322 ± 0.0010	0.2322 ± 0.0010	0.23196 ± 0.00028	4.4/5
A_{LR} (SLD)	0.23055 ± 0.00041	0.23055 ± 0.00041	0.23152 ± 0.00023	12.5/6

Table 28: Determinations of $\sin^2\theta_{\mathrm{eff}}^{\mathrm{lept}}$ from asymmetries. Averages are obtained as weighted averages assuming no correlations. The second column lists the $\sin^2\theta_{\mathrm{eff}}^{\mathrm{lept}}$ values derived from the quantities listed in the first column. The third column contains the averages of these numbers by groups of observations, where the groups are separated by the horizontal lines. The fourth column shows the cumulative averages. The χ^2 per degree of freedom for the cumulative averages is also given.

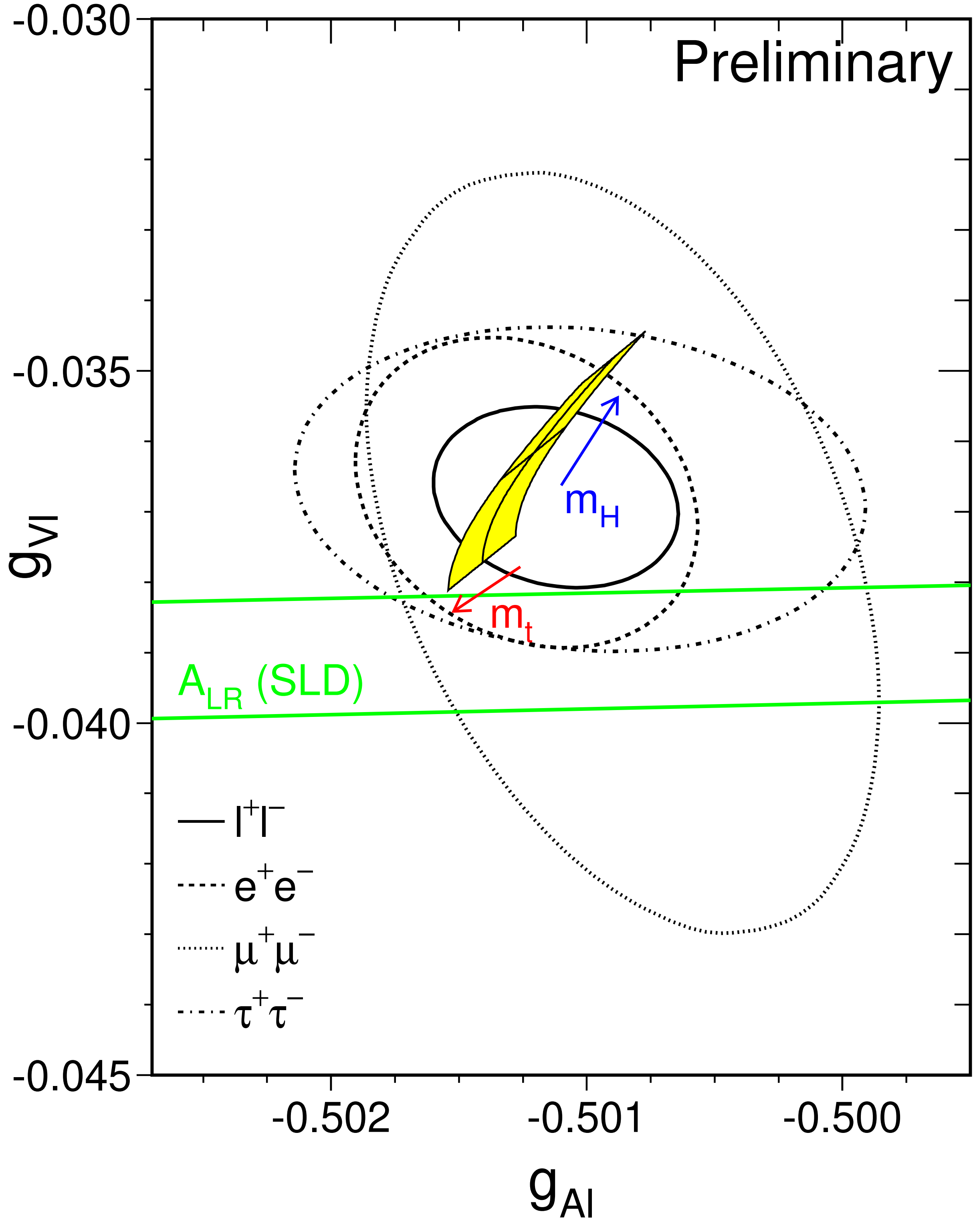

Figure 6: Contours of 68% probability in the $g_{V\ell}$-$g_{A\ell}$ plane from LEP measurements. The solid contour results from a fit assuming lepton universality. Also shown is the one standard deviation band resulting from the $A_{\rm LR}$ measurement of SLD. The shaded region corresponds to the Standard Model prediction for $m_{\rm t} = 175.6 \pm 5.5$ GeV and $m_{\rm H} = 300^{+700}_{-240}$ GeV. The arrows point in the direction of increasing values of $m_{\rm t}$ and $m_{\rm H}$.

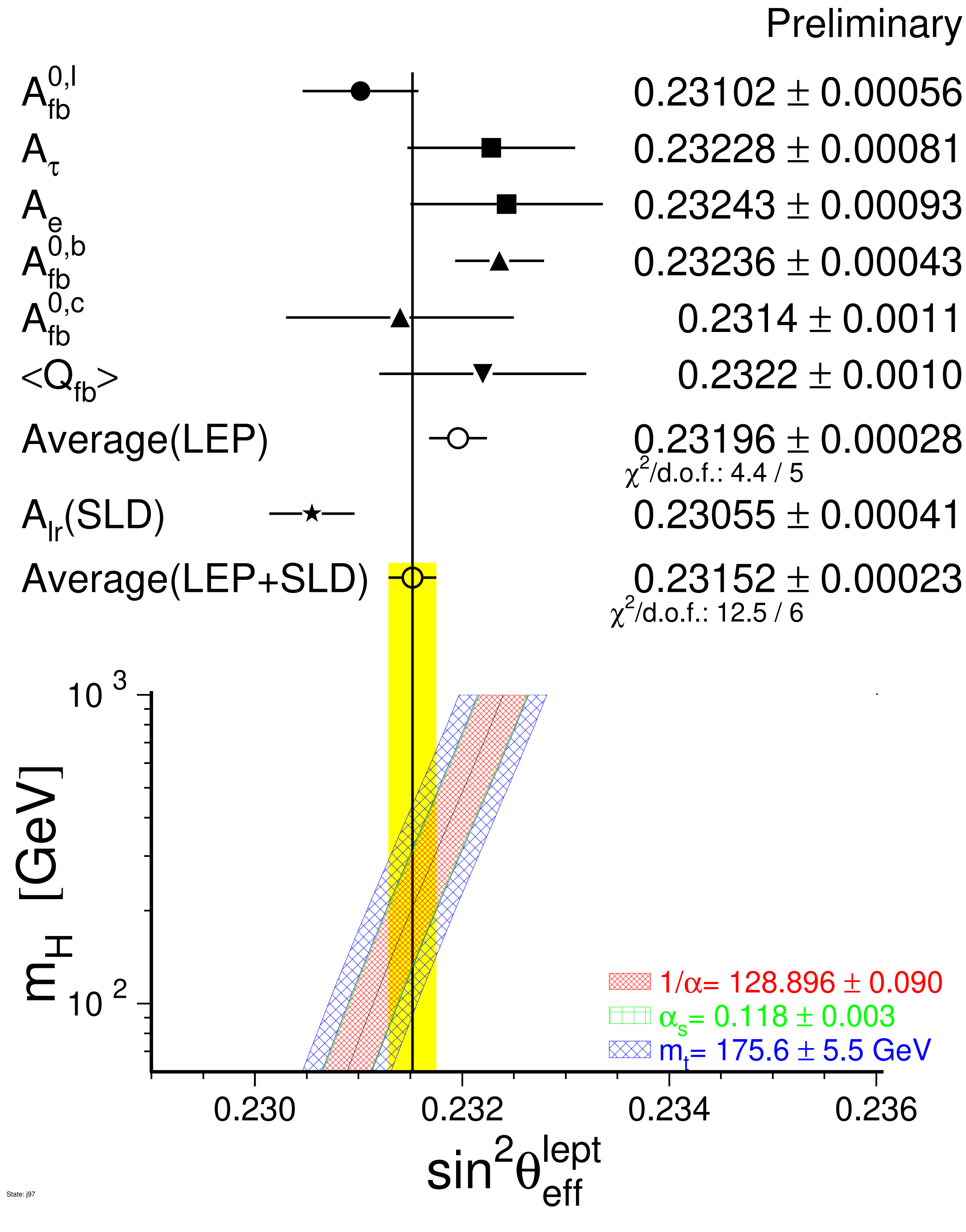

Figure 7: Comparison of several determinations of $\sin^2\theta_{\rm eff}^{\rm lept}$ from asymmetries. Also shown is the prediction of the Standard Model as a function of $m_{\rm H}$. The width of the Standard Model band is due to the uncertainties in $\alpha(m_{\rm Z}^2)$, $\alpha_s(m_{\rm Z}^2)$ and $m_{\rm t}$. The total width of the band is the linear sum of these effects.

7.4 Number of Neutrino Species

An important aspect of our measurement concerns the information related to Z decays into invisible channels. Using the results of Tables 7 and 8, the ratio of the Z decay width into invisible particles and the leptonic decay width is determined:

$$\Gamma_{\text{inv}}/\Gamma_{\ell\ell} \;=\; 5.960 \pm 0.022\,. \tag{35}$$

The Standard Model value for the ratio of the partial widths to neutrinos and charged leptons is:

$$(\Gamma_{\nu\nu}/\Gamma_{\ell\ell})_{\text{SM}} \;=\; 1.991 \pm 0.001\,. \tag{36}$$

The central value is evaluated for $m_{\text{Z}} = 91.1867$ GeV, $m_{\text{t}} = 175.6$ GeV, $m_{\text{H}} = 300$ GeV and the error quoted accounts for a variation of m_{t} in the range $m_{\text{t}} = 175.6 \pm 5.5$ GeV and a variation of m_{H} in the range 60 GeV $\leq m_{\text{H}} \leq$ 1000 GeV. The number of light neutrino species is given by the ratio of the two expressions listed above:

$$N_\nu \;=\; 2.993 \pm 0.011\,. \tag{37}$$

Alternatively, one can assume 3 neutrino species and determine the width from additional invisible decays of the Z. This yields

$$\Delta\Gamma_{\text{inv}} \;=\; -1.1 \pm 1.8 \text{ MeV}. \tag{38}$$

The negative additional width results from a measured total width that is slightly below the Standard Model expectation. This is also seen in the number of neutrino families which is slightly lower than 3. If a conservative approach is taken to limit the result to only positive values of $\Delta\Gamma_{\text{inv}}$, then the 95% CL upper limit on additional invisible decays of the Z is

$$\Delta\Gamma_{\text{inv}} \;<\; 2.9 \text{ MeV}. \tag{39}$$

7.5 Constraints on the Standard Model

The precise electroweak measurements performed at LEP can be used to check the validity of the Standard Model and, within its framework, to infer valuable information about its fundamental parameters. The accuracy of the measurements makes them sensitive to the top-quark mass, m_{t}, and to the mass of the Higgs boson, m_{H}, through loop corrections. While the leading m_{t} dependence is quadratic, the leading m_{H} dependence is logarithmic. Therefore, the inferred constraints on m_{H} are not very strong.

The LEP measurements used are summarised in Table 29a together with the Standard Model predictions. Also shown are the results from the SLD collaboration [88] as well as measurements of m_{W} from UA2 [90], CDF [91, 92], and DØ [93][5], measurements of the neutrino neutral to charged current ratios from CDHS [95], CHARM [96] and CCFR [97], and the measurements of the top quark mass by CDF [98] and DØ [99][6]. In addition, the determination of the electromagnetic coupling constant, $\alpha(m_{\text{Z}}^2)$, which is used in the fits, is shown. An additional input parameter, not shown in the table, is the Fermi constant, G_F, determined from the μ lifetime, $G_F = 1.16639 \times 10^{-5}\text{GeV}^{-2}$ [101].

Detailed studies of the theoretical uncertainties in the Standard Model predictions due to missing higher-order electroweak corrections and their interplay with QCD corrections have been carried out in

[5] See Reference 94 for a combination of these m_{W} measurements.

[6] Results on m_{t} from CDF and DØ are averaged [100] assuming a common systematic error of 3 GeV.

		Measurement with Total Error	Systematic Error	Standard Model	Pull
	$\alpha(m_Z^2)^{-1}$ [102]	128.896 ± 0.090	0.083	128.898	0.0
a)	LEP				
	line-shape and				
	lepton asymmetries:				
	m_Z [GeV]	91.1867 ± 0.0020	$^{(a)}0.0015$	91.1866	0.0
	Γ_Z [GeV]	2.4948 ± 0.0025	$^{(a)}0.0015$	2.4966	-0.7
	σ_h^0 [nb]	41.486 ± 0.053	0.052	41.467	0.4
	R_ℓ	20.775 ± 0.027	0.024	20.756	0.7
	$A_{FB}^{0,\ell}$	0.0171 ± 0.0010	0.0007	0.0162	0.9
	+ correlation matrix Table 8				
	τ polarisation:				
	$\mathcal{A}_\tau$	0.1411 ± 0.0064	0.0040	0.1470	-0.9
	$\mathcal{A}_e$	0.1399 ± 0.0073	0.0020	0.1470	-1.0
	$q\overline{q}$ charge asymmetry:				
	$\sin^2\theta_{eff}^{lept}$ ($\langle Q_{FB}\rangle$)	0.2322 ± 0.0010	0.0008	0.23152	0.7
	m_W [GeV]	80.48 ± 0.14	0.05	80.375	0.8
b)	SLD [88]				
	$\sin^2\theta_{eff}^{lept}$ (A_{LR})	0.23055 ± 0.00041	0.00014	0.23152	-2.4
c)	LEP and SLD Heavy Flavour				
	R_b^0	0.2170 ± 0.0009	0.0007	0.2158	1.3
	R_c^0	0.1734 ± 0.0048	0.0038	0.1723	0.2
	$A_{FB}^{0,b}$	0.0984 ± 0.0024	0.0010	0.1031	-2.0
	$A_{FB}^{0,c}$	0.0741 ± 0.0048	0.0025	0.0736	0.1
	$\mathcal{A}_b$	0.900 ± 0.050	0.031	0.935	-0.7
	$\mathcal{A}_c$	0.650 ± 0.058	0.029	0.668	-0.3
	+ correlation matrix Table 18				
d)	$p\overline{p}$ and νN				
	m_W [GeV] ($p\overline{p}$ [94])	80.41 ± 0.09	0.07	80.375	0.4
	$1 - m_W^2/m_Z^2$ (νN [95–97])	0.2254 ± 0.0037	0.0023	0.2231	0.6
	m_t [GeV] ($p\overline{p}$ [98–100])	175.6 ± 5.5	4.2	173.1	0.4

Table 29: Summary of measurements included in the combined analysis of Standard Model parameters. Section a) summarises LEP averages, Section b) SLD results ($\sin^2\theta_{eff}^{lept}$ includes A_{LR} and the polarised lepton asymmetries), Section c) the LEP and SLD heavy flavour results and Section d) electroweak measurements from $p\overline{p}$ colliders and νN scattering. The total errors in column 2 include the systematic errors listed in column 3. The determination of the systematic part of each error is approximate. The Standard Model results in column 4 and the pulls (difference between measurement and fit in units of the total measurement error) in column 5 are derived from the Standard Model fit including all data (Table 30, column 4) with the Higgs mass treated as a free parameter.

$^{(a)}$The systematic errors on m_Z and Γ_Z contain the errors arising from the uncertainties in the LEP energy only.

the working group on 'Precision calculations for the Z resonance' [103]. Theoretical uncertainties are evaluated by comparing different but, within our present knowledge, equivalent treatments of aspects such as resummation techniques, momentum transfer scales for vertex corrections and factorisation schemes. The impact of these intrinsic theoretical uncertainties on m_{t} and $\alpha_s(m_{\mathrm{Z}}^2)$ has been estimated by repeating the Standard Model fits in this Section using several combinations of options which were implemented in the electroweak libraries used [104] for the study performed in Reference 103. As a result the maximal variations of the central values of the fitted parameters correspond to an additional theoretical error of less than 1 GeV on m_{t}, less than 0.001 on $\alpha_s(m_{\mathrm{Z}}^2)$ and 0.1 on $\log(m_{\mathrm{H}})$. Although the theoretical error on $\log(m_{\mathrm{H}})$ is still smaller than the experimental error, it is relatively more important than the theoretical error on m_{t} or $\alpha_s(m_{\mathrm{Z}}^2)$. The theoretical error on $\alpha_s(m_{\mathrm{Z}}^2)$ covers missing higher-order electroweak corrections and uncertainties in the interplay of electroweak and QCD corrections. The effect of missing higher-order QCD corrections on $\alpha_s(m_{\mathrm{Z}}^2)$ has been estimated to be about 0.002 [105]. A discussion of theoretical uncertainties in the determination of α_s can be found in References 103 and 105. Recently, new calculations of higher-order corrections have become available [106]. However, as some of these calculations are not yet complete, and are not yet fully incorporated in the electroweak libraries, the results quoted here are still based on Ref. [104]. In addition, all theoretical errors discussed in this paragraph have been neglected for the results presented in Table 30.

At present the impact of theoretical uncertainties on the determination of m_{t} from precise electroweak measurements is small compared with the error due to the uncertainty in the value of $\alpha(m_{\mathrm{Z}}^2)$. The uncertainty in $\alpha(m_{\mathrm{Z}}^2)$ arises from the contribution of light quarks to the photon vacuum polarisation. Recently there have been several reevaluations of $\alpha(m_{\mathrm{Z}}^2)$ [102,107–110]. For the results presented in this Section, a value of $\alpha(m_{\mathrm{Z}}^2) = 1/(128.896 \pm 0.090)$ [102] is used. This uncertainty causes an error of 0.00023 on the Standard Model prediction of $\sin^2\theta_{\mathrm{eff}}^{\mathrm{lept}}$, an error of 1 GeV on m_{t}, and 0.2 on $\log(m_{\mathrm{H}})$, which are included in the results. The effect on the Standard Model prediction for $\Gamma_{\ell\ell}$ is negligible. The $\alpha_s(m_{\mathrm{Z}}^2)$ values for the Standard Model fits presented in this Section are stable against a variation of $\alpha(m_{\mathrm{Z}}^2)$ in the interval quoted.

Figure 8 shows a comparison of the leptonic partial width from LEP (Table 9) and the effective electroweak mixing angle from asymmetries measured at LEP and SLD (Table 28), with the Standard Model. Good agreement with the Standard Model prediction is observed. The star shows the prediction if, among the electroweak radiative corrections only the photon vacuum polarisation is included, showing evidence that LEP+SLD data are sensitive to electroweak corrections. Note that the error due to the uncertainty on $\alpha(m_{\mathrm{Z}}^2)$ (shown as the length of the arrow attached to the star) is as large as the experimental error on $\sin^2\theta_{\mathrm{eff}}^{\mathrm{lept}}$ from LEP and SLD. This underlines the growing importance of a precise measurement of $\sigma(\mathrm{e^+e^-} \to \mathrm{hadrons})$ at low centre-of-mass energies.

The value of $\alpha_s(m_{\mathrm{Z}}^2)$ derived from an analysis of electroweak precision tests within the Standard Model framework depends essentially on R_ℓ, Γ_{Z} and σ_{h}^0. The result is in very good agreement with the world average ($\alpha_s(m_{\mathrm{Z}}^2) = 0.118 \pm 0.003$ [101]) and is of similar precision. The strong coupling constant can also be determined from the parameter R_ℓ alone. For $m_{\mathrm{Z}} = 91.1867$ GeV, and imposing $m_{\mathrm{t}} = 175.6 \pm 5.5$ GeV as a constraint, $\alpha_s = 0.124 \pm 0.004 \pm 0.002$ is obtained, where the second error accounts for the variation of the result when varying m_{H} in the range 60 GeV $\leq m_{\mathrm{H}} \leq$ 1000 GeV.

To test the agreement between the LEP data and the Standard Model, we first perform a fit to the data (including the LEP-II m_{W} determination) leaving the top quark mass and the Higgs mass as free parameters. The result is shown in Table 30, column 2. This fit shows that the LEP data prefer a light top quark and a light Higgs, albeit with very large errors. The strongly asymmetric errors on m_{H} are due to the fact that to first order, the radiative corrections in the Standard Model are proportional to $\log(m_{\mathrm{H}})$. The correlation between the top quark mass and the Higgs mass is 0.76

(see Figure 9).

The data can also be used within the Standard Model to determine the top quark and W masses indirectly, and compare them to the direct measurements performed at the Tevatron and LEP. For this fit, we use all the results in Table 29, except the LEP-II and Tevatron m_{W} and m_{t} results. The results of the fit are shown in column 3 of Table 30. The indirect measurements of m_{W} and m_{t} from this data sample are shown in Figure 10, compared with the direct measurements. Also shown is the Standard Model predictions for Higgs masses between 60 and 1000 GeV. As can be seen in both the table and the figure, the indirect measurements prefer low m_{t} and low m_{H}.

The best constraints on m_{H} are obtained when all data, especially the direct measurements of m_{t}, are used in the fit. The results of this fit are shown in the last column of Table 30 and in Figure 9. In Figures 11 and 12 the sensitivity of the LEP and SLD measurements to the Higgs mass is shown. As can be seen, the most sensitive measurements are the asymmetries. A reduced uncertainty for the value of $\alpha(m_{\mathrm{Z}}^2)$ would therefore result in an improved constraint on m_{H}, as shown in Figure 8.

In Figure 13 the observed value of $\Delta\chi^2 \equiv \chi^2 - \chi^2_{\mathrm{min}}$ as a function of m_{H} is plotted for the fit including all data. The shaded band shows the additional error due to the missing higher order corrections. Taking this error into account yields the one-sided 95% confidence level upper limit on m_{H} of 420 GeV. The lower limit on m_{H} of approximately 77 GeV obtained from direct searches [111] has not been used in this limit determination.

	LEP including LEP-II m_{W}	all data except m_{t} and m_{W}	all data
m_{t} [GeV]	158^{+14}_{-11}	157^{+10}_{-9}	173.1 ± 5.4
m_{H} [GeV]	83^{+168}_{-49}	41^{+64}_{-21}	115^{+116}_{-66}
$\log(m_{\mathrm{H}}/\mathrm{GeV})$	$1.92^{+0.48}_{-0.39}$	$1.62^{+0.41}_{-0.31}$	$2.06^{+0.30}_{-0.37}$
$\alpha_s(m_{\mathrm{Z}}^2)$	0.121 ± 0.003	0.120 ± 0.003	0.120 ± 0.003
χ^2/d.o.f.	8/9	14/12	17/15
$\sin^2\theta_{\mathrm{eff}}^{\mathrm{lept}}$	0.23188 ± 0.00026	0.23153 ± 0.00023	0.23152 ± 0.00022
$1 - m_{\mathrm{W}}^2/m_{\mathrm{Z}}^2$	0.2246 ± 0.0008	0.2240 ± 0.0008	0.2231 ± 0.0006
m_{W} [GeV]	80.298 ± 0.043	80.329 ± 0.041	80.375 ± 0.030

Table 30: Results of the fits to LEP data alone, to all data except the direct determinations of m_{t} and m_{W} (Tevatron and LEP-II) and to all data including the top quark mass determination. As the sensitivity to m_{H} is logarithmic, both m_{H} as well as $\log(m_{\mathrm{H}}/\mathrm{GeV})$ are quoted. The bottom part of the table lists derived results for $\sin^2\theta_{\mathrm{eff}}^{\mathrm{lept}}$, $1 - m_{\mathrm{W}}^2/m_{\mathrm{Z}}^2$ and m_{W}. See text for a discussion of theoretical errors not included in the errors above.

8 Prospects for the Future

The LEP energy has now been increased; the Z phase of LEP has come to an end. However, the analyses of the LEP-I data are not yet finished. The major improvements which should happen in the near future will be:

- completion of the lineshape analysis, including final LEP energy calibrations;
- completion of the τ polarisation measurements, especially of the statistics dominated measurement of $\mathcal{A}_{\mathrm{e}}$;
- the errors on the measurements from SLD should decrease by a factor of approximately 1.6 for A_{LR}, and 2.0 for R_{b}, R_{c}, $\mathcal{A}_{\mathrm{b}}$ and $\mathcal{A}_{\mathrm{c}}$, using the data expected until the end of 1998.

In addition, the anticipated increase in statistics at LEP-II to 500 pb^{-1} per experiment will lead to substantially improved measurements of certain electroweak parameters. As a result, the measurements of m_{W} at both the Tevatron and LEP-II are likely to match the error obtained via the radiative corrections of the Z data, providing a further important test of the Standard Model. In the measurement of the WWγ and WWZ triple-gauge-boson couplings the increase in LEP-II statistics, together with the improved precision per event obtained at higher beam energy, will lead to an improvement in the current precision by a factor approaching an order of magnitude.

9 Conclusions

The combination of the many precise electroweak results yields stringent constraints on the Standard Model. All LEP measurements agree well with the predictions. Including all measurements, the data show some sensitivity to the Higgs mass.

The LEP experiments wish to stress that this report reflects a preliminary status at the time of the 1997 summer conferences. A definitive statement on these results has to wait for publication by each collaboration.

Acknowledgements

We would like to thank the CERN accelerator divisions for the efficient operation of the LEP accelerator, the precise information on the absolute energy scale and their close cooperation with the four experiments. We would also like to thank members of the CDF, DØ and SLD Collaborations for making results available to us in advance of the conferences and for useful discussions concerning their combination.

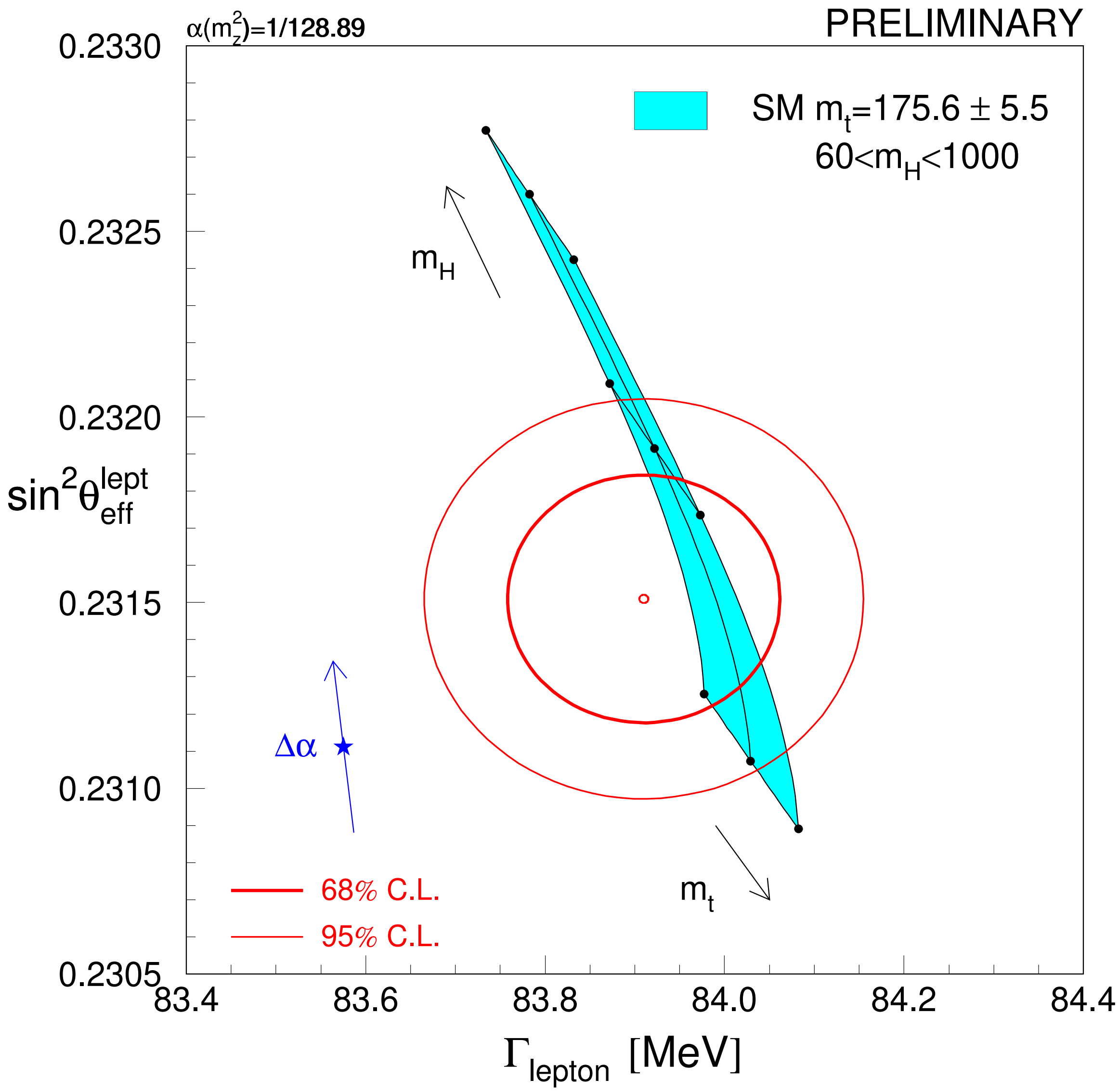

Figure 8: LEP-I+SLD measurements of $\sin^2\theta_{\rm eff}^{\rm lept}$ (Table 28) and $\Gamma_{\ell\ell}$ (Table 9) and the Standard Model prediction. The star shows the predictions if among the electroweak radiative corrections only the photon vacuum polarisation is included. The corresponding arrow shows variation of this prediction if $\alpha(m_{\rm Z}^2)$ is changed by one standard deviation. This variation gives an additional uncertainty to the Standard Model prediction shown in the figure.

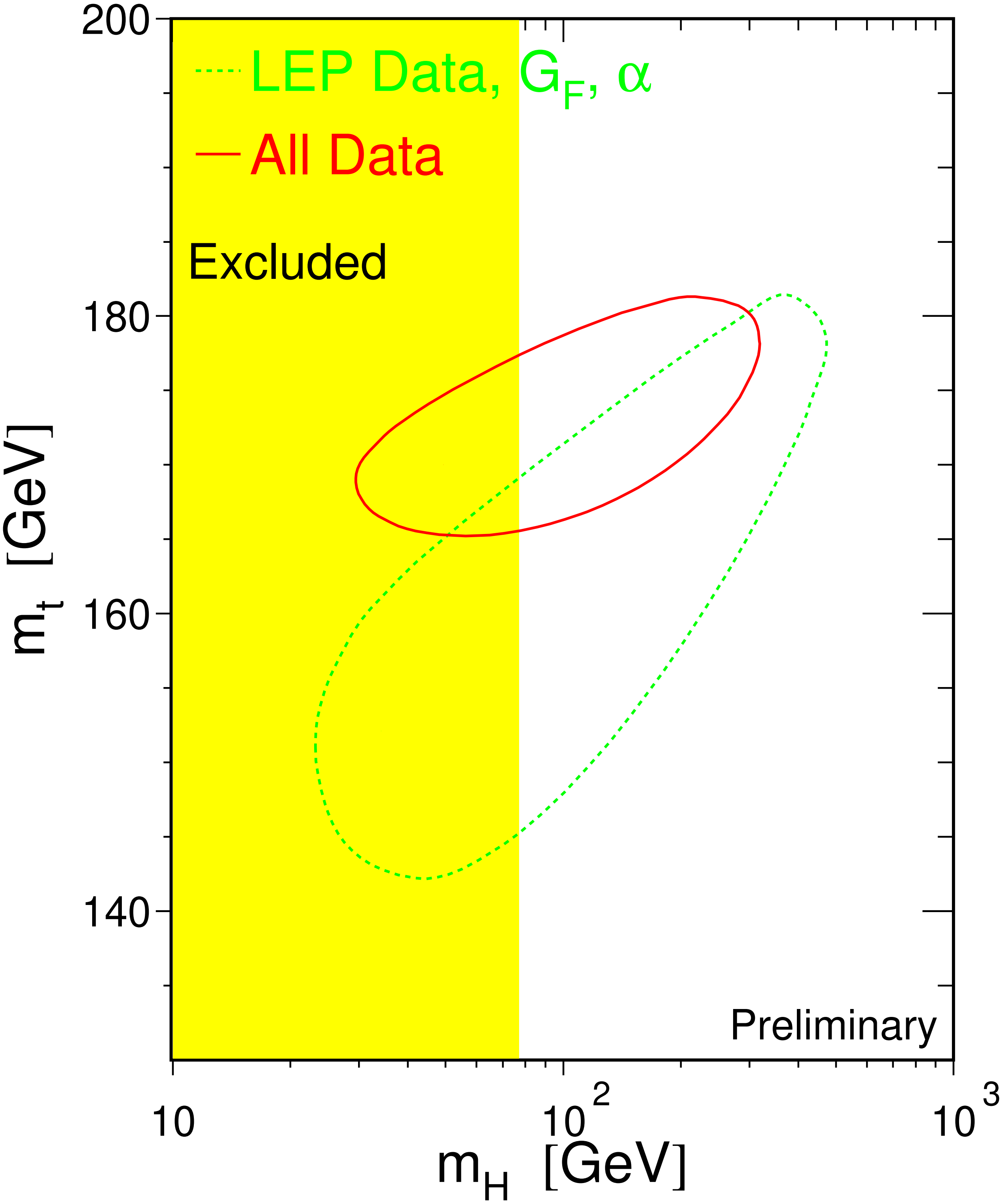

Figure 9: The 68% confidence level contours in m_{t} and m_{H} for the fits to LEP data only (dashed curve) and to all data including the CDF/DØ m_{t} measurement (solid curve). The vertical band shows the 95% CL exclusion limit on m_{H} from the direct search.

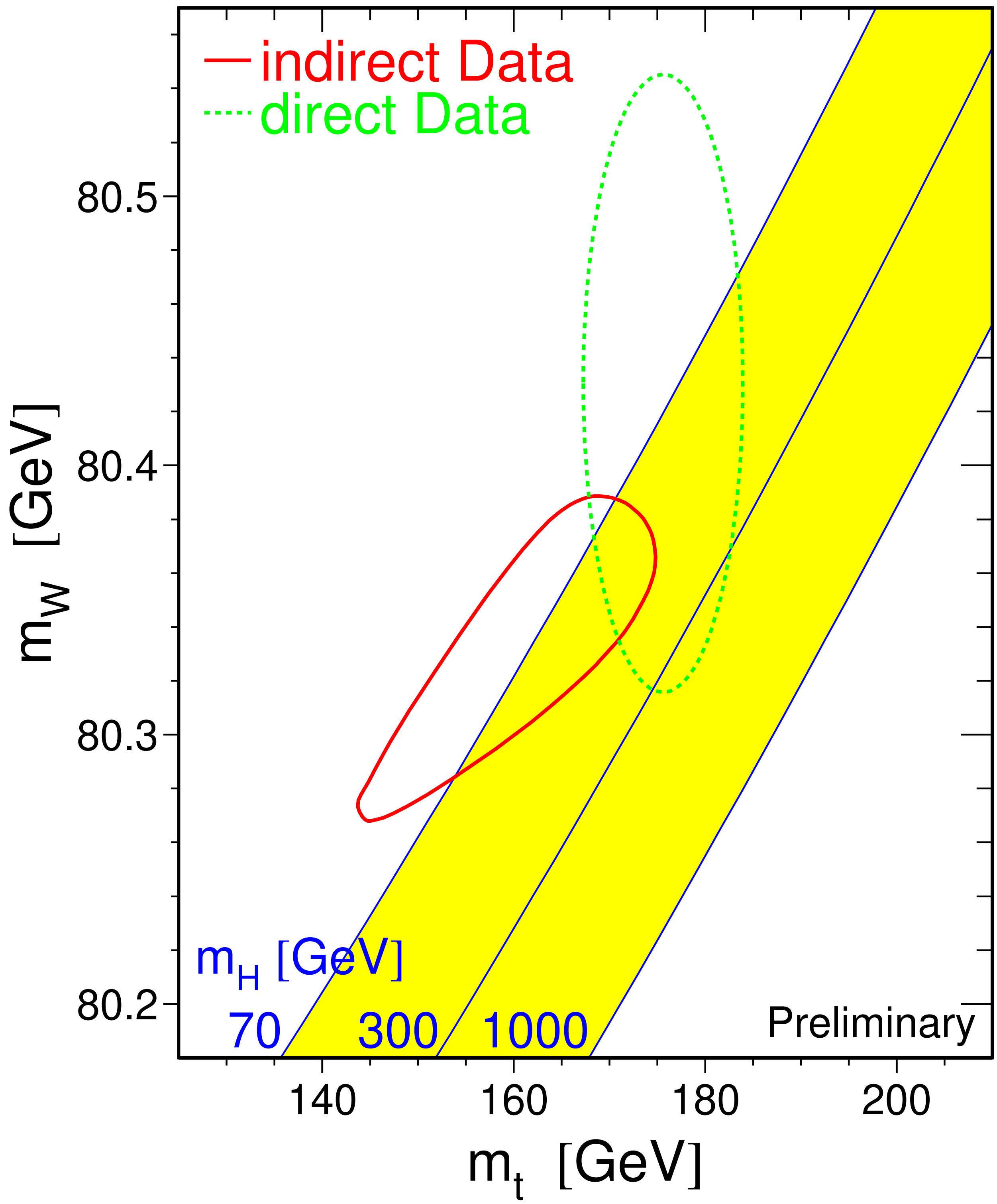

Figure 10: The comparison of the indirect measurements of m_W and m_t (LEP-I+SLD+νN data) (solid contour) and the direct measurements (Tevatron and LEP-II data) (dashed contour). In both cases the 68% CL contours are plotted. Also shown is the Standard Model relationship for the masses as a function of the Higgs mass.

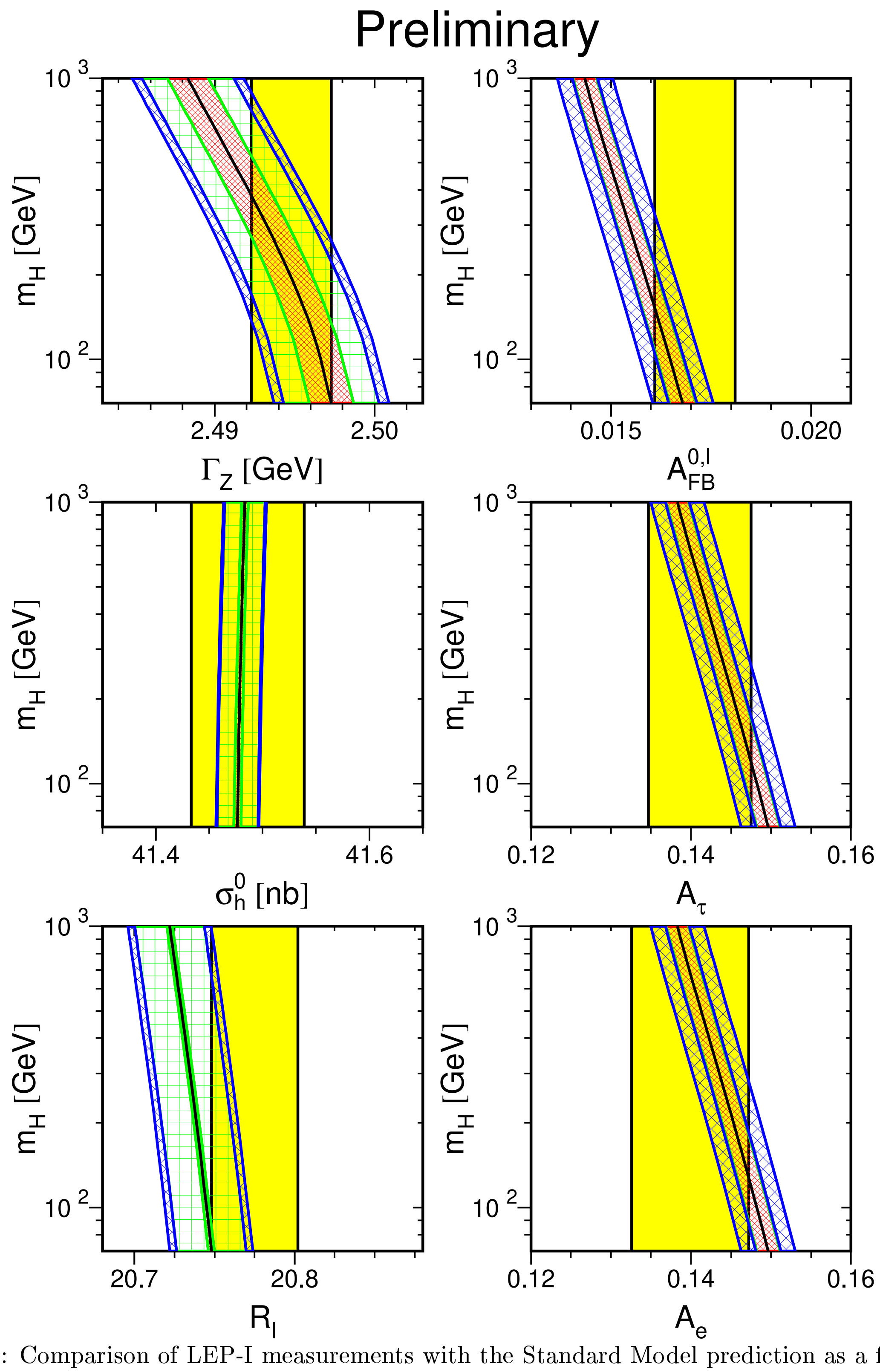

Figure 11: Comparison of LEP-I measurements with the Standard Model prediction as a function of $m_{\rm H}$. The measurement with its error is shown as the vertical band. The width of the Standard Model band is due to the uncertainties in $\alpha(m_{\rm Z}^2)$, $\alpha_s(m_{\rm Z}^2)$ and $m_{\rm t}$. The total width of the band is the linear sum of these effects. See Figure 12 for the definition of these uncertainties.

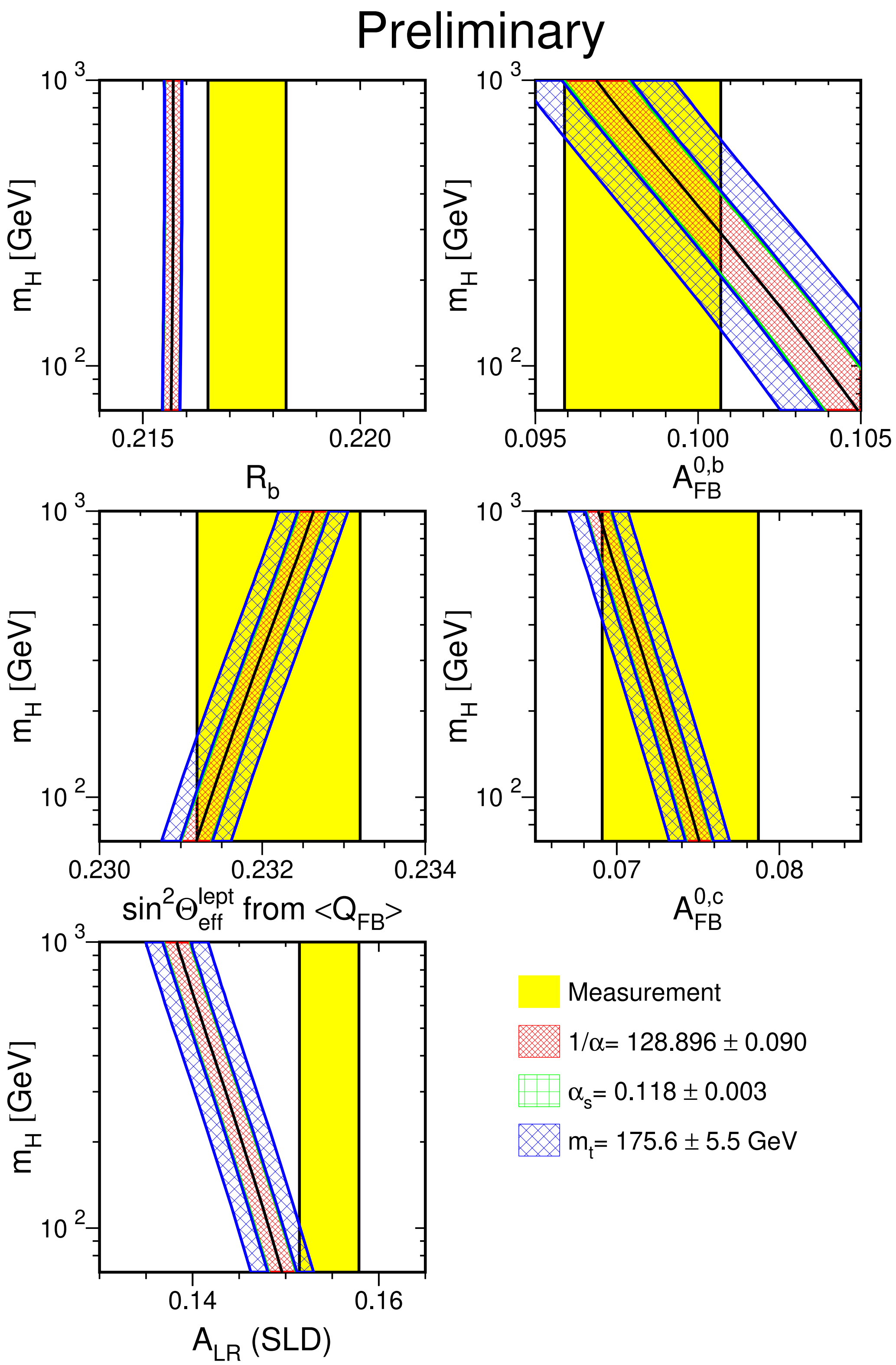

Figure 12: Comparison of LEP-I measurements with the Standard Model prediction as a function of m_{H} (*c.f.* Figure 11). Also shown is the comparison of the SLD measurement of A_{LR} with the Standard Model.

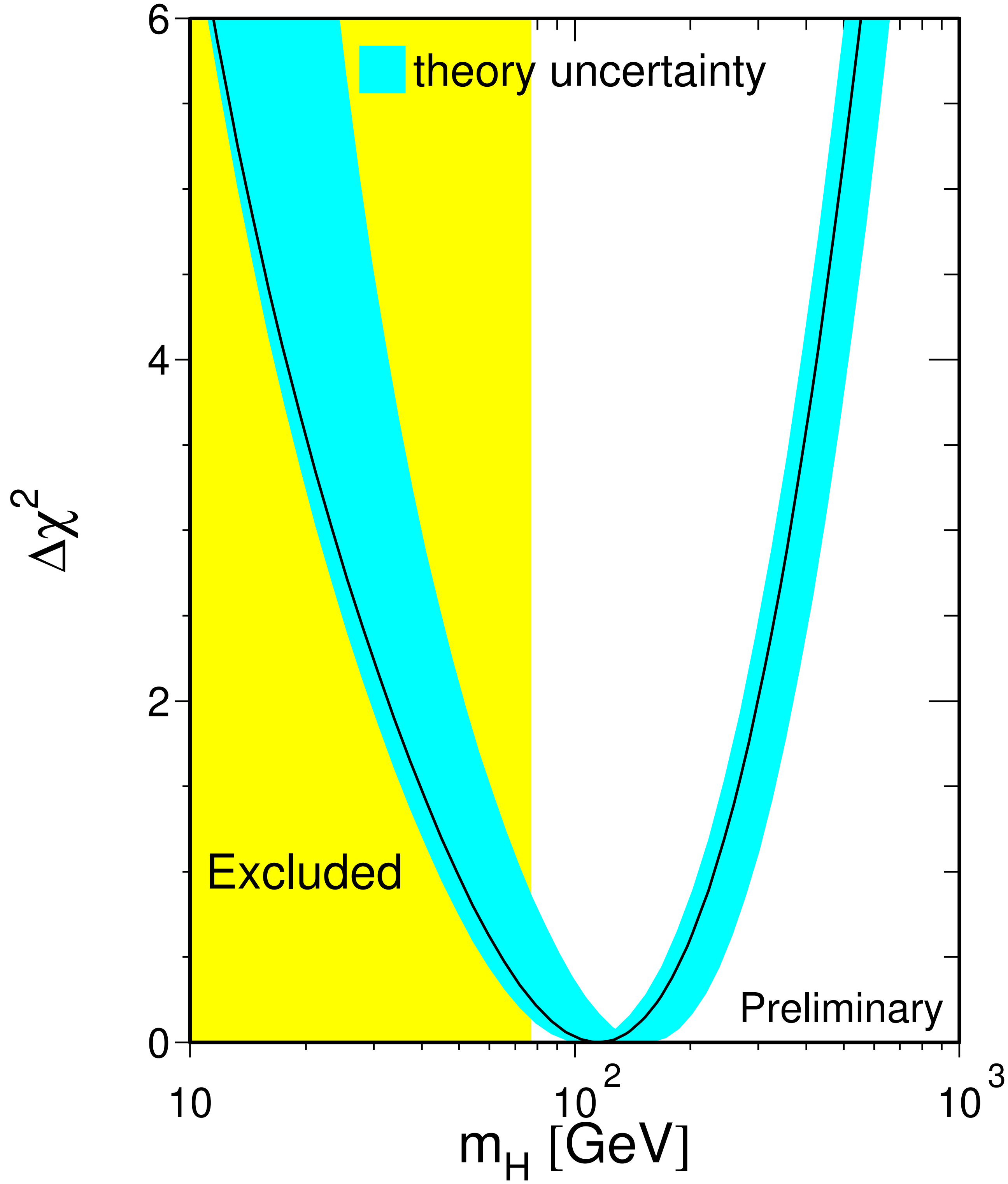

Figure 13: $\Delta\chi^2 = \chi^2 - \chi^2_{min}$ *vs.* $m_{\rm H}$ curve. The line is the result of the fit using all data (last column of Table 30); the band represents an estimate of the theoretical error due to missing higher order corrections. The vertical band shows the 95% CL exclusion limit on $m_{\rm H}$ from the direct search.

Appendix

A S-Matrix Fit Results

The full 16 parameter S-Matrix fits to the lineshape and asymmetry data taken at LEP-I and at LEP-II energies is summarised for each LEP experiment in Table 31. The average including the parameter mean values and errors and the correlation amongst them are given in Tables 32 and 33.

	ALEPH	DELPHI	L3[a]	OPAL[a]
m_Z (GeV)	91.1951±0.0056	91.1841±0.0056	91.1867±0.0056	91.1874±0.0055
Γ_Z (GeV)	2.4939±0.0044	2.4897±0.0041	2.5003±0.0043	2.4946±0.0044
$r_{\mathrm{had}}^{\mathrm{tot}}$	2.966±0.010	2.957±0.010	2.972±0.010	2.962±0.010
$r_{\mathrm{e}}^{\mathrm{tot}}$	0.14361±0.00076	0.1412±0.0010	0.14171±0.00088	0.1418±0.0011
r_{μ}^{tot}	0.14248±0.00062	0.14274±0.00069	0.14257±0.00083	0.14228±0.00066
r_{τ}^{tot}	0.14313±0.00067	0.14140±0.00097	0.1433±0.0011	0.14118±0.00088
$j_{\mathrm{had}}^{\mathrm{tot}}$	-0.18±0.27	0.36±0.28	0.30±0.28	0.03±0.27
$j_{\mathrm{e}}^{\mathrm{tot}}$	-0.007±0.041	-0.037±0.045	-0.011±0.045	-0.123±0.060
j_{μ}^{tot}	-0.018±0.030	0.052±0.030	0.028±0.036	-0.012±0.037
j_{τ}^{tot}	-0.012±0.032	0.017±0.037	0.042±0.039	-0.003±0.042
$r_{\mathrm{e}}^{\mathrm{fb}}$	0.00303±0.00072	0.00326±0.00096	0.0025±0.0013	0.0016±0.0010
r_{μ}^{fb}	0.00288±0.00048	0.00267±0.00053	0.00323±0.00067	0.00262±0.00050
r_{τ}^{fb}	0.00288±0.00055	0.00376±0.00075	0.00419±0.00094	0.00318±0.00066
$j_{\mathrm{e}}^{\mathrm{fb}}$	0.861±0.058	0.813±0.073	0.644±0.080	0.778±0.068
j_{μ}^{fb}	0.826±0.036	0.759±0.034	0.838±0.046	0.724±0.036
j_{τ}^{fb}	0.846±0.041	0.745±0.047	0.788±0.057	0.727±0.042
χ^2/d.o.f.	180/189	233/195	156/183	109/155

Table 31: S-Matrix parameters from 16-parameter fits to the data of the four LEP experiments, without the assumption of lepton universality.
[a]For the averaging procedure the L3 values of m_Z and Γ_Z are shifted by +0.3 MeV and the OPAL value of m_Z by +0.5 MeV to account for the new energy calibration.

Parameter	Average Value
m_{Z} (GeV)	91.1884±0.0031
Γ_{Z} (GeV)	2.4945±0.0025
$r^{\mathrm{tot}}_{\mathrm{had}}$	2.9637±0.0063
$r^{\mathrm{tot}}_{\mathrm{e}}$	0.14229±0.00049
r^{tot}_{μ}	0.14253±0.00036
r^{tot}_{τ}	0.14247±0.00043
$j^{\mathrm{tot}}_{\mathrm{had}}$	0.13±0.14
$j^{\mathrm{tot}}_{\mathrm{e}}$	-0.028±0.023
j^{tot}_{μ}	0.013±0.016
j^{tot}_{τ}	0.010±0.018
$r^{\mathrm{fb}}_{\mathrm{e}}$	0.00270±0.00046
r^{fb}_{μ}	0.00279±0.00027
r^{fb}_{τ}	0.00329±0.00034
$j^{\mathrm{fb}}_{\mathrm{e}}$	0.786±0.034
j^{fb}_{μ}	0.780±0.019
j^{fb}_{τ}	0.778±0.023

Table 32: Average S-Matrix parameters from the data of the four LEP experiments given in Table 31, without the assumption of lepton universality. The χ^2/d.o.f. of the average is 54/48.

	m_{Z}	Γ_{Z}	$r^{\mathrm{tot}}_{\mathrm{had}}$	$r^{\mathrm{tot}}_{\mathrm{e}}$	r^{tot}_{μ}	r^{tot}_{τ}	$j^{\mathrm{tot}}_{\mathrm{had}}$	$j^{\mathrm{tot}}_{\mathrm{e}}$	j^{tot}_{μ}	j^{tot}_{τ}	$r^{\mathrm{fb}}_{\mathrm{e}}$	r^{fb}_{μ}	r^{fb}_{τ}	$j^{\mathrm{fb}}_{\mathrm{e}}$	j^{fb}_{μ}	j^{fb}_{τ}
m_{Z}	1.00	-.10	-.07	-.03	-.06	-.05	-.75	-.25	-.30	-.28	.04	.11	.09	.01	-.02	-.01
Γ_{Z}	-.10	1.00	.80	.51	.51	.43	.16	.03	.07	.06	.00	.00	.00	.02	.05	.04
$r^{\mathrm{tot}}_{\mathrm{had}}$	-.07	.80	1.00	.59	.66	.55	.13	.01	.05	.05	.01	.01	.01	.03	.06	.05
$r^{\mathrm{tot}}_{\mathrm{e}}$	-.03	.51	.59	1.00	.42	.35	.09	.04	.04	.04	.03	.00	.00	.05	.04	.03
r^{tot}_{μ}	-.06	.51	.66	.42	1.00	.46	.10	.01	.14	.04	.01	.03	.01	.03	.10	.04
r^{tot}_{τ}	-.05	.43	.55	.35	.46	1.00	.09	.01	.04	.13	.01	.01	.03	.02	.04	.09
$j^{\mathrm{tot}}_{\mathrm{had}}$	-.75	.16	.13	.09	.10	.09	1.00	.27	.32	.30	-.04	-.11	-.09	.00	.03	.01
$j^{\mathrm{tot}}_{\mathrm{e}}$	-.25	.03	.01	.04	.01	.01	.27	1.00	.11	.10	.01	-.04	-.03	.02	.01	.00
j^{tot}_{μ}	-.30	.07	.05	.04	.14	.04	.32	.11	1.00	.12	-.01	.00	-.03	.00	.02	.00
j^{tot}_{τ}	-.28	.06	.05	.04	.04	.13	.30	.10	.12	1.00	-.01	-.04	.00	.00	.01	.01
$r^{\mathrm{fb}}_{\mathrm{e}}$	.04	.00	.01	.03	.01	.01	-.04	.01	-.01	-.01	1.00	.01	.01	.09	.00	.00
r^{fb}_{μ}	.11	.00	.01	.00	.03	.01	-.11	-.04	.00	-.04	.01	1.00	.03	.00	.17	.00
r^{fb}_{τ}	.09	.00	.01	.00	.01	.03	-.09	-.03	-.03	.00	.01	.03	1.00	.00	.00	.16
$j^{\mathrm{fb}}_{\mathrm{e}}$	.01	.02	.03	.05	.03	.02	.00	.02	.00	.00	.09	.00	.00	1.00	.00	.00
j^{fb}_{μ}	-.02	.05	.06	.04	.10	.04	.03	.01	.02	.01	.00	.17	.00	.00	1.00	.00
j^{fb}_{τ}	-.01	.04	.05	.03	.04	.09	.01	.00	.00	.01	.00	.00	.16	.00	.00	1.00

Table 33: The correlation matrix for the set of parameters given in Table 32.

B Heavy Flavour Fit including Off-Peak Asymmetries

The full 17 parameter fit to the LEP and SLD data gave the following results:

$$
\begin{aligned}
R_{\mathrm{b}}^{0} &= 0.2170 \pm 0.0009 \\
R_{\mathrm{c}}^{0} &= 0.1733 \pm 0.0048 \\
A_{\mathrm{FB}}^{\mathrm{b\bar{b}}}(-2) &= 0.048 \pm 0.010 \\
A_{\mathrm{FB}}^{\mathrm{c\bar{c}}}(-2) &= -0.038 \pm 0.019 \\
A_{\mathrm{FB}}^{\mathrm{b\bar{b}}}(\mathrm{pk}) &= 0.0969 \pm 0.0025 \\
A_{\mathrm{FB}}^{\mathrm{c\bar{c}}}(\mathrm{pk}) &= 0.0681 \pm 0.0050 \\
A_{\mathrm{FB}}^{\mathrm{b\bar{b}}}(+2) &= 0.113 \pm 0.008 \\
A_{\mathrm{FB}}^{\mathrm{c\bar{c}}}(+2) &= 0.140 \pm 0.017 \\
\mathcal{A}_{\mathrm{b}} &= 0.900 \pm 0.050 \\
\mathcal{A}_{\mathrm{c}} &= 0.651 \pm 0.058 \\
\mathrm{BR}(\mathrm{b} \to \ell) &= 0.1112 \pm 0.0020 \\
\mathrm{BR}(\mathrm{b} \to \mathrm{c} \to \bar{\ell}) &= 0.0803 \pm 0.0033 \\
\overline{\chi} &= 0.1214 \pm 0.0043 \\
f(\mathrm{D}^{+}) &= 0.221 \pm 0.020 \\
f(\mathrm{D_s}) &= 0.112 \pm 0.027 \\
f(\mathrm{c}_{baryon}) &= 0.084 \pm 0.022 \\
\mathrm{P}(\mathrm{c} \to \mathrm{D}^{*+}) \times \mathrm{BR}(\mathrm{D}^{*+} \to \pi^{+}\mathrm{D}^{0}) &= 0.1609 \pm 0.0062
\end{aligned}
$$

with a χ^2/d.o.f. of $50/(94-17)$. The corresponding correlation matrix is given in Table 34. The energy for the peak-2, peak and peak$+2$ results are respectively 89.55 GeV, 91.26 GeV and 92.94 GeV. Note that the asymmetry results shown here are not the pole asymmetries which have been shown in Section 4.3.2.

	1) R_{b}	2) R_{c}	3) $A_{\mathrm{FB}}^{\mathrm{b\bar{b}}}$ (−2)	4) $A_{\mathrm{FB}}^{\mathrm{c\bar{c}}}$ (−2)	5) $A_{\mathrm{FB}}^{\mathrm{b\bar{b}}}$ (pk)	6) $A_{\mathrm{FB}}^{\mathrm{c\bar{c}}}$ (pk)	7) $A_{\mathrm{FB}}^{\mathrm{b\bar{b}}}$ (+2)	8) $A_{\mathrm{FB}}^{\mathrm{c\bar{c}}}$ (+2)	9) $\mathcal{A}_{\mathrm{b}}$	10) $\mathcal{A}_{\mathrm{c}}$	11) BR (1)	12) BR (2)	13) $\overline{\chi}$	14) $f(\mathrm{D}^+)$	15) $f(\mathrm{D_s})$	16) $f(c_{bar.})$	17) PcDst
1)	1.00	−0.20	0.00	−0.01	−0.03	0.02	−0.01	0.01	−0.03	0.02	−0.09	−0.03	0.00	−0.18	−0.05	0.09	0.21
2)	−0.20	1.00	0.00	0.01	0.03	−0.07	0.01	−0.05	0.04	−0.04	0.09	0.13	0.01	−0.12	0.23	0.11	−0.58
3)	0.00	0.00	1.00	0.15	0.03	0.01	0.02	0.00	0.01	0.01	0.02	−0.03	0.08	0.00	0.00	0.00	0.00
4)	−0.01	0.01	0.15	1.00	0.02	0.02	0.01	0.00	0.00	0.00	0.01	−0.02	0.01	0.00	0.00	0.00	0.00
5)	−0.03	0.03	0.03	0.02	1.00	0.13	0.09	0.00	0.03	0.02	0.02	−0.15	0.24	−0.01	0.01	0.00	−0.02
6)	0.02	−0.07	0.01	0.02	0.13	1.00	0.00	0.14	0.00	0.07	0.13	−0.22	0.14	0.00	−0.01	0.00	0.04
7)	−0.01	0.01	0.02	0.01	0.09	0.00	1.00	0.14	0.01	0.00	0.00	−0.04	0.11	0.00	0.00	0.00	−0.01
8)	0.01	−0.05	0.00	0.00	0.00	0.14	0.14	1.00	0.00	0.03	0.06	−0.09	0.06	0.00	−0.01	0.00	0.03
9)	−0.03	0.04	0.01	0.00	0.03	0.00	0.01	0.00	1.00	0.08	0.01	−0.02	0.06	−0.01	0.01	0.01	−0.03
10)	0.02	−0.04	0.01	0.00	0.02	0.07	0.00	0.03	0.08	1.00	0.07	−0.18	0.10	−0.05	−0.02	0.02	0.02
11)	−0.09	0.09	0.02	0.01	0.02	0.13	0.00	0.06	0.01	0.07	1.00	−0.23	0.32	0.01	0.02	0.00	−0.06
12)	−0.03	0.13	−0.03	−0.02	−0.15	−0.22	−0.04	−0.09	−0.02	−0.18	−0.23	1.00	−0.39	0.01	0.03	0.00	−0.07
13)	0.00	0.01	0.08	0.01	0.24	0.14	0.11	0.06	0.06	0.10	0.32	−0.39	1.00	0.01	0.00	−0.01	−0.01
14)	−0.18	−0.12	0.00	0.00	−0.01	0.00	0.00	0.00	−0.01	−0.05	0.01	0.01	0.01	1.00	−0.31	−0.19	0.10
15)	−0.05	0.23	0.00	0.00	0.01	−0.01	0.00	−0.01	0.01	−0.02	0.02	0.03	0.00	−0.31	1.00	−0.25	−0.08
16)	0.09	0.11	0.00	0.00	0.00	0.00	0.00	0.00	0.01	0.02	0.00	0.00	−0.01	−0.19	−0.25	1.00	−0.04
17)	0.21	−0.58	0.00	0.00	−0.02	0.04	−0.01	0.03	−0.03	0.02	−0.06	−0.07	−0.01	0.10	−0.08	−0.04	1.00

Table 34: The correlation matrix for the set of the 17 heavy flavour parameters. BR(1) and BR(2) denote $\mathrm{BR(b \to \ell)}$ and $\mathrm{BR(b \to c \to \bar{\ell})}$ respectively, PcDst denotes $\mathrm{P(c \to D^{*+}) \times BR(D^{*+} \to \pi^+ D^0)}$.

The Measurements used in the Heavy Flavour Averages

In the following 14 tables, preliminary results are indicated by the symbol "†." The values of centre-of-mass energy are given where relevant. In each table, the result used as input to the average procedure is given followed by the statistical error, the correlated and uncorrelated systematic errors, the total systematic error, and any dependence on other electroweak parameters. In the case of the asymmetries, the measurement moved to a common energy (89.55 GeV, 91.26 GeV and 92.94 GeV, respectively, for peak−2, peak and peak+2 results) is quoted as *corrected* asymmetry.

Contributions to the correlated systematic error quoted here are from any sources of error shared with one or more other results from different experiments in the same table, and the uncorrelated errors from the remaining sources. In the case of $\mathcal{A}_{\mathrm{c}}$ and $\mathcal{A}_{\mathrm{b}}$ from SLD the quoted correlated systematic error has contributions from any source shared with one or more other measurements from LEP experiment. Constants such as $a(x)$ denote the dependence on the assumed value of x^{used}, which is also given.

	ALEPH		DELPHI		L3			OPAL		SLD
	92-95 multi [41]	90-91 lepton [33]	94† multi [42]	91-92 lepton [35]	94† multi [43]	91 shape [40]	90-91 lepton [37]	92-94 multi [44]	90-91 lepton [38]	93-96† mass [30]
R_{b}	0.2156	0.2162	0.2164	0.2146	0.2176	0.2220	0.2193	0.2175	0.2240	0.2121
Statistical	0.0009	0.0062	0.0008	0.0089	0.0015	0.0030	0.0081	0.0014	0.0110	0.0024
Uncorrelated	0.0007	0.0040	0.0006	0.0063	0.0014	0.0021	0.0047	0.0009	0.0045	0.0015
Correlated	0.0008	0.0031	0.0006	0.0020	0.0019	0.0061	0.0021	0.0012	0.0045	0.0006
Total Systematic	0.0011	0.0050	0.0009	0.0066	0.0023	0.0064	0.0051	0.0015	0.0063	0.0017
$a(R_{\mathrm{c}})$	-0.0033		-0.0041		-0.0364	-0.0209	-0.0232	-0.0183	-0.0132	-0.0068
$R_{\mathrm{c}}^{\mathrm{used}}$	0.1720		0.1720		0.1722	0.1710	0.1710	0.1720	0.1710	0.1710
$a(\mathrm{BR}(\mathrm{b} \to \ell))$						-0.0210				
$\mathrm{BR}(\mathrm{b} \to \ell)^{\mathrm{used}}$						10.50				
$a(\mathrm{BR}(\mathrm{b} \to \mathrm{c} \to \bar{\ell}))$							0.0342			
$\mathrm{BR}(\mathrm{b} \to \mathrm{c} \to \bar{\ell})^{\mathrm{used}}$							7.90			
$a(f(\mathrm{D}^+))$	-0.0010		-0.0011		-0.0087			-0.0032		-0.0007
$f(\mathrm{D}^+)^{\mathrm{used}}$	0.2330		0.2330		0.2330			0.2350		0.2590
$a(f(\mathrm{D_s}))$	-0.0001		0.0001		-0.0005			-0.0001		-0.0002
$f(\mathrm{D_s})^{\mathrm{used}}$	0.1020		0.1020		0.1020			0.0960		0.1150
$a(f(\Lambda_{\mathrm{c}}))$	0.0002		0.0002		0.0008			0.0006		-0.0004
$f(\Lambda_{\mathrm{c}})^{\mathrm{used}}$	0.0650		0.0650		0.0650			0.0640		0.0740

Table 35: The measurements of $R_{\mathrm{b}} = R_{\mathrm{b}}^0 - 0.0003$.

	ALEPH				DELPHI		OPAL		SLD
	90-91 lepton [33]	91-95† $D^{*\pm}\pi$ [34]	91-95† c count [34]	92-95† lepton [34]	91-94† c count + $D^{*\pm}\pi$ [47]	91-92 lepton [35]	90-95 $D^{*\pm}$ [48]	91-94 c count [48]	93-96† lifetime + mass [31]
R_c	0.1670	0.1724	0.1756	0.1649	0.1692	0.1640	0.1802	0.167	0.1810
Statistical	0.0054	0.0098	0.0048	0.0070	0.0080	0.0085	0.0098	0.011	0.0122
Uncorrelated	0.0149	0.0099	0.0085	0.0053	0.0071	0.0168	0.0100	0.009	0.0075
Correlated	0.0114	0.0013	0.0070	0.0092	0.0042	0.0114	0.0062	0.009	0.0024
Total Systematic	0.0188	0.0100	0.0110	0.0106	0.0083	0.0203	0.0118	0.013	0.0079
$a(R_b)$		-0.0022							-0.0215
R_b^{used}		0.2219							0.2155

Table 36: The measurements of $R_c = R_c^0 + 0.0003$.

	ALEPH			DELPHI		L3	OPAL		
	90-95 lepton [33]	90-95 lepton [33]	90-95 lepton [33]	91-94† lepton [36]	91-94† $D^{*\pm}$ [36]	90-93† lepton [37]	91-95 jet [46]	90-95† lepton [38]	90-94† $D^{*\pm}$ [50]
$\sqrt{s}$ (GeV)	88.380	89.380	90.210	89.430	89.540	89.560	89.440	89.490	89.490
$A_{\mathrm{FB}}^{\mathrm{b\bar{b}}}(-2)$	-3.51	5.45	9.07	6.37	1.99	6.90	4.10	3.54	-8.70
$A_{\mathrm{FB}}^{\mathrm{b\bar{b}}}(-2)$Corrected	5.01			6.66	2.01	6.99	4.36	3.68	-8.56
Statistical	1.80			3.86	10.48	3.50	2.10	1.73	10.80
Uncorrelated	0.04			0.16	1.12	0.34	0.25	0.16	2.53
Correlated	0.03			0.12	0.11	0.13	0.01	0.04	1.37
Total Systematic	0.05			0.19	1.12	0.37	0.25	0.16	2.88
$a(R_{\mathrm{b}})$	0.0870			-0.7233		-1.5984	-0.7300	-0.1000	
$R_{\mathrm{b}}^{\mathrm{used}}$	0.2192			0.2170		0.2160	0.2150	0.2155	
$a(R_{\mathrm{c}})$	0.0333			0.1221		0.9126	0.0700	0.1000	
$R_{\mathrm{c}}^{\mathrm{used}}$	0.1710			0.1710		0.1690	0.1730	0.1720	
$a(A_{\mathrm{FB}}^{\mathrm{c\bar{c}}}(-2))$	-0.186					-0.2684	-0.3156		
$A_{\mathrm{FB}}^{\mathrm{c\bar{c}}}(-2)^{\mathrm{used}}$	-2.34					-2.96	-2.81		
$a(\mathrm{BR}(\mathrm{b} \to \ell))$	-0.236			-0.9706		-0.7770		0.3406	
$\mathrm{BR}(\mathrm{b} \to \ell)^{\mathrm{used}}$	11.34			11.00		10.50		10.90	
$a(\mathrm{BR}(\mathrm{b} \to \mathrm{c} \to \bar{\ell}))$	-0.102			0.1580		-0.2464		-0.5298	
$\mathrm{BR}(\mathrm{b} \to \mathrm{c} \to \bar{\ell})^{\mathrm{used}}$	7.86			7.90		8.00		8.30	
$a(\overline{\chi})$	5.12			2.0533					
$\overline{\chi}^{\mathrm{used}}$	0.12460			0.12100					

Table 37: The measurements of $A_{\mathrm{FB}}^{\mathrm{b\bar{b}}}(-2)$.

	ALEPH	DELPHI			L3		OPAL		
	90-95 lepton [33]	91-94† lepton [36]	91-94† $D^{*\pm}$ [36]	91-94† jet [36]	94† jet [45]	90-95† lepton [37]	91-95 jet [46]	90-95† lepton [38]	90-94† $D^{*\pm}$ [50]
$\sqrt{s}$ (GeV)	91.210	91.230	91.230	91.230	91.220	91.260	91.210	91.240	91.240
A_{FB}^{bb}(pk)	9.88	10.75	7.23	9.95	8.55	9.63	10.04	9.10	9.50
A_{FB}^{bb}(pk)Corrected	9.97	10.81	7.29	10.01	8.63	9.63	10.13	9.14	9.54
Statistical	0.46	0.77	2.50	0.72	1.18	0.65	0.52	0.44	2.70
Uncorrelated	0.10	0.21	1.25	0.38	0.46	0.28	0.41	0.14	2.15
Correlated	0.16	0.23	0.11	0.12	0.32	0.22	0.20	0.15	0.47
Total Systematic	0.19	0.31	1.25	0.40	0.56	0.35	0.46	0.20	2.20
$a(R_b)$	-1.4613	-2.8933		-0.6000	-8.2916	-2.0736	-7.6300	-0.7000	
R_b^{used}	0.2192	0.2170		0.2210	0.2182	0.2160	0.2150	0.2155	
$a(R_c)$	1.0474	1.2214		0.2400	1.0925	1.2506	0.4600	0.6000	
R_c^{used}	0.1710	0.1710		0.1710	0.1707	0.1690	0.1730	0.1720	
$a(A_{FB}^{c\bar{c}}(pk))$	0.5068				1.1185	0.6253	0.6870		
$A_{FB}^{c\bar{c}}(pk)^{used}$	6.41				6.21	6.70	6.19		
$a(BR(b \to \ell))$	-1.3500	-3.5588				-1.5540		-0.3406	
$BR(b \to \ell)^{used}$	11.34	11.00				10.50		10.90	
$a(BR(b \to c \to \bar{\ell}))$	-0.1886	0.4740				-0.0272		-0.3532	
$BR(b \to c \to \bar{\ell})^{used}$	7.86	7.90				8.00		8.30	
$a(\overline{\chi})$	3.2930	3.5200							
$\overline{\chi}^{used}$	0.12460	0.12100							

Table 38: The measurements of $A_{FB}^{b\bar{b}}$(pk).

	ALEPH			DELPHI		L3	OPAL		
	90-95 lepton [33]	90-95 lepton [33]	90-95 lepton [33]	91-94† lepton [36]	91-94† $D^{*\pm}$ [36]	90-93† lepton [37]	91-95 jet [46]	90-95† lepton [38]	90-94† $D^{*\pm}$ [50]
$\sqrt{s}$ (GeV)	92.050	92.940	93.900	93.017	92.940	92.930	92.910	92.950	92.950
$A_{FB}^{bb}(+2)$	3.91	10.56	9.00	15.23	5.70	10.80	14.60	10.70	-2.10
$A_{FB}^{bb}(+2)$Corrected	10.00			15.15	5.70	10.98	14.63	10.69	-2.11
Statistical	1.50			3.65	9.55	2.90	1.70	1.43	9.00
Uncorrelated	0.14			0.50	1.61	0.35	0.72	0.25	2.18
Correlated	0.22			0.41	0.11	0.15	0.06	0.28	1.59
Total Systematic	0.26			0.65	1.62	0.38	0.72	0.37	2.70
$a(R_b)$	-1.86			-2.8933		-1.5984	-12.9000	-0.8000	
R_b^{used}	0.2192			0.2170		0.2160	0.2150	0.2155	
$a(R_c)$	1.43			-0.9771		0.9126	0.6900	0.8000	
R_c^{used}	0.1710			0.1710		0.1690	0.1730	0.1720	
$a(A_{FB}^{c\bar{c}}(+2))$	0.913					1.1156	1.3287		
$A_{FB}^{c\bar{c}}(+2)^{used}$	12.51					12.13	12.08		
$a(BR(b \to \ell))$	-1.65			-3.2353		-0.4200		-1.3625	
$BR(b \to \ell)^{used}$	11.34			11.00		10.50		10.90	
$a(BR(b \to c \to \bar{\ell}))$	-0.2410			0.4740		-0.5280		0.7064	
$BR(b \to c \to \bar{\ell})^{used}$	7.86			7.90		8.00		8.30	
$a(\overline{\chi})$	6.409			4.8400					
$\overline{\chi}^{used}$	0.12460			0.12100					

Table 39: The measurements of $A_{FB}^{b\bar{b}}(+2)$.

	ALEPH	DELPHI	OPAL	
	91-94† D$^{*\pm}$ [49]	91-94† D$^{*\pm}$ [36]	90-95† lepton [38]	90-94† D$^{*\pm}$ [50]
$\sqrt{s}$ (GeV)	89.400	89.540	89.490	89.490
$A_{\rm FB}^{\rm c\bar{c}}(-2)$	-4.93	0.20	-6.90	3.90
$A_{\rm FB}^{\rm c\bar{c}}(-2)$Corrected	-4.03	0.26	-6.54	4.26
Statistical	7.60	5.19	2.44	5.10
Uncorrelated	0.84	0.55	0.43	0.80
Correlated	0.04	0.07	0.21	0.30
Total Systematic	0.84	0.55	0.48	0.86
$a(R_{\rm b})$			-3.4000	
$R_{\rm b}^{\rm used}$			0.2155	
$a(R_{\rm c})$			3.2000	
$R_{\rm c}^{\rm used}$			0.1720	
$a(A_{\rm FB}^{\rm b\bar{b}}(-2))$	0.2295			
$A_{\rm FB}^{\rm b\bar{b}}(-2)^{\rm used}$	-1.34			
$a({\rm BR}({\rm b}\to\ell))$			-1.7031	
${\rm BR}({\rm b}\to\ell)^{\rm used}$			10.90	
$a({\rm BR}({\rm b}\to{\rm c}\to\bar{\ell}))$			-1.4128	
${\rm BR}({\rm b}\to{\rm c}\to\bar{\ell})^{\rm used}$			8.30	

Table 40: The measurements of $A_{\rm FB}^{\rm c\bar{c}}(-2)$.

	ALEPH		DELPHI		L3	OPAL	
	90-91 lepton [33]	91-94† D$^{*\pm}$ [49]	91-94† lepton [36]	91-94† D$^{*\pm}$ [36]	90-91 lepton [37]	90-95† lepton [38]	90-94† D$^{*\pm}$ [50]
$\sqrt{s}$ (GeV)	91.260	91.200	91.230	91.230	91.240	91.240	91.240
$A_{\rm FB}^{\rm c\bar{c}}({\rm pk})$	9.30	6.44	8.39	7.64	7.84	5.95	6.30
$A_{\rm FB}^{\rm c\bar{c}}({\rm pk})$Corrected	9.30	6.73	8.54	7.79	8.02	6.05	6.40
Statistical	2.00	1.30	1.40	1.21	3.70	0.59	1.20
Uncorrelated	1.55	0.20	0.91	0.55	2.42	0.37	0.53
Correlated	1.04	0.17	0.74	0.09	0.60	0.38	0.15
Total Systematic	1.86	0.26	1.18	0.55	2.50	0.53	0.55
$a(R_{\rm b})$			3.6167		4.3200	4.1000	
$R_{\rm b}^{\rm used}$			0.2170		0.2160	0.2155	
$a(R_{\rm c})$			-6.3514		-6.7600	-3.8000	
$R_{\rm c}^{\rm used}$			0.1710		0.1690	0.1720	
$a(A_{\rm FB}^{\rm b\bar{b}}({\rm pk}))$		-1.5110			6.4274		
$A_{\rm FB}^{\rm b\bar{b}}({\rm pk})^{\rm used}$		8.81			8.84		
$a({\rm BR}({\rm b}\to\ell))$			4.8529		3.5007	5.1094	
${\rm BR}({\rm b}\to\ell)^{\rm used}$			11.00		10.50	10.90	
$a({\rm BR}({\rm b}\to{\rm c}\to\bar{\ell}))$			-3.7920		-3.2917	-1.7660	
${\rm BR}({\rm b}\to{\rm c}\to\bar{\ell})^{\rm used}$			7.90		7.90	8.30	

Table 41: The measurements of $A_{\rm FB}^{\rm c\bar{c}}({\rm pk})$.

	ALEPH	DELPHI	OPAL	
	91-94† D*± [49]	91-94† D*± [36]	90-95† lepton [38]	90-94† D*± [50]
$\sqrt{s}$ (GeV)	93.000	92.940	92.950	92.950
$A_{\mathrm{FB}}^{\mathrm{c\bar{c}}}(+2)$	10.97	8.10	15.60	15.80
$A_{\mathrm{FB}}^{\mathrm{c\bar{c}}}(+2)$Corrected	10.81	8.10	15.57	15.77
Statistical	6.10	4.55	2.02	4.10
Uncorrelated	0.71	0.55	0.89	1.05
Correlated	0.25	0.15	0.37	0.21
Total Systematic	0.75	0.57	0.96	1.07
$a(R_{\mathrm{b}})$			9.6000	
$R_{\mathrm{b}}^{\mathrm{used}}$			0.2155	
$a(R_{\mathrm{c}})$			-8.9000	
$R_{\mathrm{c}}^{\mathrm{used}}$			0.1720	
$a(A_{\mathrm{FB}}^{\mathrm{b\bar{b}}}(+2))$	-2.0639			
$A_{\mathrm{FB}}^{\mathrm{b\bar{b}}}(+2)^{\mathrm{used}}$	12.04			
$a(\mathrm{BR}(\mathrm{b}\to\ell))$			9.5375	
$\mathrm{BR}(\mathrm{b}\to\ell)^{\mathrm{used}}$			10.90	
$a(\mathrm{BR}(\mathrm{b}\to\mathrm{c}\to\bar{\ell}))$			-1.5894	
$\mathrm{BR}(\mathrm{b}\to\mathrm{c}\to\bar{\ell})^{\mathrm{used}}$			8.30	

Table 42: The measurements of $A_{\mathrm{FB}}^{\mathrm{c\bar{c}}}(+2)$.

	SLD		
	93-95† lepton [32]	93-95† jet [32]	94-95† $K^{\pm}$ [32]
$\sqrt{s}$ (GeV)	91.280	91.280	91.280
$\mathcal{A}_{\mathrm{b}}$	0.877	0.911	0.891
Statistical	0.068	0.045	0.083
Uncorrelated	0.038	0.044	0.113
Correlated	0.022	0.002	0.002
Total Systematic	0.044	0.044	0.113
$a(R_{\mathrm{b}})$	-0.4302	-0.0442	-0.0139
$R_{\mathrm{b}}^{\mathrm{used}}$	0.2216	0.2158	0.2180
$a(R_{\mathrm{c}})$	0.0800	0.1103	0.0077
$R_{\mathrm{c}}^{\mathrm{used}}$	0.1600	0.1715	0.1710
$a(\mathcal{A}_{\mathrm{c}})$		0.0611	-0.0609
${\mathcal{A}_{\mathrm{c}}}^{\mathrm{used}}$		0.670	0.666
$a(\mathrm{BR}(\mathrm{b}\to\ell))$	-0.3176		
$\mathrm{BR}(\mathrm{b}\to\ell)^{\mathrm{used}}$	10.75		
$a(\mathrm{BR}(\mathrm{b}\to\mathrm{c}\to\bar{\ell}))$	0.1125		
$\mathrm{BR}(\mathrm{b}\to\mathrm{c}\to\bar{\ell})^{\mathrm{used}}$	8.10		
$a(\overline{\chi})$	0.3677		
$\overline{\chi}^{\mathrm{used}}$	0.12170		

Table 43: The measurements of $\mathcal{A}_{\mathrm{b}}$.

	SLD		
	93-95† lepton [32]	93-95† $D^{*\pm}$ [32]	93-95† K+vertex [32]
$\sqrt{s}$ (GeV)	91.280	91.280	91.280
$\mathcal{A}_c$	0.614	0.640	0.662
Statistical	0.104	0.110	0.066
Uncorrelated	0.040	0.053	0.040
Correlated	0.050	0.020	0.002
Total Systematic	0.064	0.057	0.040
$a(R_b)$	0.1173		
R_b^{used}	0.2216		
$a(R_c)$	-0.4112		
R_c^{used}	0.1600		
$a(\mathcal{A}_b)$		-0.1278	-0.0467
$\mathcal{A}_b{}^{used}$		0.935	0.935
$a(BR(b \to \ell))$	0.4007		
$BR(b \to \ell)^{used}$	10.75		
$a(BR(b \to c \to \ell))$	-0.5287		
$BR(b \to c \to \bar{\ell})^{used}$	8.10		
$a(\overline{\chi})$			0.0910
$\overline{\chi}^{used}$			0.13000
$a(f(D^+))$			-0.0832
$f(D^+)^{used}$			0.2590
$a(f(D_s))$			-0.0155
$f(D_s)^{used}$			0.1150
$a(f(\Lambda_c))$			0.0026
$f(\Lambda_c)^{used}$			0.0740

Table 44: The measurements of $\mathcal{A}_c$.

	ALEPH		DELPHI		L3		OPAL
	90-91 lepton [33]	92-93† multi [33]	91-92 lepton [35]	94† multi [39]	90-91 lepton [37]	92 lepton [37]	90-91 lepton [38]
$\mathrm{BR(b \to \ell)}$	11.20	11.01	11.30	10.64	11.42	10.68	10.60
Statistical	0.33	0.10	0.45	0.13	0.48	0.11	0.60
Uncorrelated	0.32	0.20	0.50	0.24	0.30	0.36	0.39
Correlated	0.27	0.21	0.46	0.36	0.21	0.26	0.53
Total Systematic	0.42	0.29	0.68	0.43	0.37	0.44	0.66
$a(R_\mathrm{b})$						-9.2571	
$R_\mathrm{b}^\mathrm{used}$						0.2160	
$a(R_\mathrm{c})$				0.2756	0.6107		0.2236
$R_\mathrm{c}^\mathrm{used}$				0.1715	0.1710		0.1710
$a(\mathrm{BR(b \to c \to \bar{\ell})})$					0.4608	-1.1700	
$\mathrm{BR(b \to c \to \bar{\ell})}^\mathrm{used}$					7.90	9.00	
$a(\overline{\chi})$		0.2075					
$\overline{\chi}^\mathrm{used}$		0.12610					

Table 45: The measurements of $\mathrm{BR(b \to \ell)}$.

	ALEPH		DELPHI		OPAL
	90-91 lepton [33]	92-93† multi [33]	91-92 lepton [35]	94† multi [39]	90-91 lepton [38]
$\mathrm{BR(b \to c \to \bar{\ell})}$	8.81	7.68	7.90	8.32	8.40
Statistical	0.25	0.18	0.49	0.29	0.40
Uncorrelated	0.40	0.25	0.95	0.40	0.57
Correlated	0.69	0.42	0.78	0.63	0.38
Total Systematic	0.80	0.49	1.23	0.75	0.68
$a(R_\mathrm{c})$				0.0919	0.3157
$R_\mathrm{c}^\mathrm{used}$				0.1715	0.1710
$a(\overline{\chi})$		-0.5108			
$\overline{\chi}^\mathrm{used}$		0.12610			

Table 46: The measurements of $\mathrm{BR(b \to c \to \bar{\ell})}$.

	ALEPH	DELPHI		L3	OPAL
	90-95 lepton [33]	91-92 lepton [35]	94† lepton [39]	90-93 lepton [37]	90-95† lepton [38]
$\overline{\chi}$	0.12461	0.14900	0.12700	0.11870	0.11390
Statistical	0.00515	0.02000	0.01600	0.00680	0.00540
Uncorrelated	0.00244	0.01044	0.00248	0.00453	0.00306
Correlated	0.00403	0.01192	0.00506	0.00257	0.00324
Total Systematic	0.00471	0.01584	0.00563	0.00521	0.00446
$a(R_{\mathrm{b}})$	0.0341			0.0004	
$R_{\mathrm{b}}^{\mathrm{used}}$	0.2192			0.2160	
$a(R_{\mathrm{c}})$	0.0009		-0.0031	0.0003	
$R_{\mathrm{c}}^{\mathrm{used}}$	0.1710		0.1715	0.1690	
$a(\mathrm{BR}(\mathrm{b} \to \ell))$	0.0524			0.0521	0.0170
$\mathrm{BR}(\mathrm{b} \to \ell)^{\mathrm{used}}$	11.34			10.50	10.90
$a(\mathrm{BR}(\mathrm{b} \to \mathrm{c} \to \bar{\ell}))$	-0.0440			-0.0427	-0.0318
$\mathrm{BR}(\mathrm{b} \to \mathrm{c} \to \bar{\ell})^{\mathrm{used}}$	7.86			8.00	8.30

Table 47: The measurements of $\overline{\chi}$.

	DELPHI	OPAL
	91-94† $\mathrm{D}^{*\pm}$ [47]	90-95 $\mathrm{D}^{*\pm}$ [48]
$\mathrm{P}(\mathrm{c} \to \mathrm{D}^{*+}) \times \mathrm{BR}(\mathrm{D}^{*+} \to \pi^+\mathrm{D}^0)$	0.1678	0.1516
Statistical	0.0069	0.0096
Uncorrelated	0.0065	0.0085
Correlated	0.0011	0.0026
Total Systematic	0.0066	0.0089

Table 48: The measurements of $\mathrm{P}(\mathrm{c} \to \mathrm{D}^{*+}) \times \mathrm{BR}(\mathrm{D}^{*+} \to \pi^+\mathrm{D}^0)$.

References

[1] The LEP Collaborations ALEPH, DELPHI, L3, OPAL the LEP Electroweak Working Group, and the SLD Heavy Flavour Group, *A Combination of Preliminary LEP Electroweak Measurements and Constraints on the Standard Model*, CERN-PPE/96-183.

[2] The LEP Collaborations ALEPH, DELPHI, L3, OPAL and the LEP Electroweak Working Group, *Combined Preliminary Data on Z Parameters from the LEP Experiments and Constraints on the Standard Model*, CERN-PPE/94-187.

[3] The LEP Experiments: ALEPH, DELPHI, L3 and OPAL, Nucl. Inst. Meth. **A378** (1996) 101.

[4] ALEPH Collaboration, D. Decamp *et al.*, Z. Phys. **C48** (1990) 365;
ALEPH Collaboration, D. Decamp *et al.*, Z. Phys. **C53** (1992) 1;
ALEPH Collaboration, D. Buskulic *et al.*, Z. Phys. **C60** (1993) 71;
ALEPH Collaboration, D. Buskulic *et al.*, Z. Phys. **C62** (1994) 539;
ALEPH Collaboration, *Preliminary Results on Z Production Cross Section and Lepton Forward-Backward Asymmetries using the 1990-1995 Data*, contributed paper to ICHEP96, Warsaw, 25-31 July 1996, **PA-07-069**; updated for EPS-HEP-97, Jerusalem.

[5] DELPHI Collaboration, P. Aarnio *et al.*, Nucl. Phys. **B367** (1991) 511;
DELPHI Collaboration, P. Abreu *et al.*, Nucl. Phys. **B417** (1994) 3;
DELPHI Collaboration, P. Abreu *et al.*, Nucl. Phys. **B418** (1994) 403;
DELPHI Collaboration, DELPHI Note 95-62 PHYS 497, contributed paper to EPS-HEP-95 Brussels, **eps0404**;
DELPHI Collaboration, DELPHI Note 97-130 CONF 109, contributed paper to EPS-HEP-97, Jerusalem, **EPS-463**.

[6] L3 Collaboration, B. Adeva *et al.*, Z. Phys. **C51** (1991) 179;
L3 Collaboration, O. Adriani *et al.*, Phys. Rep. **236** (1993) 1;
L3 Collaboration, M. Acciarri *et al.*, Z. Phys. **C62** (1994) 551;
L3 Collaboration, *Preliminary L3 Results on Electroweak Parameters using 1990-96 Data*, L3 Note 2065, March 1997, available via http://hpl3sn02.cern.ch/note/note-2065.ps.gz.

[7] OPAL Collaboration, G. Alexander *et al.*, Z. Phys. **C52** (1991) 175;
OPAL Collaboration, P.D. Acton *et al.*, Z. Phys. **C58** (1993) 219;
OPAL Collaboration, R. Akers *et al.*, Z. Phys. **C61** (1994) 19;
OPAL Collaboration, *A Preliminary Update of the Z Line Shape and Lepton Asymmetry Measurements with the 1993 and 1994 Data*, OPAL Physics Note PN166, February 1995;
OPAL Collaboration, *The Preliminary OPAL SiW luminosity analysis: Results for the 1994 Summer conferences*, OPAL Physics Note PN142, July 1994;
OPAL Collaboration, *A Preliminary Update of the Z Line Shape and Lepton Asymmetry Measurements with a Revised 1993-1994 LEP Energy and 1995 Lepton Asymmetry*, OPAL Physics Note PN242, July 1996;
OPAL Collaboration, *Measurements of Lepton Pair Asymmetries using the 1995 Data*, contributed paper to ICHEP96, Warsaw, 25-31 July 1996 **PA07-015**;
OPAL Collaboration, *A Preliminary Update of the Z Lineshape and Lepton Asymmetry Measurements with the 1995 Data*, OPAL Physics Note PN286, March 1997.

[8] A. Arbuzov, *et al.*, Phys. Lett. **B383** (1996) 238;
S. Jadach, *et al.*, Comp. Phys. Comm. **102** (1997) 229.

[9] S. Jadach, E. Richter-Wąs, B.F.L. Ward and Z. Wąs, Phys. Lett. **B353** (1995) 362.

[10] The LEP Collaborations ALEPH, DELPHI, L3, OPAL and the LEP Electroweak Working Group, *Updated Parameters of the* Z *Resonance from Combined Preliminary Data of the LEP Experiments*, CERN-PPE/93-157.

[11] F.A. Berends et al., in *Z Physics at LEP 1, Vol. 1*, ed. G. Altarelli, R. Kleiss and C. Verzegnassi, (CERN Report: CERN 89-08, 1989), p. 89.
M. Böhm et al., in *Z Physics at LEP 1, Vol. 1*, ed. G. Altarelli, R. Kleiss and C. Verzegnassi, (CERN Report: CERN 89-08, 1989), p. 203.

[12] See, for example, M. Consoli *et al.*, in "Z Physics at LEP 1", CERN Report CERN 89-08 (1989), eds G. Altarelli, R. Kleiss and C. Verzegnassi, Vol. 1, p. 7.

[13] LEP Energy Working Group note 96-07, E. Lancon and A. Blondel, *Determination of the LEP Energy Spread Using Experimental Constraints.*

[14] G. Wilkinson, *The determination of the LEP energy in the 1995 Z^0 scan*, talk presented at ICHEP96, Warsaw, 25-31 July 1996, to appear in the proceedings.

[15] LEP Energy Working Group, private communication. The contact person is Tiziano Camporesi, mail address T.Camporesi@cern.ch.

[16] A. Borrelli, M. Consoli, L. Maiani, R. Sisto, Nucl. Phys. **B 333** (1990) 357;
R.G. Stuart, Phys. Lett. **B 272** (1991) 353.

[17] A. Leike, T. Riemann, J. Rose, Phys. Lett. **B 273** (1991) 513;
T. Riemann, Phys. Lett. **B 293** (1992) 451;
S. Kirsch, T. Riemann, Comp. Phys. Comm. **88** (1995) 89.

[18] ALEPH Collaboration, D. Buskulic et al., Phys. Lett. **B 378** (1996) 373;
ALEPH Collaboration, *Measurement of fermion pair production in* e^+e^- *annihilation and interpretation in terms of new physics phenomena*, contributed paper to EPS 1997, Jerusalem, eps-hep-602.

[19] DELPHI Collaboration, *DELPHI results on the Measurement of Fermion-Pair Production at LEP energies from 130 GeV to 172 GeV*, DELPHI 97-132 CONF 110, contributed paper to EPS 1997, Jerusalem, eps-hep-464.

[20] L3 Collaboration, M. Acciarri et al., Phys. Lett. **B 370** (1996) 195;
L3 Collaboration, CERN preprint CERN-PPE/97-052;
L3 Collaboration, *Preliminary L3 Results on Z–Boson Parameters from 1990–96 Data*, L3 Note 2163, September 1997.

[21] OPAL Collaboration, CERN preprint CERN-PPE/97-101;
OPAL Collaboration, *S-Matrix Fits to the OPAL LEP1 Lineshape and Asymmetry Data and the LEP2 Cross-Section Data*, OPAL Physics Note PN319, September 1997.

[22] The LEP experiments and the LEP Electroweak Working Group, CERN preprint CERN-PPE/95-172.

[23] L3 Collaboration, O. Adriani et al., Phys. Lett. **B 315** (1993) 637;
G. Isidori, Phys. Lett. **B 314** (1993) 139;
M.W. Grünewald, S. Kirsch, CERN preprint CERN-PPE/93-188.

[24] TOPAZ Collaboration, K. Miyabayashi et al., Phys. Lett. **B 347** (1995) 171.

[25] ALEPH Collaboration, D. Buskulic *et al.*, Zeit. Phys. **C69** (1996) 183.

[26] DELPHI Collaboration, P. Abreu *et al.*, Z. Phys. **C67** (1995) 183;
DELPHI Collaboration, *An updated measurement of tau polarisation*, DELPHI 96-114 CONF 42, contributed paper to ICHEP96, Warsaw, 25-31 July 1996, **PA07-008**.

[27] L3 Collaboration, O. Acciari *et al.*, Phys. Lett. **B341** (1994) 245;
L3 Collaboration, *Measurement of the τ Polarization and the Spin Correlations in* $\mathrm{e}^+\mathrm{e}^- \rightarrow \tau^+\tau^-$, L3 note 2131, contributed paper to EPS-HEP-97, Jerusalem, **EPS-481**.

[28] OPAL Collaboration, G.Alexander *et al.*, Z. Phys. **C75** (1996) 365.

[29] The LEP Heavy Flavour Group, *Presentation of LEP Electroweak Heavy Flavour Results for Summer 1996 Conferences*, LEPHF/96-01, http://www.cern.ch/LEPEWWG/heavy/lephf9601.ps.gz.

[30] SLD Collaboration, SLAC-PUB-7585, contributed paper to EPS-HEP-97, Jerusalem, **EPS-118**.

[31] SLD Collaboration, SLAC-PUB-7594, contributed paper to EPS-HEP-97, Jerusalem, **EPS-120**.

[32] SLD Collaboration, SLAC-PUB-7629, contributed paper to EPS-HEP-97, Jerusalem, **EPS-122**;
SLD Collaboration, SLAC-PUB-7630, contributed paper to EPS-HEP-97, Jerusalem, **EPS-123**;
SLD Collaboration, contributed paper to EPS-HEP-97, Jerusalem, **EPS-124**;
SLD Collaboration, SLAC-PUB-7595, contributed paper to EPS-HEP-97, Jerusalem, **EPS-126**;
E. Etzion, talk presented at EPS-HEP-97, Jerusalem, to appear in the proceedings.

[33] ALEPH Collaboration, D. Buskulic *et al.*, Z. Phys. **C62** (1994) 179;
ALEPH Collaboration, D. Buskulic *et al.*, Phys. Lett. **B384** (1996)414;
ALEPH Collaboration., D. Buskulic *et al.*, *Measurement of the semileptonic b branching ratios from inclusive leptons in Z decays*, Contributed Paper to EPS-HEP-95 Brussels, **eps0404**.
This note may be found at http://alephwww.cern.ch/ALPUB/oldconf/HEP95/HEP95.html.

[34] ALEPH Collaboration, *Measurement of the partial decay width of the Z into $c\bar{c}$ quarks* contributed paper to ICHEP96, Warsaw, 25-31 July 1996 **PA10-016**. The results of the exclusive-exclusive and inclusive-exclusive double-tag D-meson measurements are averaged for this note;
ALEPH Collaboration, *Study of Charmed Hadron Production in Z Decays,* contributed paper to the EPS-HEP-97, Jerusalem, **EPS-623**.

[35] DELPHI Collaboration, P.Abreu et al., Z. Phys. **C66** (1995) 323.

[36] DELPHI Collaboration, P.Abreu *et al.*, Z. Phys **C65** (1995) 569;
DELPHI Collaboration, P.Abreu *et al.*, Z. Phys **C66** (1995) 341;
DELPHI Collaboration, *Measurement of the Forward-Backward Asymmetries of $e^+e^- \rightarrow Z \rightarrow b\bar{b}$ and $e^+e^- \rightarrow Z \rightarrow c\bar{c}$*, DELPHI 95-87 PHYS 522, contributed paper to EPS-HEP-95 Brussels **eps0571**.
Delphi notes are available at http://wwwcn.cern.ch/˜pubxx/www/delsec/delnote/.

[37] L3 Collaboration, O. Adriani *et al.*, Phys. Lett. **B292** (1992) 454;
L3 Collaboration, M. Acciarri *et al.*, Phys. Lett. **B335** (1994) 542;
L3 Collaboration, *Measurement of R_b and BR($\mathrm{b} \rightarrow \ell X$) from b-quark semileptonic decays,* L3 Note 1449, July 16 1993;
L3 Collaboration, *L3 Results on $A_\mathrm{FB}^\mathrm{b\bar{b}}$, $A_\mathrm{FB}^\mathrm{c\bar{c}}$ and χ for the Glasgow Conference,* L3 Note 1624;
L3 Collaboration, *L3 Results on R_b and* $\mathrm{BR}(\mathrm{b} \rightarrow \ell)$ *for the Glasgow Conference,* L3 Note 1625;
L3 Collaboration, M. Acciarri *et al.*, Z Phys. **C71** 379 (1996);
L3 Collaboration, *Measurement of the $e^-e^- \rightarrow Z \rightarrow b\bar{b}$ Forward-Backward Asymmetry Using Leptons,* L3 Note 2112, contributed paper to the EPS-HEP-97, Jerusalem, **EPS-490**;

L3 Collaboration, *Measurement of the $B^0 - \bar{B}^0$ Mixing Parameter,* L3 Note 2113, contributed paper to the EPS-HEP-97, Jerusalem, **EPS-490**.

[38] OPAL Collaboration, G. Alexander *et al.*, Z. Phys. **C70** (1996) 357;
OPAL Collaboration, R. Akers *et al.*, *Updated Measurement of the Heavy Quark Forward-Backward Asymmetries and Average B Mixing Using Leptons in Multihadronic Events*, OPAL Physics Note PN226 contributed paper to ICHEP96, Warsaw, 25-31 July 1996 **PA05-007**
OPAL Collaboration, R. Akers *et al.*, *QCD corrections to the bottom and charm forward-backward asymmetries* OPAL Physics Note PN284.

[39] DELPHI Collaboration, *Measurement of the semileptonic b branching ratios and $\bar{\chi}_b$ from inclusive leptons in Z decays,* DELPHI 97-118 CONF 100 contributed paper to the EPS-HEP-97, Jerusalem, **EPS-415**.

[40] L3 Collaboration, O. Adriani *et al.*, Phys. Lett. **B307** (1993) 237.

[41] ALEPH Collaboration, R. Barate *et al.*, Physics Letters **B 401** (1997) 150;
ALEPH Collaboration, R. Barate *et al.*, Physics Letters **B 401** (1997) 163.

[42] DELPHI Collaboration, *Measurement of the partial decay width $R_b^0 = \Gamma_{b\bar{b}}/\Gamma_{had}$ with the DELPHI detector at LEP* , DELPHI 97-106 CONF 88, contributed paper to the EPS-HEP-97, Jerusalem, **EPS-419**.

[43] L3 Collaboration, *Measurement of the Z Branching Fraction into Bottom Quarks Using Double Tag Methods,* L3 Note 2114, contributed paper to the EPS-HEP-97, Jerusalem, **EPS-489**.

[44] OPAL Collaboration, K. Ackerstaff *et al.*, Z. Phys. **C74** (1997) 1.

[45] L3 Collaboration, *Afb(bb) using a jet-charge technique on 1994 data,* L3 Note 2129.

[46] OPAL Collaboration, R. Akers *et al.*, Z. Phys. **C67** (1995) 365;
OPAL Collaboration, K.Ackerstaff *et al.*, Z. Phys. **C75** (1997) 385.

[47] DELPHI Collaboration, *Summary of R_c measurements in DELPHI,* DELPHI 96-110 CONF 37 contributed paper to ICHEP96, Warsaw, 25-31 July 1996 **PA01-060**.

[48] OPAL Collaboration, G. Alexander *et al.*, Z. Phys. **C72** (1996) 1;
OPAL Collaboration, K. Ackerstaff *et al.*, CERN-PPE/97-093, accepted by Zeit. Phys. C.

[49] ALEPH Collaboration, D. Buskulic *et al.*, Z. Phys. **C62** (1994) 1;
ALEPH Collaboration, D. Buskulic *et al.*, *The Forward–Backward Asymmetry for Charm Quarks at the Z pole: an Update*, Contributed Paper to EPS-HEP-95 Brussels, **eps0634**.
This note may be found at http://alephwww.cern.ch/ALPUB/oldconf/HEP95/HEP95.html.

[50] OPAL Collaboration, G. Alexander *et al.*, Z. Phys. **C73** (1996) 379.

[51] D. Bardin *et al.*, Z. Phys. **C44** (1989) 493; Comp. Phys. Comm. **59** (1990) 303; Nucl. Phys. **B351**(1991) 1; Phys. Lett. **B255** (1991) 290 and CERN-TH 6443/92 (May 1992).

[52] The LEP Heavy Flavour Group, *QCD Corrections to $A_{\mathrm{FB}}^{\mathrm{b\bar{b}}}$ and $A_{\mathrm{FB}}^{\mathrm{c\bar{c}}}$ Measurements at LEPI*, LEPHF/97-01, http://www.cern.ch/LEPEWWG/heavy/.

[53] ALEPH Collaboration, D. Decamp *et al.*, Phys. Lett. **B259** (1991) 377.

[54] ALEPH Collaboration, ALEPH-Note 93-041 PHYSIC 93-032 (1993);
ALEPH Collaboration, ALEPH-Note 93-042 PHYSIC 93-033 (1993);
ALEPH Collaboration, ALEPH-Note 93-044 PHYSIC 93-035 (1993).

[55] ALEPH Collaboration, D. Buskulic *et al.*, Z. Phys. **C71** (1996) 357.

[56] DELPHI Collaboration, P. Abreu *et al.*, Phys. Lett. **B277** (1992) 371.

[57] DELPHI Collaboration, *Measurement of the Inclusive Charge Flow in Hadronic Z Decays,* DELPHI 96-19 PHYS 594.

[58] L3 Collaboration, *Forward-Backward charge asymmetry measurement on 91-94 data*, L3 Note 2063.

[59] OPAL Collaboration, P. D. Acton *et al.*, Phys. Lett. **B294** (1992) 436.

[60] OPAL Collaboration, *A determination of* $\sin^2\theta_W$ *from an inclusive sample of multihadronic events,* OPAL Physics Note PN195 (1995).

[61] T. Sjöstrand, Comp. Phys. Comm. **82** (1994) 74.

[62] G. Marchesini *et al.*, Comp. Phys. Comm. **67** (1992) 465.

[63] ALEPH Collaboration, R. Barate, *et al.*, Phys. Lett. **B401** (1997) 347.

[64] DELPHI Collaboration, P. Abreu, *et al.*, Phys. Lett. **B397** (1997) 158.

[65] L3 Collaboration, M. Acciarri, *et al.*, Phys. Lett. **B398** (1997) 223.

[66] OPAL Collaboration, K. Ackerstaff, *et al.*, Phys. Lett. **B389** (1996) 416.

[67] WW Cross-sections Working Group, W. Beenacker (convenor), F.A. Berends (convenor), *et al.*, "WW Cross-sections and Distributions", in *Physics at LEP2*, edited by G. Altarelli, T. Sjöstrand and F. Zwirner (CERN, Geneva, 1996), CERN 96-01, vol. 1.

[68] M. Rijssenbeek, talk presented at ICHEP96, Warsaw, 25-31 July 1996, to appear in the proceedings.

[69] LEP Energy Group, "LEP Energy Calibration in 1996", LEP Energy Group/97-01.

[70] D. Bardin, *et al.*, Comp. Phys. Comm. **104** (1997) 161.

[71] ALEPH Collaboration, *Measurement of the W-pair cross section in* e^+e^- *collisions at 172 GeV*, CERN-PPE/97-102, submitted to Phys. Lett. B;
ALEPH Collaboration, *W mass measurement through direct reconstruction in ALEPH*, contributed paper to EPS-HEP-97, Jerusalem, **EPS-600**.

[72] DELPHI Collaboration, *Measurement of the W-pair cross-section and of the W mass in* e^+e^- *interactions at 172 GeV*, DELPHI 97-108 CONF 90, contributed paper to EPS-HEP-97, Jerusalem, **EPS-347**.

[73] L3 Collaboration, M. Acciarri, *et al.*, Phys. Lett. **B407** (1997) 419;
L3 Collaboration, M. Acciarri, *et al.*, *Measurements of Mass, Width and Gauge Couplings of the W Boson at LEP*, CERN-PPE/97-98, submitted to Phys. Lett. B.

[74] OPAL Collaboration, *Measurement of the Mass of the W Boson Mass and* $W^+ W^-$ *Production and Decay Properties in* e^+e^- *Collisions at* $\sqrt{s} = 172$ *GeV*, CERN-PPE/97-116, accepted by Zeit. f. Physik C.

[75] W Mass Working Group, Z. Kunszt (convenor), W. J. Stirling (convenor), *et al.*, "Determination of the Mass of the W Boson", in *Physics at LEP2*, edited by G. Altarelli, T. Sjöstrand and F. Zwirner (CERN, Geneva, 1996), CERN 96-01, vol. 1.

[76] The ALEPH Collaboration, Contrib. paper to LP97 Hamburg, LP-257.
The ALEPH Collaboration, Contrib. paper to EPS-HEP97 Jerusalem, EPS/97-601.

[77] DELPHI Collaboration, P. Abreu *et al.*, Phys. Lett. **B397** (1997) 158;
DELPHI Collaboration, *Measurement of Trilinear Gauge Couplings in* e^+e^- *Collisions at 161 GeV and 172 GeV,* Contrib. paper to EPS-HEP97 Jerusalem, EPS/97-295, and DELPHI 97-113 CONF 95.

[78] L3 Collaboration, M. Acciarri *et al.*, Phys. Lett. **B398** (1997) 223,
L3 Collaboration, M. Acciarri *et al.*, CERN-PPE/97-98, submitted to Phys.Lett.B.

[79] OPAL Collaboration, K. Ackerstaff *et al.*, Phys. Lett. **B397** (1997) 147,
OPAL Collaboration, *Measurement of triple Gauge Boson Couplings from* W^+W^- *Production at* $\sqrt{s} = 172$ *GeV,* CERN-PPE/97-125, submitted to Zeit. f. Physik C.

[80] CDF Collaboration, F. Abe *et al.*, Phys. Rev. Lett. **75** (1995) 1017,
CDF Collaboration, F. Abe *et al.*, Phys. Rev. Lett. **78** (1997) 4536.

[81] DØ Collaboration, S. Abachi *et al.*, Phys. Rev. Lett. **75** (1995) 1023,
S. Abachi *et al.*, Phys. Rev. Lett. **75** (1995) 1034,
S. Abachi *et al.*, Phys. Rev. Lett. **77** (1996) 3303,
S. Abachi *et al.*, Phys. Rev. Lett. **78** (1997) 3634,
S. Abachi *et al.*, Fermilab-Pub-97/088-E, submitted to Phys. Rev.D ,
B. Abbott *et al.*, Fermilab-Pub-97/136-E, submitted to Phys. Rev. Lett.

[82] K. Gaemers and G. Gounaris, Zeit. Phys. **C1** (1979) 259.

[83] K. Hagiwara, R.D. Peccei, D. Zeppenfeld, K. Hikasa, Nucl. Phys. **B282** (1987) 253.

[84] M. Bilenky, J.L. Kneur, F.M. Renard and D. Schildknecht, Nucl. Phys. **B409** (1993) 22.
M. Bilenky, J.L. Kneur, F.M. Renard and D. Schildknecht, Nucl. Phys. **B419** (1994) 240.

[85] I. Kuss and D. Schildknecht, Phys. Lett. **B383** (1996) 470.

[86] G. Gounaris and C.G. Papadopoulos, DEMO-HEP-96/04, THES-TP 96/11, hep-ph/9612378.

[87] Physics at LEP2, Edited by G. Altarelli, T. Sjostrand and F. Zwirner, Report on the LEP2 workshop 1995, CERN 96-01 (1996) Vol 1 p525.

[88] SLD Collaboration, P. Rowson, talk presented at Moriond 97.

[89] CHARM II Collaboration, P. Vilain *et al.*, Phys. Lett. **B335** (1994) 246.

[90] UA2 Collaboration, J. Alitti *et al.*, Phys. Lett. **B276** (1992) 354.

[91] CDF Collaboration, F. Abe *et al.*, Phys. Rev. Lett. **65** (1990) 2243;
CDF Collaboration, F. Abe *et al.*, Phys. Rev. **D43** (1991) 2070.

[92] CDF Collaboration, F. Abe *et al.*, Phys. Rev. Lett. **75** (1995) 11;
CDF Collaboration, F. Abe *et al.*, Phys. Rev. **D52** (1995) 4784.
A. Gordon, talk presented at XXXIInd Rencontres de Moriond, Les Arcs, 16-22 March 1997, to appear in the proceedings.

[93] DØ Collaboration, S. Abachi *et al.*, Phys. Rev. Lett. **77** (1996), 3309;
K. Streets, talk presented at Hadron Collider Physics 97, Stony Brook, to appear in the proceedings.

[94] Y.K. Kim, talk presented at the Lepton-Photon Symposium 1997, Hamburg, 28 July - 1 Aug, 1997, to appear in the proceedings.

[95] CDHS Collaboration, H. Abramowicz *et al.*, Phys. Rev. Lett. **57** (1986) 298;
CDHS Collaboration, A. Blondel *et al.*, Z. Phys. **C45** (1990) 361.

[96] CHARM Collaboration, J.V. Allaby *et al.*, Phys. Lett. **B177** (1986) 446;
CHARM Collaboration, J.V. Allaby *et al.*, Z. Phys. **C36** (1987) 611.

[97] CCFR Collaboration, K. McFarland, *A Precision Measurement of Electroweak Parameters in Neutrino-Nucleon Scattering*, FERMILAB-Pub-97/001-E, January 1997, submitted to Phys. Rev. Lett.

[98] CDF Collaboration, J. Lys, *Top Mass Measurements at CDF,* Proc. ICHEP96, Warsaw, 25-31 July 1996, 1196.

[99] DØ Collaboration, S. Abachi *et al.*, Phys. Rev. Lett. **79** (1997) 1197.

[100] R. Raja, talk presented at XXXIInd Rencontres de Moriond, Les Arcs, 16-22 March 1997, to appear in the proceedings.

[101] R.M. Barnett, *et al.*, Phys. Rev. **D54** (1996) 1.

[102] S. Eidelmann and F. Jegerlehner, Z. Phys. **C67** (1995) 585.

[103] *Reports of the working group on precision calculations for the Z resonance*, eds. D. Bardin, W. Hollik and G. Passarino, CERN Yellow Report 95-03, Geneva, 31 March 1995.

[104] Electroweak libraries:
ZFITTER: see Reference 51;
BHM (G. Burgers, W. Hollik and M. Martinez): W. Hollik, Fortschr. Phys. **38** (1990) 3, 165;
M. Consoli, W. Hollik and F. Jegerlehner: Proceedings of the Workshop on Z physics at LEP I, CERN Report 89-08 Vol.I,7 and G. Burgers, F. Jegerlehner, B. Kniehl and J. Kühn: the same proceedings, CERN Report 89-08 Vol.I, 55;
TOPAZ0: G. Montagna, O. Nicrosini, G. Passarino, F. Piccinnii and R. Pittau, Nucl. Phys. **B401** (1993) 3; Comp. Phys. Comm. **76** (1993) 328.
These computer codes are upgraded by including the results of [103] and references therein.

[105] T. Hebbeker, M. Martinez, G. Passarino and G. Quast, Phys. Lett. **B331** (1994) 165;
P.A. Raczka and A. Szymacha, Phys. Rev. **D54** (1996) 3073;
D.E. Soper and L.R. Surguladze, Phys. Rev. **D54** (1996) 4566.

[106] See, for example, A. Czarnecki and J. Kühn, Phys. Rev. Lett. **77** (1996) 3955;
G. Degrassi, P. Gambino and A. Sirlin, Phys. Lett. **B394** (1997) 188.

[107] M. L. Swartz, Phys. Rev. **D53** (1996) 5268.

[108] A.D. Martin and D. Zeppenfeld, Phys. Lett. **B345** (1994) 558.

[109] H. Burkhardt and B. Pietrzyk, Phys. Lett. **B356** (1995) 398.

[110] R. Alemany, *et al.*, *Improved Determination of the Hadronic Contribution to the Muon* $(g-2)$ *and to* $\alpha(m_Z)$ *Using new Data from Hadronic* τ *Decays*, LAL 97-02, Feb 1997.

[111] P. Janot, *Searches for New Particles at Present Colliders*, talk presented at EPS-HEP-97, Jerusalem, to appear in the proceedings.